Synthesis and Characterization of Telechelic Hydroxyl Functional Poly(N-vinylpyrrolidone)

by

Rueben Pfukwa

Thesis presented in partial fulfillment of the requirements for the degree of
Master of Science (Polymer Science)

at

Stellenbosch University

Supervisor: Prof. Bert Klumperman

Department of Chemistry and Polymer Science

Faculty of Science

March 2008

Declaration

I, the undersigned, hereby declare that the work contained in this thesis is my own work and that I have not previously in its entirety or in part submitted it at any university for a degree.

…………………   ..……………

Rueben Pfukwa   March 2008

<u>Abstract</u>

Reversible addition fragmentation chain transfer (RAFT)-mediated polymerization has emerged as a versatile method for preparing polymers with control over molecular weight and polydispersity. Inherent in its mechanism is the retention of the chain transfer agent, the RAFT agent, at the polymer chain ends. Typically RAFT agents are made up of two parts, the so called R (leaving) and Z (thiocarbonyl thio, stabilizing) groups. These are retained as the α-and the ω-end groups of the final polymer, respectively. RAFT polymerization offers a ready method for preparing polymers with well defined end functionalities.

The α-end functionality can easily be built into the R group. The Z group, however, is thermally unstable and can impart color and smell to the polymer. Hence, two new methods for Z end group removal were introduced. Both methods take advantage of the facile reaction between thiocarbonyl thio compounds and radicals. By matching the functionalities of the R group (α-end group) with that of the end modified ω-chain end, both methods offer an easy route to accessing telechelic functional polymers. End functional polymers have many important uses in industry and in the biomedical field.

An alcohol functional xanthate RAFT agent was synthesized and successfully used to conduct the RAFT-mediated polymerization of N-vinylpyrrolidone (NVP). Characterization by NMR and MALDI ToF MS confirmed that α-hydroxyl-ω-xanthate-functional PVP was easily produced.

In the first end group modification method radicals were generated as in atom transfer radical addition (ATRA). A hydroxyl functional α-haloester was used as the ATRA initiator with a Cu catalyst system. The alkyl radical produced by this ATRA initiator then replaced the Z group giving a telechelic hydroxyl functional polymer. NMR analysis showed that the thiocarbonyl thio end group was completely removed. The hydroxyl functionality was quantified by derivatizing with trichloro acetyl isocyanate and subsequent analysis by NMR. MALDI ToF MS analysis, however, was inconclusive.

In the second method the thiocarbonyl thio end group was removed by simply heating the polymer with hydrogen peroxide, thereby replacing the Z group with a hydroxyl end group at the ω-chain end, giving a telechelic functional polymer. The telechelic hydroxyl functional polymer was subsequently crosslinked with a trifunctional isocyanate to make a PVP hydrogel. This confirmed that the end-modified polymer was indeed telechelic. The swelling kinetics of this hydrogel were determined in water at 37 ^{o}C.

Opsomming

Die omkeerbaar addisie-fragmentasie-kettingoordrag (OAFO)-beheerde polimerisasie proses is 'n veelsydige metode vir die bereiding van polimere met gekontrolleerde molekulêre massas en poliverspreiding. Die meganisme van die reaksie behels die behoud van die kettingoordragverbinding aan die punte van die polimeerketting. OAFO-verbindings bestaan tipies uit twee dele: die sogenaamde R-(verlatende) groep en die Z-(tiokarbonieltio, stabiliserende) groep. Hierdie groepe word onderskeidelik as die α-en die ω-endgroepe van die finale polimeer behou. RAFT-verbindings kan gebruik word om polimere met goed gedefineerde end-funksionaliteite te berei.

Die α-endfunksionaliteit kan maklik in die R-groep ingebou word. Die Z-groep is egter termies onstabiel en kan kleur en 'n onaangename reuk aan die polimeer verleen. Gevolglik is twee nuwe metodes voorgestel vir die verwydering van die Z-endgroep. Beide metodes trek voordeel uit die maklike reaksie tussen tiokarbonieltioverbindings en radikale. Deur die funksionaliteite van die R-groep (α-endgroep) met dié van die endgewysigde ω-kettingpunt te pas, bied beide metodes 'n eenvouding roete vir die bereiding van teecheliese funksionele polimere. Endfunksionele polimere het baie belangrike gebruike in die nywerheid en in die biomediese gebied.

'n Alkoholfunksionele xantaat RAFT-verbinding met alkoholfunksionaliteit is suksesvol berei en gebruik in die OAFO-beheerde polimerisasie van N-vinielpirollideen (NVP). KMR-analise en MALDI ToF MS het bevestig dat die α-hidroksiel-ω-xantaat-funksionele PVP suksesvol en maklik berei is.

In die eerste endgroep wysigingsmetode is radikale gegenereer soos in die atoomoordragradikaaladdisie (AORA). Hiervoor is 'n α-halo-ester as AORA-afsetter gebruik, tesame met 'n Cu-katalissisteem. Die alkielradikaal wat ontstaan het het vervolgens die Z-groep vervang, wat op sy beurt tot die onstataan van 'n teecheliese polimeer met hidroksielfunksionaliteit aanleiding gegee het. KMR-analise het bewys dat die tiokarbonieltio-endgroep volledig verwyder is. Die hidroksielfunksionaliteit is gekwantifiseer deur 'n derivaat daarvan te maak met

trichloroasetielisosianaat, asook deur die daaropvolgende KMR-analise. Resultate wat met behulp van MALDI-ToF-MS verkry is, was egter onoortuigend.

In die tweede metode is die tiokarbonieltio-endgroepe vewyder deur eenvoudig die polimeer met waterstofperoksied te verhit. Op dié manier is die Z-groep met 'n hidroksielendgroep aan die ω-ketting punt vervang, wat weer aanleiding gegee het tot 'n telecheliese hidroksielfunksionele polimeer. Hierdie polimeer is daarna gekruisbind met 'n trifunksionele isosianaat om 'n PVP-hidrogel te berei. Dit het bewys dat die endgewysigde polimeer inderdaad telechelies was. Die swelkinetika van hierdie hidrogel is in water by 37 ^{o}C bepaal.

To my parents, siblings, relatives, friends and colleagues, and to Helen, my sweet love, my beloved XX partner.

<u>Acknowledgements</u>

Table of Contents

Table of Figures

Table of Schemes

List of Symbols

[ACP]	Concentration of ACP
C_{tr}	Chain transfer constant
Da	Dalton
f	Initiator efficiency factor
f	Fractional water content
f_n^{OH}	Relative hydroxyl end functionality
k_{add}	Addition rate constant
k_d	Dissociation constant
k_{frag}	Fragmentation rate constant
k_p	Propagation rate constant
k_t	Termination rate constant
k_{dec}	Decomposition rate constant
[M]	Monomer concentration
$[M]_0$	Initial monomer concentration
M_c	Molecular weight between crosslinks
M_{C+}	Molar mass of cationizing ion
M_M	Molar mass of repeat unit
M_n	Number average molar mass
M_n^{NMR}	M_n determined by NMR
M_n^{SEC}	M_n determined by SEC
M_n^{Theor}	Theoretical M_n value
Mr_{NVP}	Molar mass of NVP
Mr_{HEECP}	Molar mass of HEECP
M_w/M_n	Ratio of weight average molar mass to number average molar mass
$M_{X,Y}$	Molar mass of end groups X and/or Y
m/z	Mass to charge ratio
t	time
W_t	Weight of water in hydrogel at time t
W_∞	weight of water in hydrogel at equilibrium swelling

List of Abbreviations

ACP   4,4'-Azobis(4-cyanopentanol)

AGET   Activators generated by electron transfer

AIBN   2,2'-Azobisisobutyronitrile

ARGET   Activators regenerated by electron transfer

ATRA   Atom Transfer Radical Addition

ATRP   Atom Transfer Radical Polymerization

COSY   (2-Dimensional NMR) Correlation Spectroscopy

CRP   Controlled Radical Polymerization

CTA   Chain Transfer Agent

DDI   Distilled Deionized (water)

DEP   Dead End Polymerization

ESI MS   Electrospray Ionisation Mass Spectrometry

EWC   Equilibrium Water Content

FRP   Free Radical Polymerization

GPEC   Gradient Polymer Elution Chromatography

HEBP   2-Hydroxyethyl 2'-Bromopropionate

HEECP   2-Hydroxyethyl 2-(ethoxycarbonothioylthio)propanoate

HPLC   High Performance Liquid Chromatography

IR   Infrared spectroscopy

LCCC   Liquid Chromatography *under* Critical Conditions

LRP   Living Radical Polymerization

MALDI ToF MS   Matrix Assisted Laser Desorption Ionization Time of Flight Mass
                            Spectroscopy

Me$_6$TREN   Tris[2-(dimethylamino)ethyl]amine

NMP   Nitroxide Mediated Polymerization

NMR   Nuclear Magnetic Resonance

NVP   N-vinyl pyrrolidone

PDI	Polydispersity Index
PEG	Poly(ethylene glycol)
PMDETA	*N,N,N',N",N"*-pentamethyldiethylenetriamine
PMMA	Poly(methyl methacrylate)
PS	Polystyrene
PVP	Poly(N-vinylpyrrolidone)
RAFT	Reversible Addition Fragmentation chain Transfer
RES	Reticulo Endothelial System
SEC	Size Exclusion Chromatography
TAI	Trichloroacetyl isocyanate
TEMPO	2,2,6,6-tetramethylpiperidnyloxyl
TERP	Organotellerium Mediated Radical Polymerization
TLC	Thin Layer Chromatography
UV-vis	Ultraviolet visible
VAc	Vinyl acetate

Chapter 1

General Introduction and objective

1.1 Introduction

Advances in materials science demand the provision of smart materials, i.e. materials with advanced properties and increased sophistication. This will make these materials better suited for their intended uses. As some of these materials are selected from polymers, this establishes a very important niche for polymer chemists. The polymer materials find employment in important fields like medicine and electrical engineering. Frequently these smart materials need to have well defined functional groups, pendant or located at the chain ends. This is illustrated schematically in Figure 1.1 below.

Pendant functional polymer

End functional polymers

mono end functional polymer

hetero telechelic end functional polymer

telechelic functional polymer
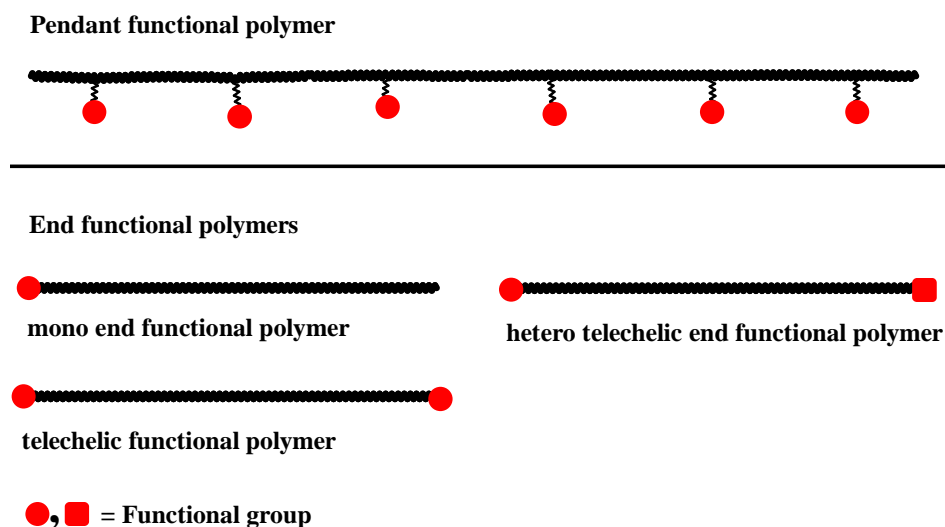
●,■ = Functional group

Figure 1.1. Schematic illustration of pendant functional and end functional polymers.

The presence of the functional groups enables the further application of the usual organic synthetic procedures to these materials as routes to making advanced structures. In medicine, for example, biomolecules can be covalently attached to the polymers at these functional groups to make polymeric

drug delivery vehicles with improved pharmacokinetic properties.[1] These biomolecules include proteins, peptides and liposomes or low molecular weight organic drug conjugates. The challenge, therefore, is for the polymer chemist to come up with simple and effective ways to introduce the functional groups into the polymer structure.

1.2 Objective of this work

In this work, two simple methods of making telechelic hydroxyl functional Poly(N-vinylpyrrolidone) (PVP) are introduced. PVP is a polymer of choice in numerous biomedical applications due to its excellent biocompatibility. It also has numerous industrial applications and is also widely applied in cosmetics. It is therefore an interesting polymer system. The details of this work are briefly outlined in the section below. The end functional PVP, prepared here, is subsequently characterized by SEC, NMR, UV and MALDI ToF MS.

1.3 Layout of thesis

1.3.1 Chapter 1. Introduction

This chapter gives a very brief insight into why functional polymers are important. It also contains a short outlines on the details of the rest of the work.

1.3.2 Chapter 2. Historical and theoretical background

Chapter 2 contains a brief overview on the chemistry of CRP as well as the shortcomings of this process. LRP[2] techniques are then introduced with a greater emphasis on RAFT[3] as it is the method used in this work. A brief outline on methods used to make end functional polymers is also given as well as methods used to make PVP.

1.3.3 Chapter 3. RAFT-mediated polymerization of NVP

In this chapter the RAFT-mediated polymerization of NVP is described. The preparation of an alcohol functional xanthate chain transfer (RAFT) agent is described. Its ability to mediate the polymerization of NVP to give α-hydroxyl-ω-xanthate functional PVP is assessed. The subsequently made PVP is characterized by SEC, NMR and MALDI ToF MS.

1.3.4 Chapter 4. Thiocarbonyl thio end group removal by an ATRA based radical exchange process for the preparation of α,ω-hydroxyl telechelic functional PVP

An ATRA based radical exchange process is introduced as an efficient way to remove the ω-xanthate end group. By using a hydroxyl functional ATRA initiator, this technique results in the replacement of the xanthate end group with a hydroxyl functional one. As the starting polymer material was already α-hydroxyl end functional, this offers an easy route to make telechelic hydroxyl functional PVP. The telechelic functional PVP is subsequently characterized by the relevant spectroscopic techniques. The hydroxyl functionality is quantified by derivatizing with trichloro acetyl isocyanate (TAI).

1.3.5 Chapter 5. Thiocarbonyl thio end group removal by an ATRA based radical exchange process for the preparation of α,ω-hydroxyl telechelic functional PVP

In this chapter a facile method for the removal of the xanthate end group by merely heating a mixture of the polymer solution with H_2O_2 is introduced. This process is shown to result in the replacement of the xanthate end group with a hydroxyl end moiety resulting in telechelic hydroxyl functional PVP. The telechelic hydroxyl functional PVP is then crosslinked by reacting with a trifunctional isocyanate to give a PVP hydrogel. The swelling behavior of this hydrogel, in DDI water, is also assessed.

1.3.6 Chapter 6. Conclusions and outlook

This chapter gives a short overview of the achievements in this work. It also contains a brief overview of the problems encountered in this work as well as an overview of possible methods to rectify these problems in future work.

References

1. R. Duncan, *Nat. Rev. Drug Discovery*, 2003. **2**: p.347-360.

2. W.A. Braunecker and K. Matyjaszewski, *Prog. Polym. Sci.*, 2007. **32**: p.93-146.

3. G. Moad, E. Rizzardo and S.H. Thang, *Aust. J. Chem.*, 2005. **58**: p.379-410.

Chapter 2

Historical and theoretical background

2.1 Why the need for well defined end functional polymers?

End functional polymers have an important economic position. They are used industrially to make block copolymers which find numerous applications as thermoplastic elastomers, dispersants, lubricants and as nonionic surfactants. They are also used to make polymer networks with well defined segment lengths. From the industrial and ultimately the economical standpoint this requires that these (pre)polymers have well defined end group functionalities. This is important for optimizing the formation of the advanced structures especially considering the chemistries utilized in making them into complex architectures. For example telechelic functional polymers terminated with alcohol and carboxylic acid functionalities are used to make their respective polyesters via condensation reactions. Hydroxyl telechelic functional polymers are reacted with difunctional isocyanates to form polyurethanes. When they are intended for making networks, the telechelic functional polymer is reacted stoichiometrically with a multifunctional crosslinking molecule bearing a complimentary functionality. This leads to a well defined polymer network which is very important for correlating structure property relationships.

2.2 Methods of preparing end functional polymers

End functional polymers are mainly prepared by living ionic polymerization and by the free radical polymerization mechanism. However, living ionic polymerization processes suffer from the fact that very stringent reaction conditions have to be employed. They require a complete absence of moisture and they are also intolerant to functional groups. Hence when end functional polymers are desired, functional group protection chemistry has to be used, inevitably adding more reaction steps and from the industrial perspective adding to the costs.[1] Living ionic polymerization is also restricted to a few monomer types. Radical polymerization methods are, therefore, generally used to prepare functional polymers. These are applicable to a wider range of monomers and are generally very tolerant to functional groups either on the initiators or on the monomers.

2.3 Free radical polymerization

FRP is a chain growth polymerization technique. The basic reactions of this process are shown in Scheme 2.1.
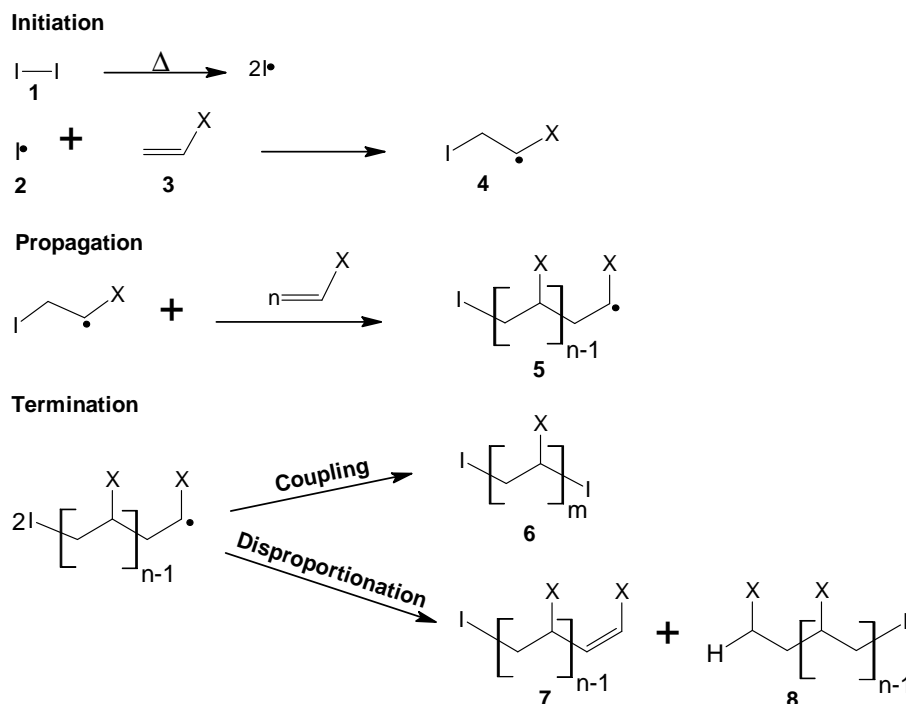
Scheme 2.1. Basic reactions in free radical polymerization.

In the initiation step, primary radicals are generated by thermally or photochemically induced homolysis of the initiator. In Scheme 1.1 initiation is illustrated by thermally induced homolysis. Typical initiators used are azo compounds like AIBN or peroxide initiators like benzoyl peroxide.[2] The primary radicals (**2**, Scheme 2.1) add to the monomers to produce the propagating radicals (**4**, Scheme 2.1). Propagation is the chain building stage whereby the polymer chain grows by further addition of monomers. Chain growth is terminated by bimolecular reactions either by coupling of propagating radicals or by disproportionation reactions. Propagation is first order with respect to radical concentration, whilst termination is second order. A number of other chain breaking reactions can also take place; these are mainly chain transfer reactions to monomer and to solvent. The latter happens when polymerization is carried out in solution.

2.3.1 Attractive features of FRP processes

FRP reactions are very robust! They have a reasonable tolerance to traces of impurities like stabilizers, and oxygen. They also exhibit a high level of tolerance to functional groups like alcohols, carboxylic acids and tertiary amine groups. Added to this they are also applicable to virtually all unsaturated monomer ranges, hence they are widely used in industry and in research labs to make functional polymers.

2.3.2 Drawbacks of FRP processes

Despite its robust nature and its remarkable versatility, conventional free radical polymerization has its drawbacks. Control of molecular weight is poor and molecular weight distributions are broad. Chain transfer reactions to monomer and to solvent are always present and chain functionalization is not always quantitative. This is a hindrance when polymers with precisely controlled molecular weight distributions and accurately known end functionalities are required for making advanced structures. Nevertheless FRP has been applied to make end functional polymers.

2.3.3 End functional polymers by FRP

Telechelic functional polymers by radical polymerization were first obtained via the so called DEP.[3,4] The procedure relies on using a very high initiator concentration resulting in high radical concentrations. These conditions favor primary radical termination and therefore lead to a low degree of polymerization. All initiator is used up before all monomers have reacted resulting in oligomers. Success of this procedure depends on the complete exclusion of termination events like chain to solvent or chain to monomer in order to get completely α,ω-telechelic functional polymer.[3] Termination should only be by combination. High conversions are not ideal as they retard the termination step by the Tromsdorff-Norrish (gel) effect.[3,5] DEP is however, restricted to monomers that terminate mainly by primary radical termination like styrene.[5,6]

α,ω-Telechelic functional polymers have also been accessed by using chain transfer agents which do not have transferable hydrogen atoms. Examples include substituted disulfides or carbon tetrachloride. This procedure was however limited by the fact that a lot of monomers were not compatible with the limited range of suitable chain transfer agents available.[7]

Cho and Kim reported the use of a combination of functional azo initiators and chain transfer agents, with the same functionality as a route to accessing α, ω-telechelic functional polymers. This they called a two component iniferters system (iniferters -*ini*tiators-trans*fer* agent *ter*minators).[8] The group of Rizzardo also utilized substituted allylic disulfides containing the appropriate functionalities to prepare α, ω-PS and PMMA.[7]

In all the examples considered in this case, the shortcomings of FRP were evident in that conversion of end functionalities was not quantitative and the polymers prepared were characterized by high M_w/M_n ratios. These shortcomings, among other concerns, have provided the impetus to "tame" the FRP process in order to realize the full benefits of its robust and versatile nature culminating in the invention of several LRP processes.

2.4 Living Radical Polymerization

The problems encountered with conventional radical polymerization have recently been countered with the advent of LRP processes.[2,9,10] The most successful of these methods are NMP,[11] ATRP[12,13] and RAFT.[14-16] There are other methods of controlled radical polymerization[9] e.g. TERP and Stibine Mediated Polymerization, however only NMP, ATRP and RAFT will be discussed here given that they are most studied so far. There has been a lot of debate on what is the best terminology to use i.e. *Controlled* or *Living radical polymerizations*? In this work only the term living will be used as the processes considered yield living polymers. This is because whilst termination reactions are not totally eradicated, the polymers produced show characteristics of living polymers, e.g. the ability to chain extend and form block copolymers.

2.4.1 Features of LRP

Considered broadly, the LRP processes aim to suppress reactions that irreversibly terminate growing chains and make the chains grow simultaneously. A dynamic equilibrium is established between a low concentration of propagating radicals/growing chains ($P_n\bullet$, Scheme 2.2) and a much larger concentration of dormant chains (P_n–X) thereby enabling all the chains to grow at the same time making the process living.

Initiation $\xrightarrow[\quad k_p \quad]{\quad M \quad}$ $P_n^{\bullet}$

$P_n^{\bullet}$ + X $\underset{\xleftarrow{\quad\quad}}{\xrightarrow{\quad k_d \quad}}$ $P_n\text{-X}$ $\underset{\xleftarrow[\quad k_d \quad]{}}{\xrightarrow{\quad k_a \quad}}$ $P_n^{\bullet}$ + X

$P_n^{\bullet}$ + $P_m^{\bullet}$ $\xrightarrow[\quad k_t \quad]{}$ dead chains $\xleftarrow{\quad k_t \quad}$
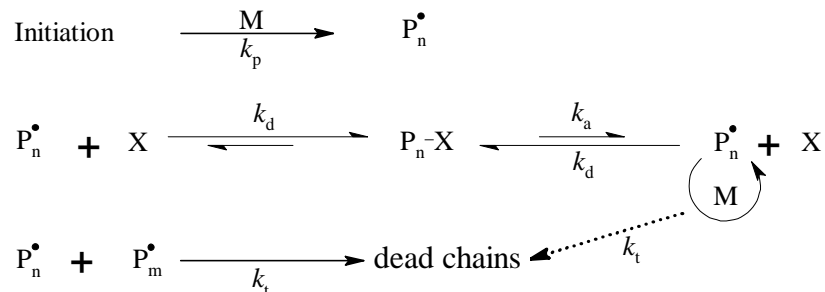
Scheme 2.2. The mechanistic basis of living radical polymerization processes.

In NMP and ATRP this is achieved by reversibly capping the growing chains with stable nitroxide radicals and halogens respectively (= X) to give the dormant forms (P_n–X). These can be reactivated by homolytic cleavage of the P_n–X bond.[2] In RAFT on the other hand the "livingness" is attained by degenerative transfer between the propagating radicals/growing chains and certain thiocarbonyl thio compounds.[9] The exchange reactions must be very fast in order to give all the chains a chance to grow at the same rate. The dormant chains should be favored thermodynamically so as to keep a low steady state concentration of propagating radicals and minimize termination.[2] If initiation is fast and termination events are rendered insignificant all chains can grow at the same rate, molecular weights evolve linearly with conversion and the polymers have low polydispersities. The features of these LRP systems were thoroughly considered by Quirk and Lee[17] and they made the following recommendations for the polymerizations systems to be considered as living.

- When all monomer is consumed, chain growth can be resumed by adding more monomer
- Molecular weights evolve linearly with conversion
- The number of polymer chains is not affected by conversion
- Molecular weight is predetermined by the reaction's stoichiometry, initial monomer and chain transfer agent concentrations, as well as conversion
- PDI values are low and decrease with conversion
- Block copolymers can be prepared if monomers are added one after the other
- Chain end functionalities are predictable and retained quantitatively

These processes are now considered individually below. NMP and ATRP will be considered briefly here, whilst RAFT will be covered in more detail given that it is the LRP system used in this work.

2.4.2 NMP

In NMP, **X** is a stable nitroxide radical e.g. TEMPO (**11**).
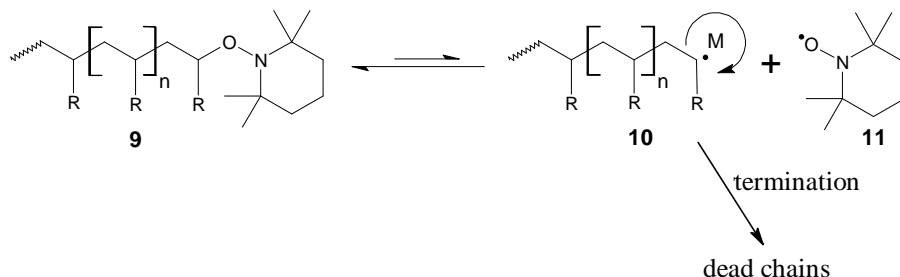
Scheme 2.3. Illustration of a TEMPO mediated NMP

A dynamic equilibrium is established between dormant alkoxyamine terminated chains (**9**) and the propagating radicals/growing chains (**10**). The dormant species are activated by a thermally induced homolytic cleavage of the alkoxyamine's C–O bond to give again the propagating radical and the stable nitroxide radical (**11**).[2] This is illustrated in Scheme 1.3. For the system to exhibit living behavior, the nitroxide radical should not:

- initiate chain growth
- react with itself
- take part in side reactions like β–hydrogen abstraction.
- be unstable

In the earliest work on this method, TEMPO was used as the stable nitroxide radical.[18,19]

2.4.3 ATRP

ATRP is a transition metal complex catalyzed process. The ingredients include a transition metal complex, an alkyl halide and the monomer. The metal complex undergoes a one electron oxidation step which is accompanied by a reversible abstraction of the halogen atom from the alkyl halide. This results in the metal complex being oxidized and the formation of an alkyl radical, which subsequently initiates the polymerization.[2] The polymer chain grows until it abstracts back the halogen from the metal complex (deactivation) to give the dormant species (P_n–X, Scheme 2.4, where X is the halogen) and the metal complex in a lower oxidation state. The activation and

deactivation reactions can occur repeatedly to establish a dynamic equilibrium between active and dormant chains.[2] This reaction profile is illustrated below

$$R-X \ + \ [ML_y]^xX \ \rightleftharpoons \ R^\bullet \ + \ [ML_y]^{x+1}X_2$$

$$R^\bullet \ \xrightarrow{M} \ P_n^\bullet \ + \ [ML_y]^{x+1}X_2 \ \rightleftharpoons \ P_n-X \ + \ [ML_y]^xX$$

termination

$$P_n^\bullet \ + \ P_m^\bullet \ \longrightarrow \ \text{dead chains}$$
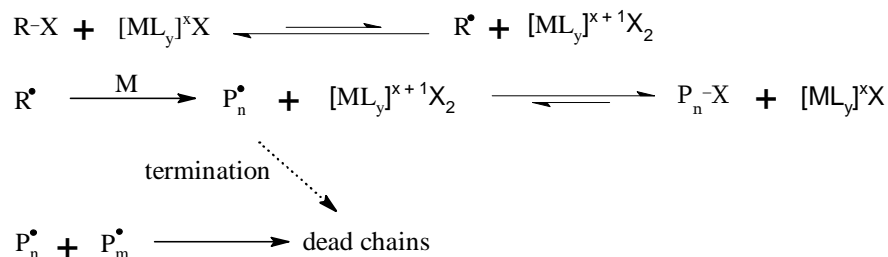
Scheme 2.4. The mechanistic basis of ATRP.

Copper based catalytic systems have been the most studied, by the group of Matyjaszewski[20,21] and are the most versatile. Other transition metal catalyst systems used include Ruthenium, Iron, Molybdenum, Chromium, Rhenium, Rhodium, Nickel and Palladium.[12,13] For the more successful copper based systems, multidentate nitrogen ligands are the most effective.[22] For maximum catalytic efficiency, the ligands have to be chosen carefully. Their activity decreases with coordination number as well as with the number of linking carbon atoms.[22] The effects of the nature of the alkyl halide as initiator have also been studied.[23]

2.4.4 RAFT

RAFT is probably the most successful LRP process. This is because it is compatible with the widest range of monomer classes including those with acid functionality. These can not be polymerized easily under ATRP conditions.[9] The chain transfer agents used for RAFT are selected from dithioesters, trithiocarbonates, dithiocarbamates, and xanthates. The generic structures of all commonly used RAFT agents are shown in Figure 2.1:
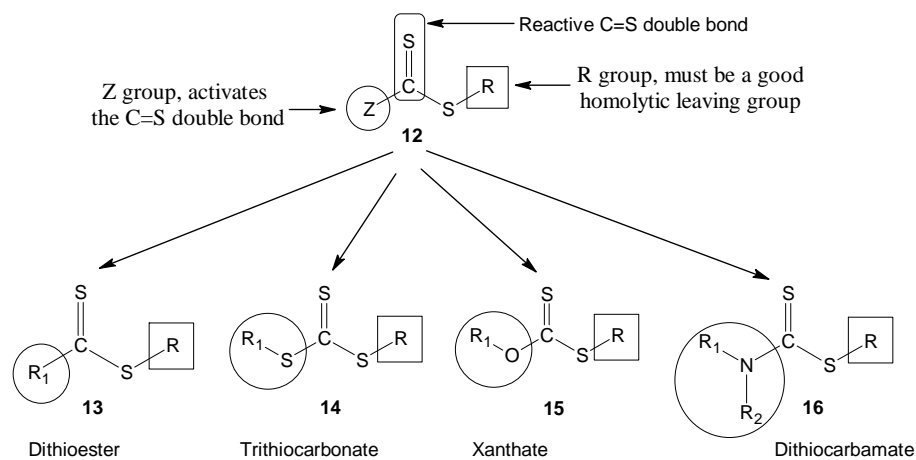
Figure 2.1. Generic structures of all commonly used RAFT agents.

2.4.4.1 Mechanism of the RAFT process

Scheme 2.5 shows the mechanism of the RAFT process as it is generally accepted in literature.[14,15]
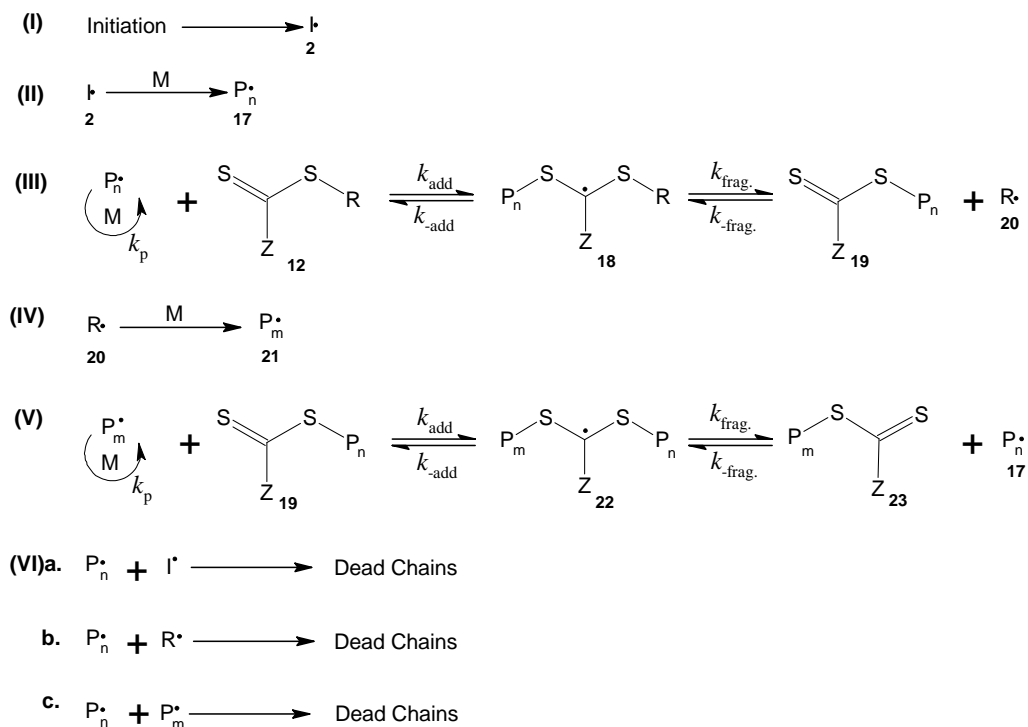
Scheme 2.5. The RAFT mechanism.

Initiation is usually as in conventional radical polymerization, by azo compounds, such as AIBN, or by peroxides, such as benzoyl peroxide. However other methods can be used, including thermal initiation for styrene[24] and ultraviolet (UV) irradiation.[25] After initiation the propagating radicals

(**17**) add to the CTA (**12**) to give the intermediate radical (**18**) which subsequently fragments to give the new radical (**20**) as well as the dormant chain (**19**). The radical (**20**) then reinitiates polymer chain growth. The propagating radicals $P_n\bullet$ (**17**) and $P_m\bullet$ (**21**) then rapidly equilibrate between the dormant forms (**19**) and (**23**) capped with the thiocarbonyl moiety, and their actively propagating forms, equation (**V**). Termination events can still happen as in conventional radical polymerization, however they are limited by keeping a low concentration of active radical species.

The fast equilibration between the actively propagating forms and the dormant thiocarbonyl capped forms thus ensures that all chains get a chance to grow at the same time. Equilibrium (**V**) is considered the main equilibrium as it ensures a rapid exchange between active and dormant forms of all growing chains ensuring that they all grow at the same rate and thus ensuring polymers with controlled molecular weight distribution and predictable molar mass.[9] It is also the stage in which most monomer is consumed. Overall the RAFT process can be considered as an insertion of monomers between the thiocarbonyl thio and the R group, ZC(S)S–R, bond of the RAFT agent by a radical chain reaction.

2.4.4.2 For a successful RAFT mediated polymerization

In the most ideal case for RAFT to be a living process, it must adhere to the characteristics described earlier (Section 2.4.1). All polymer chain growth must be initiated at the same time and more so by the R group reinitiating radical (**20**) of the RAFT agent (Scheme 2.5) and the contribution of chains initiated by the initiator derived radicals should be negligible.[2,9,26] However, despite the need for rapid dormant-active form interchange, the thermodynamic equilibrium must favor the dormant chain forms (in this case **19** and **23**). This helps to ensure a low propagating radical concentration so as to minimize bimolecular termination events. Other chain breaking events like chain transfer to monomer and to solvent should also be minimized.

2.4.4.3 Choice of RAFT agent

An appropriate RAFT agent should have a high chain transfer constant, C_{tr}, in order to ensure a rapid and quantitative initiation of chain growth. The C_{tr} of the dormant chains/macro CTAs (**19** and **23**) should be high as well to ensure fast equilibration between the dormant and active forms.[27] Therefore, the Z and R groups of the RAFT agent should be chosen carefully and should be tailored

with the reactivity of the monomer to be polymerized. The important considerations were given by Moad *et al.*[14] as follows:

- the C=S double bond of the RAFT agent and the macro RAFT agent (**19** and **23** respectively) should have a high k_{add}

- the intermediate radicals (**18** and **22**) should fragment easily to give the active radical species and should not participate in side reactions.

- in equilibrium (III) $k_{frag} \geq k_{-add}$

- **R•** (**20**) should reinitiate the polymerization rapidly and efficiently.

All these considerations bear down to the structure of the Z and R groups.

2.4.4.4 The Z group

The Z group mainly functions to influence the reactivity of the C=S double bond towards radical attack as well as stabilizing the intermediate radical species (**18** and **22**, Scheme 2.5) that are subsequently formed.[24,28,29] The generic forms of all RAFT agents' Z groups are given in Fig. 2.1. R_1 can be of aryl or alkyl functionality. Chiefari et. al[24] found that the reactivity of the C=S double bond towards propagating radicals, decreased in the order shown in Fig. 2.2, in polystyrene polymerizations.
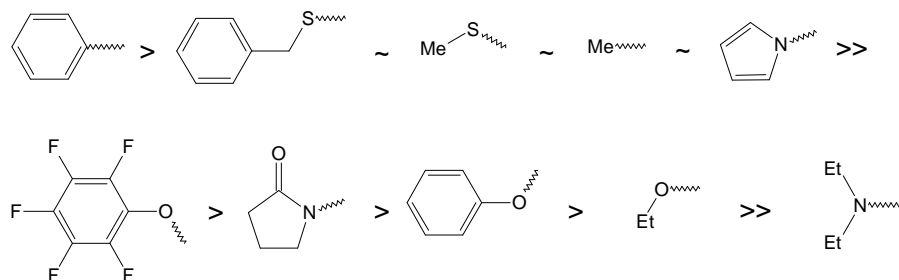
Figure 2.2. Decreasing order of ability of various Z groups to activate the C=S double bond of RAFT agents.

The stability of the radical intermediates (**18** and **22**) has therefore been rationalized to be affected by resonance stabilization as well as electronic effects emanating from the Z group.[14,26,30] Indeed the chain transfer coefficients of the RAFT agents also generally decrease in the following order: dithiobenzoates > trithiocarbonates > dithioalkanoates > xanthates > dithiocarbamates. This general classification also gives control over most monomers.[26] It must also be kept in mind that whilst the Z group stabilizes the intermediate radicals, it must also maintain appropriate fragmentation rates of

the intermediate radical.[29-31] Xanthate and dithiocarbamate RAFT agents, exhibit a low C_{tr} towards monomers stabilized by an electron withdrawing group, e.g. styrene and acrylates. This has been attributed to the interaction of these CTAs' oxygen and nitrogen lone electron pairs, respectively, with the C=S double bond as depicted in the zwitterionic canonical forms below.[2,9,27,32]
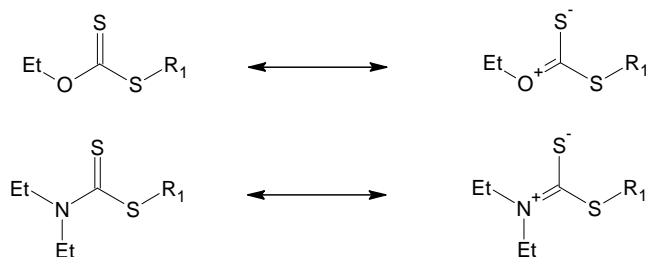
Scheme 2.6. Canonical forms of xanthates and dithiocarbamates.

This lowers the reactivity of the C=S double bond thereby lowering k_{add} (Scheme 2.5) and reducing the extent of uniform polymer chain growth resulting in polymers with high molecular weight distributions being produced.[33] However, if the O or the N atoms, of the xanthates and the dithiocarbamates respectively, are adjacent to electron withdrawing groups, like –CH_2CF_3, their lone electron pairs become less available to interact with the C=S double bond. This then enables good control over molecular weight distribution in the polymerization of the stabilized monomers.[33] Xanthate RAFT agents, however, give good control with poorly stabilized vinyl monomers like VAc[32,34-36] and NVP[35-38] which are fast propagating.

2.4.4.5 The R group

The R group has two main roles:

- It must be a good homolytic leaving group and more so a better one than $P_n{}^\bullet$, in the intermediate radical (**18**) in order for the equilibrium below to favor the production of the reinitiating radicals (**R•**, **20**, Scheme 2.7). These must be produced as fast as possible to ensure that all chains get formed and start growing at the same time.

- The radical **R•** (**20**) must also efficiently reinitiate the polymerization.
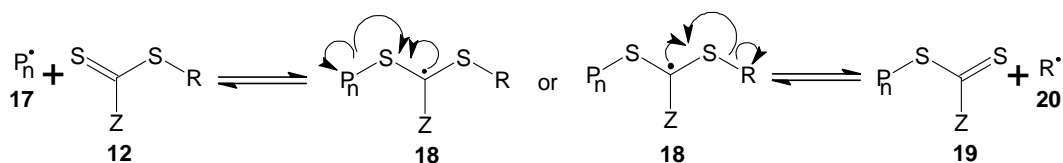
Scheme 2.7. Illustrating the directions the intermediate radical (18) can fragment towards.

Moad *et al.* noted that for R to be a good homolytic leaving group, due attention has to be paid to electronic and steric factors as well as substituents that increase the stability of the reinitiating radical.[39] The following trend for reduction in apparent transfer constants for various RAFT agents in bulk styrene polymerizations at 110°C was established.[27,39]
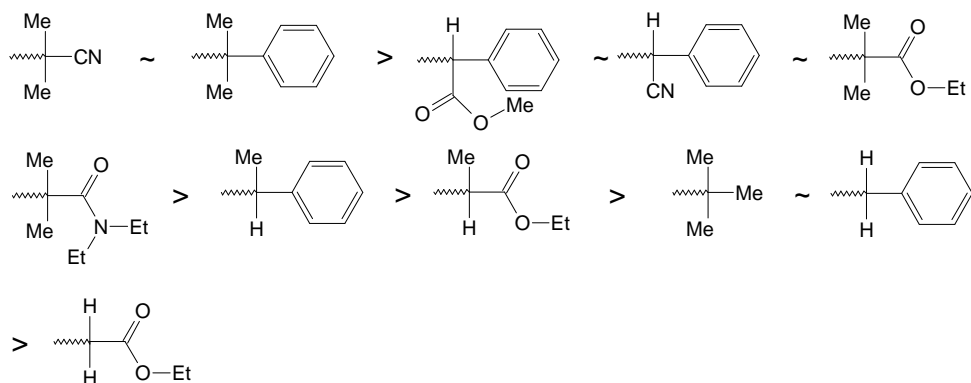
Figure 2.3. General trend for leaving group ability of R group determined in styrene polymerizations.

In concluding this discussion, the wide variety of RAFT agents differing in structural details of the R and Z groups enable one to carefully select RAFT agents typically suited for the particular monomer class. Recent reviews by Moad *et al.*[14] and by Favier and Charreyre[26] highlight the major considerations to be made when choosing RAFT agents for particular monomers. The latter review, in particular, also considers the relevant experimental requirements for a successful RAFT mediated polymerization.

Good correlations between theoretical and experimental molecular weights as well as low polydispersity indexes are all good indicators of a well controlled RAFT mediated polymerization.[9] Livingness is confirmed by the presence/retention of the thiocarbonyl thio moiety at the polymer chains' ω-chain end. Evidence of this presence has been provided by NMR,[16] UV-vis[38,40] ESI MS,[40,41] and MALDI ToF MS.[41,42] Added to confirming the livingness of RAFT made polymers, this evidence also serves to confirm the mechanism of the RAFT process.[9,14] The ability to chain

extend or form block copolymers by simply adding more monomer, and initiator, has also served to confirm livingness.[43-45] This approach, to making block copolymers is illustrated in Scheme 2.8.
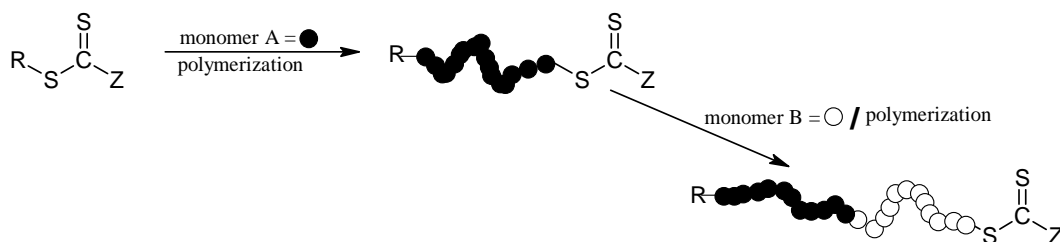
Scheme 2.8. Preparation of block copolymers by the RAFT process.

2.4.4.6 Shortcomings of RAFT mediated polymerization

Retardation is by far the most debated problem with most RAFT mediated systems. It has been attributed to a lot of things. From experimental techniques to issues intrinsic with the RAFT mediated polymerization system itself. Poor deoxygenation, impurities in monomer and/or solvent as well as residual inhibitor in monomer can all retard the rate of a free radical polymerization. Plummer *et al.*[46] showed that impurities in the RAFT agent itself can also retard a RAFT mediated polymerization. Retardation also increases with increasing RAFT agent concentration.[9]

On issues inherent to the system, slow fragmentation[27,28,47,48] and intermediate radical termination,[45,49,50] of the intermediated radicals (**18** and **22** in Scheme 2.5) have been pointed out as causes of retardation. Slow fragmentation is related to increased stability of the intermediate radicals. It has been put forward as the cause of retardation in RAFT mediated polymerizations of acrylates were dithiobenzoates[27,48] where used as the CTAs. The increased stabilization has been attributed to delocalization of the radical with the phenyl group.[51] This gives it the longer lifetime necessary for it to participate in side reactions.

Recently Geelen and Klumperman[49] provided direct evidence of termination reactions involving the intermediate radicals (**18** and **22**) in a (real) RAFT-mediated polymerization. They also showed that the termination products take no further part in the polymerization reaction through out its duration. This has provided evidence of the role of radical termination in retardation experienced in RAFT. On the other hand, it has also been shown that slow re-initiation by the leaving group radical (**20**) Scheme 2.5, manifests itself as an apparent inhibition period, i.e. the initialization period.[48]

Initialization[52] is defined as the process by which the starting RAFT agent is consumed, whilst the initialization period is the time this process takes to complete.

2.4.4.7 Advantages of RAFT mediated polymerization

Compared to all the other LRPs for making polymers, RAFT is the most versatile given that it is adaptable to the widest monomer range. This is especially true for the unstabilised vinyl monomers, mainly vinyl acetate and N-vinylpyrrolidone which are difficult to polymerize with methods like ATRP and NMP. (Meth)acrylic acids can be polymerized easily by RAFT.[53-55] However they can not be polymerized directly by ATRP as they destroy the catalyst by coordinating to it and by protonating nitrogen containing ligands.[2,13] RAFT-mediated polymerizations largely require just the CTA to be added to an otherwise conventional FRP reaction mixture under typical FRP conditions. This makes them attractive in that they require a minimum perturbation to the typical FRP reaction conditions.[15]

2.4.5 Preparation of end functional polymers by RAFT

A feature inherent in the RAFT-mediated polymerization mechanism is the retention of the RAFT agent's R and Z groups, as the α and the ω end groups of the polymer respectively. This enables excellent control over chain end functionalities. Also it immediately offers two direct methods to make end functional polymers:

2.4.5.1 Building the functionality into the R-group (α-end functionalization)

Functional groups can be built into the RAFT agent at the R group termini to provide polymer chains with α-end functional groups in one step. This strategy is very attractive due to the excellent tolerance to functional groups exhibited by the RAFT process. This method has been used to prepare polymers with α-alcohol,[56-59] acid[47,60,61] and amine[57,62] functionalities. RAFT agents bearing charged groups at the R group have also been prepared to mediate aqueous RAFT-mediated polymerizations with good control over molecular weights.[63] Azide functional RAFT agents have also been prepared.[64] They were used to mediate styrene and *N,N*-dimethylacrylamide polymerizations yielding polymers with good control over molecular weight. These α-azido end functional polymers were later converted into α-alcohol, acrylate and methacrylate functional polymers by "clicking" the appropriate alkynes.

2.4.5.2 Building the functionality into the Z-group (ω-end functionalization)

The retention of the thiocarbonyl thio moiety (Z-group) in the final polymer entails that functionality can be built into the Z-group to give ω-end functional polymers. However this approach suffers from a number of significant problems.

- Thiocarbonyl thio compounds are usually colored (and odorous) and the color is retained in the polymer products produced by the RAFT process. This may be undesirable depending on application.

- The C–S bond is relatively labile; the Z-group bearing chain end can therefore decompose releasing odorous and possibly toxic compounds which can contaminate the polymer.

- Thiocarbonyl thio compounds are hydrolytically unstable in basic aqueous media.[65] They are also unstable in the presence of primary and secondary amines.[62]

2.4.5.3 Methods for thiocarbonyl thio end group removal

The problems encountered due to the presence of the thiocarbonyl thio end groups have given impetus to the need to develop efficient (post polymerization) methods to selectively remove and/or replace them with more stable end groups. Scheme 2.9 below gives an overview of the methods that have been used to treat polymers prepared by the RAFT process and the end groups that are produced. These methods, of end group modification, take advantage of the facile reactions that thiocarbonyl thio compounds undergo with radicals,[66] nucleophiles[67] and ionic reducing agents.[68]

Their nucleophilic susceptibility has been utilized by aminolysing the thiocarbonyl thio end groups into thiol end groups.[59,69,70] Thiocarbonyl thio groups can also be reduced to thiols by borohydrides.[57,71] A frequent problem with this technique, however, is that the thiol terminated polymers tend to couple to give polymeric disulfides of twice the original molecular weight. This can be suppressed by using reducing agents like sodium bisulfite[59] and tris(2-carboxyethyl)phosphine.[72]

Complete desulphurization can be effected by radical-induced reduction using tributylstannane.[62] More recently Chong *et al.*[73] used N-ethylpiperidine hypophosphite, a hypophosphite salt to completely desulfurize the Z-end group replacing it with hydrogen. This method was recommended over using tributyl stannane due to the ease with which the hypophosphite's byproducts can be

removed compared to stannane derived byproducts which are also toxic. Destarac and coworkers[74] used a peroxide initiator/secondary alcohol couple to replace the Z group with H.
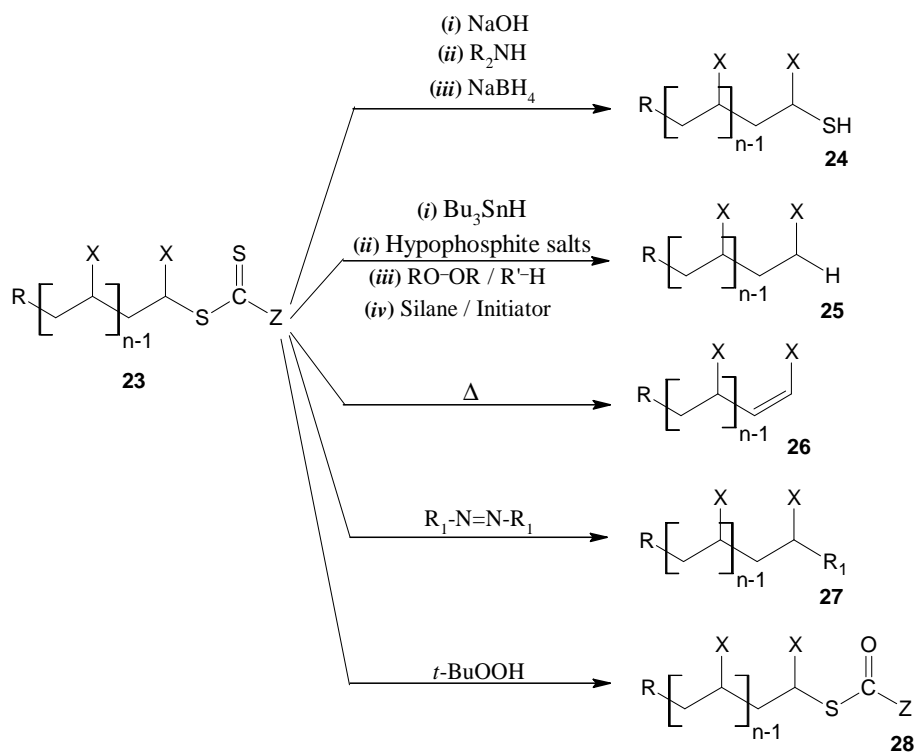
Scheme 2.9. End group modification methods reported in literature.

Perrier *et al.*[75] reported the removal of the Z group by applying a huge excess of radicals, generated *in situ* by conventional azo initiators, to the polymer sample, Scheme 2.2. They claimed a total desulphurization of the polymer chains' ω-chain end. Of significance with this method is the fact that when **R** equals **R₁** (Scheme 1.2) and both bear a functional group, then a telechelic functional polymer is produced. This method also serves to regenerate the RAFT agent. These authors did not, however, provide evidence of complete structural resolution of the modified chain ends. They only gave ^{1}H-NMR evidence showing the disappearance of the peaks characteristics thiocarbonyl thio moiety. Postma and coworkers[62] found this method to give incomplete (95%) end group removal for polystyrene with butyl trithiocarbonate end groups under the same conditions as recommended by Perrier. They rationalized the effectiveness of the method to depend on the leaving group ability of the polymeric radical (**32**) Scheme 2.2.
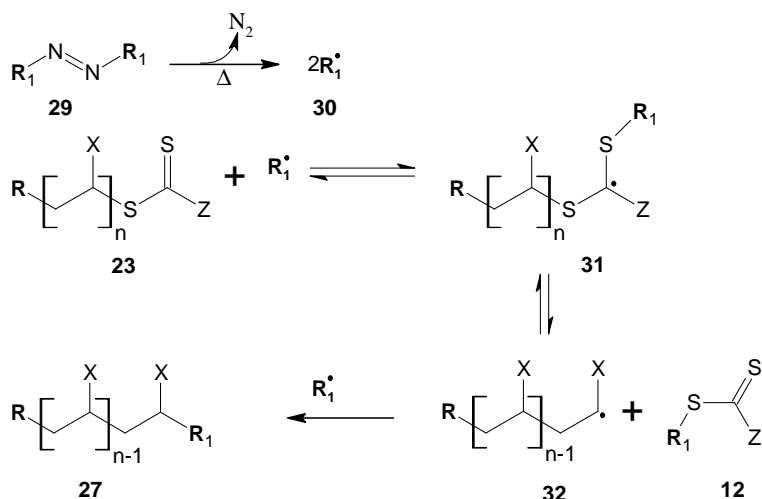
Scheme 2.21. Perrier's end group modification strategy.

Thermal elimination has also been used to cleave off the thiocarbonyl thio end groups. Trithiocarbonates chain ends were cleanly removed from polystyrene.[62,76] For poly (butyl acrylate) the major product consisted of chain ends produced by disproportionation.[76] UV irradiation was also shown to be a useful method for thiocarbonyl thio end group removal.[45]

In Chapters 4 and 5 of this work, two methods of end modifying the thiocarbonyl thio chain ends of polymers made by the RAFT process will be reported. The first (in Chapter 4) is based on ATRA. Here a flood of radicals, generated *in situ* from an appropriate alkyl halide, in a transition metal catalyzed process, removes the thiocarbonyl thio moiety and "caps" the polymer's ω-chain end. With appropriate selection of a functional RAFT agent and a functional alkyl halide a telechelic functional polymer is produced. In the second process, in Chapter 5, it is shown that the thiocarbonyl thio end group can also be removed by merely heating the polymer with a huge excess of hydrogen peroxide and simultaneously capping the chain end with an OH group from the hydrogen peroxide. Both methods are an extension to the work of Perrier *et al.*[75] as they rely on applying a flood of radicals to the polymer solution as a way of removing the thiocarbonyl thio end group.

2.5 End group analysis of polymers

The determination of end groups is very important in order to fully understand the polymer's chemical structure as well as to relate properties to polymer structure. Traditionally polymers are

analyzed by SEC to obtain information on the average molar mass as well as the molecular weight distributions. However, a typical SEC trace is usually a broad envelope and it does not show any information on the macromolecular structure of the individual polymer chains. End group analysis requires prior knowledge of what the likely end group structures are going to be. Methods that have been used to analyze end groups include UV,[69,72,77] NMR,[70,78-80] HPLC[59,81] as well as mass spectrometry.[30,41,59,82,83] Other methods include IR and classical titration methods for polymers terminated with *e.g.* carboxylic acid groups.[9]

2.5.1 Analysis by UV, IR and NMR

End group analysis with UV and IR is most effective when the end group chromophores do not absorb near those of the backbone to enable their distinction from possible interfering signals from initiator derived by products. With NMR as well, end group resolution can be difficult if the end group signals appear too close to the much larger signals of the polymer backbone. These problems can, however, be circumvented by chemically derivatizing the end groups so that they can be measured easily and more clearly. A particular example is in the case of hydroxyl, amino, or carboxyl end terminated polymers. Derivatization with TAI, which undergoes a quick and facile reaction with these functional groups, gives carbamate derivatives with an imidic hydrogen. The imidic hydrogen signal has chemical shifts that appear well clear of the backbone signals (8–11 ppm).[84] The α-methylene protons of the carbamate derivative also give a distinctive signal with a chemical shift between 4.0–5.0 ppm.[84] This enables end functionalities to be calculated easily.[79,80,84] This is illustrated in Chapters 4 and 5 where this method is used to estimate the extent of chain end functionalization. UV, IR and NMR spectroscopy, however, also have the problem that they provide an average image of the polymer sample. They are limited to polymers with a low degree of polymerization and they do not give information on the functionality type distribution.

2.5.2 Liquid chromatographic methods

Information on functionality type distribution can be obtained by HPLC methods, mainly LCCC[85] and GPEC.[85] With LCCC, retention is independent of molecular weight and is on the basis of (end group) functionality.[85] Quantitative results can also be obtained by this process with the latter.[59] GPEC, on the other hand, separates polymer chains on the basis of their partition coefficient between the column and the mobile phase.[85] Gao *et al.*[81] used a two dimensional combination of

GPEC and SEC to obtain information on chain end functionality distribution as well as on and molecular weight distribution of α, ω-dihydroxylpolystyrene prepared by a combination of ATRP and click chemistry.

2.5.3 Mass spectrometry

Traditionally mass spectroscopy was applicable to low molecular weight organic and inorganic compounds given that they have to be converted into (intact) gas phase ions. However, the recent development of ingenious ionization techniques like MALDI[82,86] has extended the mass range that can be analyzed by this technique. Mass spectroscopy has since become a very popular tool for structural analysis of synthetic polymers. High resolution mass spectra can be obtained with MALDI coupled to a time of flight detector (MALDI ToF) with the concomitant use of other special technical features like delayed extraction.[82] Peaks in a MALDI ToF spectrum are generated from (intact) individual polymer chains, thereby enabling structural identification of the polymer. The mass of the end groups is obtained by subtracting the mass of the cationizing agent and that of the appropriate number of repeat units as inferred from the mass to charge ratio (*m/z*) of the intact oligomer ion peak in the spectrum.[82] With additional information from the synthetic procedure used and from other spectroscopic techniques like NMR, the end group structure can then be elucidated. This is illustrated in Chapters 3, 4 and 5 where MALDI ToF MS and NMR are used to generate information on the structure of the end groups capping the RAFT made PVP chains. MALDI can also be coupled (off-line) to liquid chromatographic techniques like LCCC to map the structural heterogeneity of synthetic polymers.[41,59]

2.6 Poly (N-vinylpyrrolidone)

Poly (N-vinylpyrrolidone) (Figure 2.4) is the polymer formed from N-vinylpyrrolidone.

33
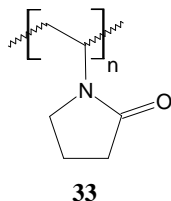
Figure 2.4. Poly(N-vinylpyrrolidone).

PVP is an important polymer with a whole range of uses. It finds use in numerous cosmetic formulations as a binder, hair fixative and suspending agent.[87,88] Products with PVP range from shampoos, eyeliners, several hair grooming aids, lipstick, shaving preparation products and several skin care products.[87] It is used as a clarifying agent in beverages and vinegar, and as a stabilizer in mineral concentrates.[88] PVP has also been used as a suspension stabilizer in oil in water suspension polymerization systems.[89] Its other numerous uses have been reviewed.[88]

2.6.1 Biomedical applications

PVP is one of the most promising biocompatible polymers owing to its amphiphilic nature and bio-inertness which makes it very biocompatible. Medically, PVP was first used as a blood plasma extender during World War II. Its intravenous application was, however, stopped after it was found that it did not break down easily in the body, but settled in the RES were it caused storage problems hence all its bio-applications of high molecular weight PVP are now restricted to systems were its introduced orally or when it is used topically.[90,91] It is widely used in the pharmaceutical industry as a tablet binder and in the formulation of antiseptics. Its complex with Iodine, marketed as Betadine is an important topical disinfectant.[88]

2.6.2 Polymer drug conjugates

PVP is also finding increased usage in formulations of polymer-drug conjugates. Covalent conjugation of PVP to bioactive compounds and small molecular weight organic compounds (PVPlation) has been shown to improve their aqueous solubility, reduce their toxicity and reduce their uptake by the RES without impairing the therapeutic effect of these polymer-drug conjugates.[92-95] PVPlation of bioactive compounds and small molecular weight organic compounds results in an increase in the molecular weight of these pharmaceutical agents. This reduces their renal clearance, subsequently increasing their plasma circulation half-lives. Generally these biomolecules are unstable, but their conjugation with polymers increases their stability *in vivo*. It has been postulated that the polymer conjugates sterically hinder reactions with immune cells. This then protects the biomolecules from proteolytic attack resulting in an increase in their bioavailability.[95,96] Therefore smaller doses are required without diminishing the pharmacokinetic effects of the drugs.

Compared to PEG, one of the most successful biopolymers, PVP has been shown to be a better polymeric modifier. PVP-biomolecule conjugates had significantly better therapeutic effectiveness than PEG-biomolecule conjugates of the same molecular weight. They were retained longer in the blood.[97] Also being a vinyl monomer, it (NVP) can be copolymerized with other vinyl monomers bearing functional groups to make PVP-copolymers with pendant functionalities. These side chain functionalities then act as loci for attachment of bioactive compounds resulting in an increased drug loading capacity. For example, the copolymer of NVP and a derivative of 5-Fluorouracil (allyloxycarbonyloxymethyl-5-fluorouracil) was prepared and used as a polymer-drug conjugate for the slow release of 5-Fluorouracil, a popular antimetabolite.[98] In some cases the copolymer systems include NVP copolymerized with its own derivatives. Ferruti and coworkers[99,100] prepared 1-vinylpyrrolidin-2-one derivatives carboxylated at the 3-position of the lactam ring, determined their reactivity ratios[99] and copolymerized them with NVP. The subsequent PVP copolymer, pendant carboxylic acid functional groups, was then used, in a series of reactions to attach glutathione as a model biomolecule.[100] By varying the number of pendant functionalities, the drug loading capacity of this system was also varied.

2.6.3 End functional PVP systems

PVPlation (described above) makes use of end functional PVP oligomers which, with application of organic synthetic chemistry, get covalently linked to bioactive compounds. This requires that the PVP has well defined end group functionalities which will be the loci for the attachment of the biomolecules. Up to now these are almost exclusively prepared by conventional FRP methods in the presence of functionalized CTAs[101] or in functionalized chain-transfer active solvents such as isopropoxyethanol.[90,102] However, as with each conventional FRP process, the products have large polydispersities and chain end functionalization is not quantitative.[102] The inconvenience of this is illustrated by the fact that when it is intended for PVPlation, it has to be fractionated in order to adjust molecular size and obtain polymers with narrow molecular weight distribution before being conjugated to the bioactive molecules.[92,103]

A survey of published literature, to date, revealed that there is no report on synthesis of end-functionalized PVP oligomers by any of the recently devised LRP techniques. In this work, it will be shown that α-hydroxyl functional PVP can be prepared easily by RAFT mediated polymerization

using an alcohol functional xanthate RAFT agent (Chapter 3). End group conversion is quantitative and good control over molecular weight distribution is also achieved.

2.6.4 In biomimetic hydrogels

Hydrogels are three-dimensional hydrophilic crosslinked polymer networks that do not dissolve but swell in water.[104] They are capable of imbibing enormous volumes of water, many times greater than their weight.

Owing to its hydrophilic nature and remarkable biocompatibility, PVP based hydrogels have numerous uses in the biomedical field where they are used as vitreous substitutes,[105] wound dressings,[106] as drug delivery vehicles[107] and for making soft contact lenses.[108] Industrially PVP based gel systems have found use as thickeners, flocculants, adsorbents[108] and in the removal and separation of metal ions from industrial waste water contaminated with heavy metal ions.[109] It is easy therefore, to understand the attraction for research groups to making PVP based gels with better characterized properties as these can readily find a niche in the biomedical and industrial fields. In this work the hydroxyl telechelic functional PVP prepared will be chemically crosslinked, by reacting with a tri-arm isocyanate crosslinker to give a hydrogel. This technique, however, will only be used as a way to illustrate that the material is indeed telechelic functional.

2.6.5 Polymerization of NVP

In light of the discussions above, highlighting the uses of PVP, the polymerization of NVP by the free radical mechanism will now be discussed. NVP can be polymerized by both ionic and free radical mechanisms, but the former method is considered to be of no practical value as it only gives rise to oligomers.[88] PVP is therefore almost exclusively prepared by a free radical mechanism in organic or in aqueous media using azo compounds and hydrogen peroxide as initiators respectively.[88] It can also be polymerized in bulk, with initiation by azo compounds.[88] The shortcomings of conventional FRP as a route for accessing end functional PVP have already been described (see Section 2.6.2). This leaves LRP processes as the reactions best suited to produce PVP with control over both molecular weight and end groups.

2.6.6 LRP of NVP

There have not been that many reports in the literature as yet on the LRP of PVP. The vinyl group of the monomer is not stabilized by resonance. As a result its propagating radicals are very reactive and have a huge propensity to participate in side reactions, like disproportionation and chain transfer, making it difficult to "tame".

2.6.6.1 NMP

Attempts to control its polymerization by NMP were not very successful as the polymers produced had high polydispersities (1.8–2.2).[110]

2.6.6.2 ATRP

NVP, up to now, has largely remained beyond the reigns of metal catalyzed living radical polymerization. The first report on the ATRP of NVP was made by Matyjaszewski and coworkers[111] under copper catalyzed conditions. These workers claimed to have made PVP with M_n of 2000 with very good control (PDI = 1.15). They did not, however, give conditions for this process. In a very recent communication, Lu *et al.*[112] reported the copper catalyzed ATRP of NVP. They used a cyclic ligand, 5,5,7,12,12,14-hexamethyl-1,4,8,11-tetra-azacyclo-tetradecane (Me$_6$Cyclam), and CuCl and CuCl$_2$ as catalysts in 1,4-dioxane and isopropanol as solvents at room temperature to produce PVP with good control over M_n (PDI ~1.2–1.38). This is the first work in the open literature to detail a successful ATRP of NVP. The general outlook, however, for ATRP of NVP is that catalysts with very fast activation (and therefore very high activity) have to be developed in order to fully realize the efficient ATRP of NVP.

2.6.6.3 Organostibine mediated LRP

Ray *et al.*[113] recently showed that the organostibines **34**, **35** and **36**, promote the living radical polymerization of NVP.
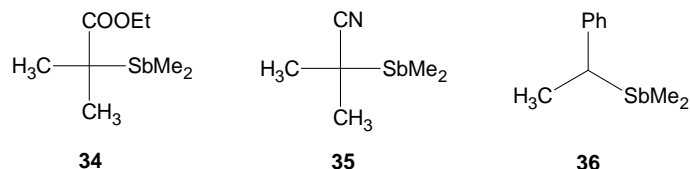
Figure 2.5. Organostibines used to mediate the LRP of NVP.

PVP with excellent control over molecular weights and low polydispersities (1.07–1.29) was produced. Molecular weights of up to 80 000 were attained. A slight decrease in control with increasing conversion was attributed to the occurrence of head to head addition reactions. These produced an organostibine PVP derivative that was incapable of regenerating propagating radicals and behaved essentially as dead polymer. Good control (PDI < 1.4) was still attained despite this. The livingness of this system was also confirmed by the preparation of several diblock copolymers.

2.6.6.4 TERP

Very recently Yusa[114] and coworkers have shown that the polymerization of NVP can be mediated by organo-telluride transfer agents to give PVP with excellent control over M_n and low PDI. They compared results for PVP made by TERP and RAFT mediated polymerizations and found both systems to yield PVP with well defined characteristics. In their work they found the TERP mediated product to give polymer with molecular weight distributions ranging between 1.0–1.1 whilst for the RAFT process it ranged from 1.1–1.2 implying better control was attainable with the TERP process than with RAFT.

2.6.6.5 RAFT

To date RAFT mediated polymerizations are the most studied system for the controlled living radical polymerization of NVP although it must still be mentioned that not much has been published on this. Dithiobenzoates, trithiocarbonates, dithiocarbamates and xanthates have all been employed as CTAs for its RAFT mediated polymerization. Dithiobenzoates have been shown to retard the polymerization of NVP[115] as well as give poor control over molecular weight distributions, giving polymers with polydispersities of 1.6–1.9. The thiocarbonyl thio moiety is, however, retained in the final polymer.[110] Molecular weight distributions have also been found to be broad with trithiocarbonates with polydispersities ranging from 1.5–2.3.[110] The polymerization of NVP with the dithiocarbamate **39** was reported by Devasia *et al.*[37] Their best control over molecular weight

distribution was obtained with molar ratios of monomer/RAFT agent = 100 and RAFT agent to AIBN ratio was 8 at 80 °C in dioxane to give polymer with PDI of 1.3. Moad[14] and coworkers described the RAFT mediated polymerization of NVP, in methanol at 60 °C, with xanthate **47** to give PVP of M_n = 17000 with a PDI index of 1.35. Wan *et al.*[115] reported that the RAFT mediated polymerization of NVP with xanthates **46a** and **b** proceeded with simultaneous control of molecular weight and tacticity when the polymerization was carried out in fluoroalcohol solvents. They found that the syndiotacticity increased with increasing the ratio of fluoroalcohol solvent to monomer (NVP) as well as by reducing reaction temperature. Xanthates **46a** and **b** however showed inhibition periods of 1 and 6 hours respectively. This was attributed to the fact that the benzylic radicals have poor leaving group ability with NVP.
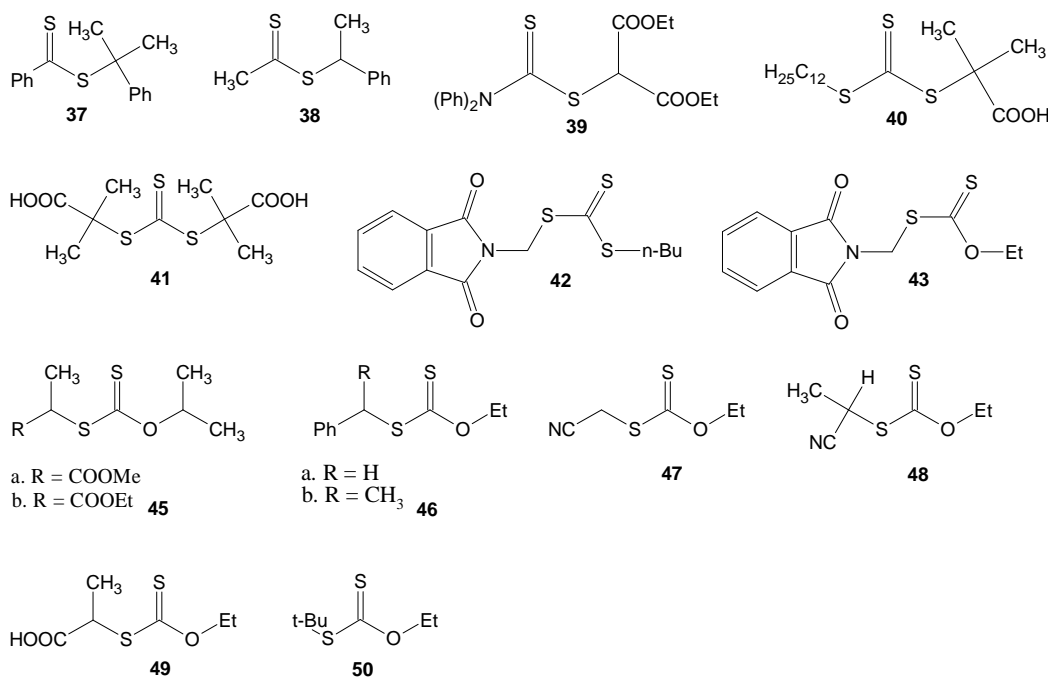
Figure 2.6. RAFT CTAs used to mediate the LRP of NVP.

Postma *et al.*[38] also reported the RAFT-mediated polymerization of NVP with the phthalimidomethyl trithiocarbonate **42** and the S-phthalimidomethyl xanthate **43**. The trithiocarbonate CTA **42** inhibited the polymerization initially before the polymerization commenced. The inhibition was attributed to the relative stability of the RAFT intermediate. The subsequently made polymers were also characterized by high M_w/M_n values (1.48–1.61). However, xanthate RAFT agent **43** gave no discernible inhibition period and the polymerization proceeded with good control over molecular weight distribution. PDI values of between 1.16–1.27 were

obtained for low molecular weight targets (< 10000g/mol). Recently Pound *et al.*[35] have shown that unstabilised monomers (VAc and NVP) also exhibit selective initialization. The RAFT mediated polymerizations of VAc and NVP with the xanthate CTAs (**48**, **49** and **50**) were probed with *in-situ* ^{1}H-NMR spectroscopy. For the polymerization of NVP with xanthate CTA **48** the xanthate was consumed in the first 275 minutes to give the single monomer adduct. No significant polymerization was observed within this period and the first monomer addition proceeded with high selectivity. The initialization behavior of the various xanthate CTAs employed in this study were found to be determined by the nature of the R group. Xanthate CTAs with a *tert*-butyl R group exhibited poor initialization behavior for these monomers. This was attributed to the fact that the monomer derived radicals had better leaving group ability compared to the R group radical, thereby causing hybrid behavior.[35] These studies also served to show that in-situ ^{1}H-NMR is a useful tool to screen the efficacy of RAFT agent CTAs. This being done by correlating initialization behavior to the leaving and reinitiating behavior of the R groups of the CTAs and subsequently to the M_w/M_n ratios.[35,36] In this work, the RAFT-mediated polymerization of NVP, by an alcohol functional xanthate RAFT agent will be described in Chapter 3.

References

(1)   A. Hirao and M. Hayashi, *Acta Polym.*, 1999. **50**: p.219-231.

(2)   K. Matyjaszewski and T. P. Davis, *Handbook of Radical Polymerization*. 2002, John Wiley & Sons: Hoboken, NJ.

(3)   A. V. Tobolsky, *J. Am. Chem. Soc.*, 1960. **82**: p.1277-1280.

(4)   A. V. Tobolsky, *J. Am. Chem. Soc.*, 1958. **80**: p.5927-5929.

(5)   G. David, J.-J. Robin and B. Boutevin, *J. Polym. Sci., Part A: Polym. Chem.*, 2001. **39**: p.2740-2750.

(6)   G. David, B. Boutevin, J.-J. Robin, C. Loubat and N. Zydowicz, *Polym. Int.*, 2002. **51**: p.800-807.

(7)   G. F. Meijs, T. C. Morton, E. Rizzardo and S. H. Thang, *Macromolecules*, 1991. **24**: p.3689-3695.

(8)   I. Cho and J. Kim, *Polymer*, 1999. **40**: p.1577-1580.

(9)   G. Moad and D. H. Solomon, *The Chemistry of Radical Polymerization*. Second ed. 2006, Elsevier: Amsterdam.

(10)   W. A. Braunecker and K. Matyjaszewski, *Prog. Polym. Sci.*, 2007. **32**: p.93-146.

(11)   C. J. Hawker, A. W. Bosman and E. Harth, *Chem. Rev.*, 2001. **101**: p.3661-3688.

(12)   M. Kamigaito, T. Ando and M. Sawamoto, *Chem. Rev.*, 2001. **101**: p.3689-3745.

(13)   K. Matyjaszewski and J. Xia, *Chem. Rev.*, 2001. **101**: p.2921-2990.

(14)   G. Moad, E. Rizzardo and S. H. Thang, *Aust. J. Chem.*, 2005. **58**: p.379-410.

(15)   S. Perrier and P. Takolpuckdee, *J. Polym. Sci., Part A: Polym. Chem.*, 2005. **43**: p.5347-5393.

(16)   J. Chiefari, Y. K. B. Chong, F. Ercole, J. Krstina, J. Jeffery, T. P. T. Le, R. T. A. Mayadunne, G. F. Meijs, C. L. Moad, G. Moad, E. Rizzardo and S. H. Thang, *Macromolecules*, 1998. **31**: p.5559-5562.

(17)   R. P. Quirk and B. Lee, *Polym. Int.*, 1992. **27**: p.359-367.

(18)   D. H. Solomon, E. Rizzardo and P. Cacioli, *Eur. Pat. Appl.*, 1985: p.66.

(19)   M. K. Georges, R. P. N. Veregin, P. M. Kazmaier and G. K. Hamer, *Macromolecules*, 1993. **26**: p.2987-2988.

(20)   T. Pintauer and K. Matyjaszewski, *Coord. Chem. Rev.*, 2005. **249**: p.1155-1184.

(21)   T. E. Patten and K. Matyjaszewski, *Acc. Chem. Res.*, 1999. **32**: p.895-903.

(22)   W. Tang and K. Matyjaszewski, *Macromolecules*, 2006. **39**: p.4953-4959.

(23)   W. Tang and K. Matyjaszewski, *Macromolecules*, 2007. **40**: p.1858-1863.

(24)   J. Chiefari, R. T. A. Mayadunne, C. L. Moad, G. Moad, E. Rizzardo, A. Postma, M. A. Skidmore and S. H. Thang, *Macromolecules*, 2003. **36**: p.2273-2283.

(25)   J. F. Quinn, L. Barner, C. Barner-Kowollik, E. Rizzardo and T. P. Davis, *Macromolecules*, 2002. **35**: p.7620-7627.

(26)   A. Favier and M. T. Charreyre, *Macromol. Rapid Commun.*, 2006. **27**: p.653-692.

(27)   G. Moad, J. Chiefari, B. Y. Chong, J. Krstina, R. T. A. Mayadunne, A. Postma, E. Rizzardo and S. H. Thang, *Polym. Int.*, 2000. **49**: p.993-1001.

(28)   J. F. Quinn, E. Rizzardo and T. P. Davis, *Chem. Commun.*, 2001. p.1044-1045.

(29)   C. Barner-Kowollik, J. F. Quinn, T. L. Nguyen, J. P. A. Heuts and T. P. Davis, *Macromolecules*, 2001. **34**: p.7849-7857.

(30)   C. Schilli, M. G. Lanzendorfer and A. H. E. Muller, *Macromolecules*, 2002. **35**: p.6819-6827.

(31)   A. Favier, M. T. Charreyre, P. Chaumont and C. Pichot, *Macromolecules*, 2002. **35**: p.8271-8280.

(32)   M. H. Stenzel, L. Cummins, G. E. Roberts, T. P. Davis, P. Vana and C. Barner-Kowollik, *Macromol. Chem. Phys.*, 2003. **204**: p.1160-1168.

(33)   M. Destarac, W. Bzducha, D. Taton, I. Gauthier-Gillaizeau and S. Z. Zard, *Macromol. Rapid Commun.*, 2002. **23**: p.1049-1054.

(34)   J. Bernard, A. Favier, T. P. Davis, Christopher Barner-Kowollik and M. H. Stenzel, *Polymer*, 2006. **47**: p.1073-1080.

(35)   G. Pound, J. B. McLeary, J. M. McKenzie, R. F. M. Lange and B. Klumperman, *Macromolecules*, 2006. **39**: p.7796-7797.

(36)   B. Klumperman, J. B. McLeary, E. T. A. v. d. Dungen and G. Pound, *Macromol. Symp.*, 2007. **248**: p.141-149.

(37)   R. Devasia, R. L. Bindu, R. Borsali, N. Mougin and Y. Gnanou, *Macromol. Symp.*, 2005. **229**: p.8-17.

(38)   A. Postma, T. P. Davis, G. Li, G. Moad and M. S. O'Shea, *Macromolecules*, 2006. **39**: p.5307-5318.

(39)   B. Y. K. Chong, J. Krstina, T. P. T. Le, G. Moad, A. Postma, E. Rizzardo and S. H. Thang, *Macromolecules*, 2003. **36**: p.2256-2272.

(40)   A. A. Toy, P. Vana, T. P. Davis and C. Barner-Kowollik, *Macromolecules*, 2004. **37**: p.744-751.

(41)   X. Jiang, P. J. Schoenmakers, J. L. J. v. Dongen, X. Lou, V. Lima and J. Brokken-Zijp, *Anal. Chem.*, 2003. **75**: p.5517-5524.

(42)   A. Favier, C. Ladavie, M. T. Charreyre and C. Pichot, *Macromolecules*, 2004. **37**: p.2026-2034.

(43)   R. T. A. Mayadunne, E. Rizzardo, J. Chiefari, J. Krstina, Graeme Moad, A. Postma and S. H. Thang, *Macromolecules*, 2000. **33**: p.243-245.

(44)   B. Y. K. Chong, T. P. T. Le, G. Moad, E. Rizzardo and S. H. Thang, *Macromolecules*, 1999. **32**: p.2071-2074.

(45)   H. d. Brouwer, M. A. J. Schellekens, B. Klumperman, M. Monteiro and A. L. German, *J. Polym. Sci., Part A: Polym. Chem.*, 2000. **38**: p.3596-3603.

(46)   R. Plummer, Y.-K. Goh, A. K. Whittaker and M. J. Monteiro, *Macromolecules*, 2005. **38**: p.5352-5355.

(47)   S. Perrier, C. Barner-Kowollik, J. F. Quinn, P. Vana and T. P. Davis, *Macromolecules*, 2002. **35**: p.8300.

(48)   J. B. McLeary, J. M. McKenzie, M. P. Tonge, R. D. Sanderson and B. Klumperman, *Chem. Commun.*, 2004: p.1950.

(49)   P. Geelen and a. B. Klumperman, *Macromolecules*, 2007. **40***(11)*: p.3914-3920.

(50)   R. Venkatesh, B. B. P. Staal, B. Klumperman and M. J. Monteiro, *Macromolecules*, 2004. **37**: p.7906-7917.

(51)   C. Barner-Kowollik, M. Buback, B. Charleux, M. L. Coote, M. Drache, T. Fukuda, A. Goto, B. Klumperman, A. B. Lowe, J. B. McLeary, G. Moad, M. J. Monteiro, R. D. Sanderson, M. P. Tonge and P. Vana, *J. Polym. Sci., Part A: Polym. Chem.*, 2006. **44**: p.5809-5831.

(52)   J. B. McLeary, F. M. Calitz, J. M. McKenzie, M. P. Tonge, R. D. Sanderson and B. Klumperman, *Macromolecules*, 2004. **37**: p.2383-2394.

(53)   B. T. T. Pham, D. Nguyen, C. J. Ferguson, B. S. Hawkett, A. K. Serelis and C. H. Such, *Macromolecules*, 2003. **36**: p.8907-8909.

(54)   D. Taton, A. Z. Wilczewska and M. Destarac, *Macromol. Rapid Commun.*, 2001. **22**: p.1497.

(55)   C. Ladaviere, N. Dorr and J. P. Claverie, *Macromolecules*, 2001. **34**: p.5370.

(56)   Y. K. Chong, F. Ercole, G. Moad, E. Rizzardo, S. H. Thang and A. G. Anderson, *Macromolecules*, 1999. **32** p.6895.

(57) G. Moad, Y. K. Chong, A. Postma, E. Rizzardo and S. H. Thang, *Polymer*, 2005. **46**: p.8458-8468.

(58) J. T. Lai and R. Shea, *J. Polym. Sci., Part A: Polym. Chem.*, 2006. **44**: p.4298-4316.

(59) V. Lima, X. Jiang, J. Brokken-Zijp, P. J. Schoenmakers, B. Klumperman and R. V. d. Linde, *J. Polym. Sci., Part A: Polym. Chem.*, 2005. **43**: p.959-973.

(60) J. T. Lai, D. Filla and R. Shea, *Macromolecules*, 2002. **35**: p.6754-6756.

(61) M. L. Coote and L. Radom, *Macromolecules*, 2004. **37**: p.590.

(62) A. Postma, T. P. Davis, R. A. Evans, G. Li, G. Moad and M. S. O'Shea, *Macromolecules*, 2006. **39**: p.5293-5306.

(63) C. L. McCormick and A. B. Lowe, *Acc. Chem. Res.*, 2004. **37**: p.312-325.

(64) S. R. Gondi, A. P. Vogt and B. S. Sumerlin, *Macromolecules*, 2007. **40**: p.474-481.

(65) D. B. Thomas, A. J. Convertine, R. D. Hester, A. B. Lowe and C. L. McCormick, *Macromolecules*, 2004. **37**: p.1735-1741.

(66) S. Z. Zard, *Angew. Chem., Int. Ed. Engl.*, 1997. **36**: p.612-685.

(67) E. A. Castro, *Chem. Rev.*, 1999. **999**: p.3505-3524.

(68) J. Boivin, R. Jrad, S. Juge and V. T. Nguyen, *Org. Lett.*, 2003. **5**: p.1645-1648.

(69) X.-P. Qiu and F. M. Winnik, *Macromol. Rapid Commun.*, 2006. **27**: p.1648-1653.

(70) J. Xu, J. He, D. Fan, X. Wang and Y. Yang, *Macromolecules*, 2006. **39**: p.8616-8624.

(71) B. S. Sumerlin, A. B. Lowe, P. A. Stroud, P. Zhang, M. W. Urban and C. L. McCormick, *Langmuir*, 2003. **19**: p.5559-5562.

(72) C. W. Scales, A. J. Convertine and C. L. McCormick, *Biomacromolecules*, 2006. **7**: p.1389-1392.

(73) Y. K. Chong, G. Moad, E. Rizzardo and S. Thang, *Macromolecules*, 2007. **40**: p.9262-9271.

(74) M. Destarac, C. Kalai, L. Petit, A. Z. Wilczewska, G. Mignani and S. Z. Zard, *Polym. Prepr. (Am. Chem. Soc., Div. Polym. Chem.)*, 2005. **46(2)**: p.372-373.

(75) S. Perrier, P. Takolpuckdee and C. A. Mars, *Macromolecules*, 2005. **38**: p.2033-2036.

(76) A. Postma, T. P. Davis, G. Moad and M. S. O'Shea, *Macromolecules*, 2005. **38**: p.5371-5374.

(77) Y.-Z. You, D. S. Manickam, Q.-H. Zhou and D. Oupicky, *Biomacromolecules*, 2007. **8**: p.2038-2044.

(78) M.-F. Llauro, J. Loiseau, F. Boison, F. Delolme, C. Ladaviere and J. Claverie, *J. Polym. Sci., Part A: Polym. Chem.*, 2004. **42**: p.5439-5462.

(79)   A. R. Donovan and G. Moad, *Polymer*, 2005. **46**: p.5005-5011.

(80)   A. Postma, T. P. Davis, A. R. Donovan, G. Li, G. Moad, R. Mulder and M. S. O'Shea, *Polymer*, 2006. **47**: p.1899-1911.

(81)   H. Gao, G. Louche, B. S. Summerlin, N. Jahed, P. Golas and K. Matyjaszewski, *Macromolecules*, 2005. **38**: p.8979-8982.

(82)   G. Montaudo, F. Samperi and M. S. Montaudo, *Prog. Polym. Sci.*, 2006. **31**: p.277-357.

(83)   S. D. Hanton, *Chem. Rev.*, 2001. **101**: p.527-569.

(84)   J. C. Ronda, A. Sierra, A. Mantecon and V. Cadiz, *Macromol. Chem. Phys.*, 1994. **195**: p.3445-3457.

(85)   H. J. A. Philipsen, *J. Chromatogr., A*, 2004. **1037**: p.329-350.

(86)   H. Pasch and W. Schrepp, *MALDI-ToF Mass Spectrometry of Synthetic Polymers*. 2003, Springer: Berlin.

(87)   N. Bindu, *International Journal of Toxicology*, 1998. **17**: p.95-130.

(88)   F. Haaf, A. Sanner and F. Straub, *Polym. J.* , 1985. **17**: p.143-152.

(89)   T. L. U. Nguyen, K. Eagles, T. P. Davis, C. Barner-Kowollik and M. H. Stenzel, *J. Polym. Sci., Part A: Polym. Chem.*, 2006. **44**: p.4372-4383.

(90)   E. Ranucci, L. Macchi, R. Annunziata, P. Ferruti and F. Chiellini, *Macromol. Biosci.*, 2004. **4**: p.706-713.

(91)   S. Trimpina, P. Eichhorn, H. J. Radera, K. Mullena and T. P. Knepper, *J. Chromatogr., A*, 2001. **938**: p.67-77.

(92)   H. Kamada, Y. Tsutsumi, Y. Yamamoto, T. Kihira, Y. Kaneda, Y. Mu, H. Kodaira, S. Tsunoda, S. Nakagawa and T. Mayumi, *Cancer Res.*, 2000. **60**: p.6416-6420.

(93)   A. J. M. D'Souza, R. L. Schowen and E. M. Topp, *J. Controlled Release*, 2004. **94**: p.91-100.

(94)   Y. Kaneda, Y. Tsutsumi, Y. Yoshioka, H. Kamada, Y. Yamamoto, H. Kodaira, S. Tsunoda, T. Okamoto, Y. Mukai, H. Shibata, S. Nakagawa and T. Mayumi, *Biomaterials*, 2004. **25**: p.3259-3266.

(95)   S. Tsunoda, H. Kamada, Y. Yamamoto, T. Ishikawa, J. Matsui, K. Koizumi, Y. Kaneda, Y. Tsutsumi, Y. Ohsugi, T. Hirano and T. Mayumia, *J. Controlled Release*, 2000. **68**: p.335-341.

(96)   V. P. Torchilin, T. S. Levchenko, K. R. Whiteman, A. A. Yaroslavov, A. M. Tsatsakis, A. K. Rizos, E. V. Michailova and M. I. Shtilman, *Biomaterials*, 2001. **22**: p.3035-3044.

(97)   Y. Kaneda, Y. Tsutsumi, Y. Yoshioka, H. Kamada, Y. Yamamoto, H. Kodaira, S.-i. Tsunoda, T. Okamoto, Y. Mukai, H. Shibata, S. Nakagawa and T. Mayumi, *Biomaterials*, 2004. **25**: p.3259-3266.

(98)   Z. Liu, N. Fullwood and S. Rimmer, *J. Mater. Chem.*, 2000. **10**: p.1771-1775.

(99)   M. Bencini, E. Ranucci, P. Ferruti, C. Oldani, E. Licandro and S. Maiorana, *Macromolecules*, 2005. **38**: p.8211-8219.

(100)   M. Bencini, E. Ranucci, P. Ferruti and A. Manfredi, *Macromol. Rapid Commun.*, 2006. **27**: p.1060-1066.

(101)   E. Ranucci, P. Ferruti, R. Annunziata, I. Gerges and G. Spinelli, *Macromol. Biosci.*, 2006. **6**: p.216-227.

(102)   L. Luo, M. Ranger, D. G. Lessard, D. e. L. Garrec, S. Gori, J.-C. Leroux, S. Rimmer and D. Smith, *Macromolecules*, 2004. **37**: p.4008-4013.

(103)   H. Kodaira, Y. Tsutsumi, Y. Yoshioka, H. Kamada, Y. Kaneda, Y. Yamamoto, S. Tsunoda, T. Okamoto, Y. Mukai, H. Shibata, S. Nakagawa and T. Mayumi, *Biomaterials*, 2004. **25**: p.4309-4315.

(104)   A. S. Hoffman, *Adv. Drug Delivery Rev.*, 2002. **43**: p.3-12.

(105)   T. V. Chirila and Y. Hong, *Polym. Int.*, 1998. **46**: p.183-195.

(106)   S. O. Rogero, S. M. Malmonge, A. B. Lugão, T. I. Ikeda, L. Miyamaru and Á. S. Cruz, *Artif. Organs*, 2003. **27**: p.424-427.

(107)   K. I. Shantha and D. R. K. Harding, *Eur. Polym. J.*, 2003. **39**: p.63-68.

(108)   C. C. Anderson, F. Rodriguez and D. A. Thurston, *Journal of Applied Polymer Science*, 1979. **23**: p.2453-2462.

(109)   E.-S. A. Hegazy, S. E. A. ElAal, M. F. A. Taleb and A. M. Dessouki, *J. Appl. Polym. Sci.*, 2004. **92**: p.2642-2652.

(110)   P. Bilalis, M. Pitsikalis and N. Hadjichristidis, *J. Polym. Sci., Part A: Polym. Chem.*, 2006. **44**: p.659-665.

(111)   V. Coessens, T. Pintauer and K. Matyjaszewski, *Prog. Polym. Sci.*, 2001. **26**: p.337-377.

(112)   X. Lu, S. Gong, L. Meng, C. Li, S. Yang and L. Zhang, *Polymer*, 2007. **48**: p.2835-2842.

(113)   B. Ray, M. Kotani and S. Yamago, *Macromolecules*, 2006. **39**: p.5259-5265.

(114)   S. Yusa, S. Yamago, M. Sugahara, S. Morikawa, T. Yamamoto and Y. Morishima, *Macromolecules*, 2007. **40**: p.5907-5915.

(115)   D. Wan, K. Satoh, M. Kamigaito and Y. Okamoto, *Macromolecules*, 2005. **38**: p.10397-10405.

Chapter 3

RAFT mediated polymerization of N-vinylpyrrolidone

3.1 Introduction

The propagating radical of NVP is not conjugated and hence is poorly stabilized and therefore very reactive. An analogy can be drawn with VAc which also produces a poorly stabilized and highly reactive propagating radical. It has been rationalized that since the propagating radical, resulting from the addition of VAc, is a poor homolytic leaving group, the intermediate radical adducts (**18** and **22**, Scheme 2.5, Chapter 2) are more stable than their anticipated products and hence they fragment slowly.[1] The low reactivity of the xanthate CTAs C=S double bond towards radical addition[2,3] is best suited for these unstabilized and fast propagating monomers. It allows for efficient addition of their propagating radicals onto the C=S double bond. It also allows for the facile fragmentation of their intermediate radical adducts. This then ensures control over the polymerization. Their xanthates' ability to delocalize O's lone pair of electrons onto the C=S double bond increases the electron density at the radical centre. This destabilizes the intermediate radical adducts thereby increasing their fragmentation rate as compared to the case with methyl or phenyl Z group substituents.[1,4]

The conventional FRP of NVP in the presence of functionalized "irreversible" CTAs like mercaptans or functionalized solvents like isopropoxyethanol yields end functional oligomers. However, it leads to polymers with broad molecular weight distributions.[5] The end group conversion is also not quantitative.[5] In light of this an alcohol end functional RAFT agent (**1**), HEECP, was designed to mediate the polymerization of NVP. To date there is only one other report in literature detailing the synthesis of hydroxyl terminated xanthates and their use in RAFT mediated polymerizations. Lai and Shea[6] prepared alcohol functional xanthates by mixing molar equivalents of an alcohol, carbon disulfide and sodium hydroxide to form a xanthate salt. This was then alkylated with chloroform and acetone in the presence of a phase transfer agent to give a carboxyl functional xanthate. The carboxylic acid functional xanthate was then esterified with ethylene glycol, via acid catalysis, to give the hydroxyl functional xanthate. In general however, xanthate

RAFT agents can be readily prepared in one pot by simply alkylating the parent xanthate anion. It can be easily prepared by adding carbon disulfide to an alkoxide before adding the alkylating agent. Xanthate salts, fortunately, are also available commercially.
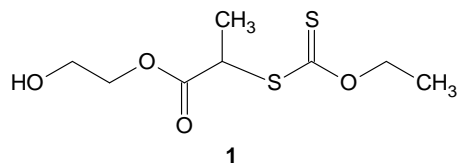
Figure 3.1. Hydroxyl functional RAFT agent (HEECP) used in the RAFT mediated LRP of NVP.

The R and Z group designations of RAFT agents are given in Figure. 2.1, Chapter 2. The *O*-ethyl substituent, of the Z group was chosen on the basis of the similarity in RAFT mediated polymerization behaviors of NVP to VAc. Coote and Radom have shown that, for VAc in RAFT, the alkyl group on the oxygen must be a poor homolytic leaving group compared to the conventional R group.[1] In earlier studies by Stenzel *et al.*[4] an ethyl substituent, on the oxygen, was shown to give the lowest retardation in VAc polymerization by RAFT.[4] In analogy with VAc, the ethoxy Z group was also used in the present study. The R group should be a good homolytic leaving group so that in the pre-equilibrium (equilibrium III, Scheme 2.5, Chapter 2) fragmentation favors the release of the R group radical (R•). This helps to achieve maximum reinitiating efficiency and to avoid the initial formation of high molecular weight polymers. It has been shown that propionic acid esters are efficient reinitiators in VAc RAFT mediated polymerization.[7]

3.2 Synthesis of HEECP

Xanthate **1** was readily prepared in good yields (> 80%) and high purity by a simple two step procedure. The first step involved the preparation of the alcohol functional alkylating agent, HEBP (**4**), before reacting it with the xanthate salt to give the RAFT agent. The synthesis of HEBP has been described in work focused on ATRP as it is also used as an ATRP initiator for making hydroxyl end functional polymers.[8,9]
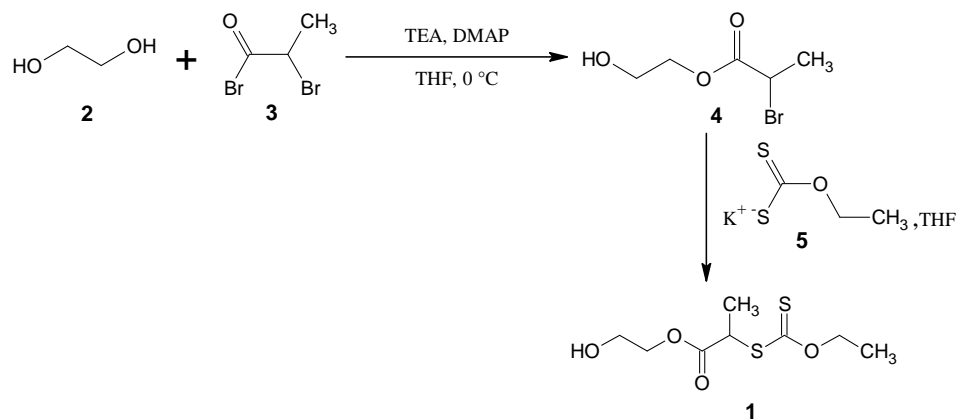
Scheme 3.1. Preparation of HEECP.

3.2.1 Materials

Ethylene glycol 99+%, triethyl amine (TEA), 99%, dicyclo hexylcarbodiimide (DCC) , 4-dimethyl aminopyridine (DMAP) and 2-bromopropionyl bromide, 97% (all Aldrich) were used received. Tetrahydrofuran (THF) was distilled from lithium aluminum hydride (LiAlH$_4$) and kept over molecular sieves. Diethyl ether (DEE) and ethanol (EtOH) were purified by drying over anhydrous magnesium sulfate (MgSO$_4$) (Saarchem) for 24hrs and distilling under a nitrogen atmosphere. The purified EtOH was kept over molecular sieves. NaCl 99.5% (R & S enterprises), HCl 32% (Saarchem) and sodium hydrogen carbonate (NaHCO$_3$) were used as received. Potassium ethyl xanthogenate 99.5% (Sigma-Aldrich) was used as received. Silica gel 60 for column chromatography was purchased from Macherey-Nagel. Silica gel/TLC aluminum cards were purchased from Sigma Aldrich. Color fixed indicator pH paper 0–14 was from Macherey-Nagel. Iodine, resublimed, was bought from Saarchem. Hexane was distilled under standard conditions. Ethyl acetate was used as received. Sodium cyanide 95%+ (Aldrich), hydrazine sulphate 99.0% (Analar), 3-acetyl-1-propanol 96% (Aldrich), Bromine (Merck) and sodium bisulfite 98% (Analytical reagents) were used as received. Chloroform, dichloromethane, and acetone were used as received. NVP 99% was bought from Aldrich. NVP was dried over anhydrous MgSO$_4$ overnight, flushed with argon for 30 minutes and distilled under vacuum (b.p. 74 °C at 3.60 mmHg) and stored over molecular sieves in the fridge (< 4 °C).

3.2.2 Preparation of HEBP

HEBP was prepared as described by Qin *et al.*[9] with a few alterations. Ethylene glycol (31 g, 500 mmol), anhydrous THF (150 ml), TEA (8.0 mL, 57 mmol) and DMAP (0.70 g, 5.7 mmol) were added to a 500 mL 3-necked round bottomed flask which was subsequently cooled to 0 °C in ice. A solution of 2-bromo propionyl bromide (10.8 g, 50 mmol) was then added dropwise under a nitrogen atmosphere. A white precipitate ($Et_3N^+HBr^-$) formed immediately. The mixture was allowed to stir overnight, coming to room temperature on its own accord in the process. The mixture was filtered and the filtrate concentrated. The remaining liquid was redissolved in DDI water (200 mL) and extracted with DEE (3 x 50 mL). The combined ether extracts were washed with HCl (5%, 3 x 50 mL), $NaHCO_3$ solution (3 x 50 mL) and distilled water and then dried over anhydrous $MgSO_4$ and the solvent was removed. The remaining liquid was distilled under vacuum (bp 86~89 °C at 5.6 mmHg) to give 5.41 g (55%) of HEBP as a colorless liquid. Purity was confirmed by ^{1}H-NMR spectroscopy (~99%). HEBP was prepared as described here every time in the rest of this work and isolated yields ranged between 50–60%.

^{1}H-NMR ($CDCl_3$): δ (ppm) = 1.85(d, 3 H, **CH₃**–CHBr–), 2.60(broad singlet, 1 H, **H**O–CH2–CH2–), 3.87(t, 2 H, HO–**CH₂**–CH₂–), 4.31(t, 2 H, HO–CH₂–**CH₂**–O–), 4.42(q, 1 H, –C**H**Br–CH₃).

3.2.3 Preparation of HEECP

Potassium ethyl xanthogenate (**6**) (4.66 g, 30 mol) was dissolved in EtOH (60 mL) in a 250 mL round bottom flask. 2-Hydroxyethyl 2-bromopropionate (4 g, 20 mol) was added and the mixture was allowed to stir overnight. The white precipitate (KBr) was filtered off and the solvent was evaporated before re-dissolving the remaining liquid in 200 mL of ether and filtering to remove solids. The mixture was concentrated and purified by column chromatography (eluent: hexane/ethyl acetate, 3:1) to give HEECP as a light yellow oily liquid, 5.79 g (83.46%). Purity was checked by TLC ($R_f = 0.30$) and confirmed by ^{1}H-NMR ($\geq$ 98%) spectroscopy.

^{1}H-NMR ($CDCl_3$): δ (ppm) = 1.40(t, 3 H, **CH₃**–CH₂–), 1.58(d, 3 H, **CH₃**–CH–), 2.11(broad singlet,1H, –O**H**), 3.82(d, 2 H, –**CH₂**–CH₂–), 4.26(q, 2 H, –**CH₂**–CH₂–), 4.40(q, 1 H, –C**H**–CH₃–), 4.62(q, 2 H, –**CH₂**–CH₃).

3.3 Polymerization system

3.3.1 The initiator

In order to obtain a maximum amount of chains terminated with hydroxyl functionality, a hydroxyl functional azo initiator, 4,4'-azobis(4-cyanopentanol) (**6**) (ACP), prepared as described by Clouet *et al.*[10], was used.
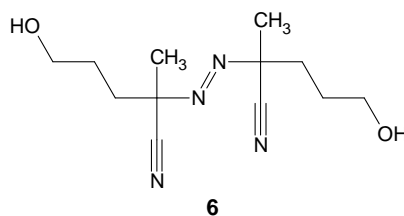
Figure 3.2. Structure of the hydroxyl functional initiator used.

Hydrazine sulphate (14.3 g, 0.11 mol) was dissolved in 150 mL water in a 3-necked 500 mL round bottom flask. 5-Hydroxy-pentane-2-one (22.5 g, 0.22 mol) was added followed by the slow addition of a solution of sodium cyanide (10.8 g, 0.22 mol) in 100 mL water and the mixture was allowed to stand overnight. The reaction mixture was cooled to ~0 °C, by placing the flask in an ice bath, and made acidic by slowly adding aqueous hydrochloric acid (15%). Bromine (32 g, 0.2 mol) was then added dropwise over a period of 5 h with the temperature being kept at around 0 °C with intense stirring and the reaction was allowed to stand overnight. Excess bromine (yellow color) was removed by adding sodium bisulphite solution. A white precipitate was filtered off. This precipitate (5.20 g) corresponded to the higher melting point isomer of this azo compound.[10] It was dried under vacuum and gave a melting range between 93–96 °C. The filtrate was washed with several portions of a mixture methylene chloride/acetone (2:1 mL) the aqueous phase discarded and the organic portions combined. The solvent was evaporated and the solid residue obtained was recrystalized from ethanol to give 3.70 g of the low melting isomer of this initiator. It melted in the range 81–84 °C. The combined yield of the two isomers was 8.9 g (~33% yield). Although no distinction was necessary on which isomer to use, only the lower melting isomer was used in the rest of this work as it had the highest purity (97% by NMR). ^{1}H-NMR (CDCl$_3$): δ (ppm) = 1.50–1.64(m, 2 H, –CH$_2$–**CH$_2$**–CH$_2$), 1.72(s, 3 H, **CH$_3$**–), 1.74-1.83 (m, 2 H,–**CH$_2$**–C(CH$_3$)(CN)–), 2.05–2.19(m, 2 H, –CH$_2$–**CH$_2$**–CH$_2$–), 2.20–2.32(m, 2 H,–**CH$_2$**–C(CH$_3$)(CN) –), 3.70(t, 2 H, –**CH$_2$**–OH).

3.3.2 General polymerization procedure

The RAFT mediated LRP of NVP using HEECP as the RAFT agent was conducted. The molecular weights, polydispersity indexes and conversions obtained are given in Table 3.1. All polymerizations were conducted in bulk at 60 ^{o}C with initiation by ACP.

Table 3.1. RAFT mediated bulk polymerization of NVP with ACP as initiator at 60 ^{o}C

run	time (h)	$[M]_o/[HEECP]_o/[ACP]$	$^aM_n^{Theor}$. (g/mol)	$^bConv.$ (%)	$^cM_n^{Calc}$. (g/mol)	M_n^{NMR} (g/mol)	M_n^{SEC} (g/mol)	M_w/M_n
1	7	223.0/5.65 /1.0	4 868	49	2 385	2711	2 798	1.30
2	7	224.5/5.25/1.0	4 970	45	2 263	2930	2 725	1.29
3	7	218.0/5.05/1.0	5 001	49	2 451	2201	2 483	1.31
4	7	410.0/4.96/1.0	9 192	63	5 791	6220	6740	1.26

^{a} M_n values expected at 100% conversions, determined using equation 3.2.

^{b} Conversions were determined by weighing the purified and dried polymer (= yield{g}) and then calculated as yield{g}/([NVP+HEECP+ACP] {g}) ✖ 100%

^{c} M_n values calculated as follows: $^cConv.$ ✖ $^aM_n^{Theor}$.

For runs 1–3, the following procedure was typical: (e.g. for run 1) a dry Schlenk flask was charged with HEECP (0.25 g, 1.06 mmol), ACP (52.60 mg, 0.208 mmol), NVP, (5.00 g, 40.5 mmol) and a magnetic stirrer bar successively. It was thoroughly degassed by four freeze pump thaw cycles, backfilled with argon, sealed and immersed into an oil bath preheated and thermostated at 60 ^{o}C. The polymerization was the allowed to run for 7 h. It was typical in all the cases that the reaction mixture became very viscous around 6–7 h and stirring was greatly hampered. The reactions were allowed to run for 7 h and stopped by removing the reaction flasks from the oil baths and opening them. The reaction mixtures were diluted with THF and the polymer was isolated by precipitation from diethyl ether. For runs 1–3, these samples were also used in the end group modifying reactions described in Chapters 4 and 5. They were precipitated twice from diethyl ether and subjected to Soxhlet extraction with diethyl ether for 48 h, to remove residual monomer and finally dried in a vacuum oven at 40 ^{o}C for 24 h. Theoretical molecular weights (M_n^{Theor}.) were calculated using equation 3.2, a simplified version of equation 3.1.

$$M_n^{\text{theor.}} = \frac{[NVP]_0}{[HEECP]_0 + 2f[ACP]_0(1 - e^{-k_d t})} \times Mr_{NVP} \times \text{Conversion} + Mr_{HEECP} \tag{3.1}$$

Mr_{NVP} and Mr_{HEECP} are the molecular weights of the monomer and the RAFT agent respectively. $[NVP]_0$, $[HEECP]_0$ and $[ACP]_0$ account for the initial concentrations of the monomer, RAFT agent and the initiator respectively. f is the initiator efficiency factor and k_d is the rate constant for initiator decomposition. f values for ACP with NVP have not been reported yet. However, its k_d was found to be 1.28×10^{-5} s^{-1} in acetone at 60 $^{\circ}$C.[10] Its activation energy for decomposition is 120.92 kJ/mol^{-1} which is close to values for other azo compounds like AIBN (121.34–138.07 kJ/mol^{-1}) and 4,4'–azobis(4–cyanopentanoic acid) (117.15–133.89 kJ/mol^{-1}). This implies that the electronic effects of substituents in ACP do not affect the decomposition of the azo compounds.[10] It appeared valid therefore, to assume f values determined for AIBN in conventional FRP at 60 $^{\circ}$C (~0.5–0.6) to hold here as well. The f values are not constant and tend to reduce in highly viscous media. Viscosity increases with increasing conversion therefore, it follows that f values will also reduce with increasing conversion. f values can, therefore, be lower than 0.5 and the second term in the denominator also becomes very low[11] (i.e. the number of initiator derived chains is negligible). In a typical RAFT-mediated polymerization, the fraction of initiator derived chains is minimal. It is therefore, legitimate to reduce equation 3.1 to equation 3.2.

$$M_n^{\text{Theor.}} = \frac{[NVP]_0}{[HEECP]_0} \times Mr_{NVP} \times \text{Conversion} + Mr_{HEECP} \tag{3.2}$$

For runs 1-3 (Table 3.1), conversions were determined gravimetrically and M_n was calculated using equation 2. Molecular weights were also determined by ^{1}H-NMR spectroscopy. For the run from which samples were taken, ACP (52.4 mg, 0.207 mmol), HEECP (250.8 mg, 1.05 mmol), NVP (10 g, 89.98 mmol) and a magnetic stirrer bar were added to a dry 50 mL Schlenk flask. The reaction mixture was thoroughly degassed by 5 successive freeze pump thaw cycles, backfilled with argon and sealed before being immersed in an oil bath thermostated at 60 $^{\circ}$C. Samples were withdrawn at timed intervals, using a degassed syringe, to assess the evolution of molecular weight by SEC and conversion (by NMR) with time. The NMR samples (to determine conversions) were immediately prepared after each sampling, in CDCl$_3$ as the NMR solvent whilst the rest of the sample was added, dropwise, to diethyl ether to precipitate the polymer. Where no precipitate was obtained, all volatiles

were removed and the sample concentrated. These samples were prepared for SEC. MALDI ToF analysis was carried out on samples 1, 2 and 3 in order to fully characterize their structures whilst two dimensional NMR spectroscopy was carried out on sample 3 in order to gain more insight on its end group structure.

3.4 Analysis

3.4.1 NMR

One dimensional ^{1}H (400 MHz) NMR and ^{13}C NMR spectra as well as two dimensional COSY were acquired with a Varian VXR-Unity in CDCl$_3$ (unless specified otherwise). All chemical shifts are reported in parts per million (ppm) with tetramethylsilane (TMS) as a reference.

3.4.2 SEC

SEC analysis was carried out using a Shimadzu, LC-10AD pump, a triple detector array in series: Waters 2487 dual wavelength UV detector (320 nm), Viscotek 270 light scattering (RALLS/LALLS) and Viscometry (in series) and a Waters 2414 Differential Refractive Index (DRI) detector (35 ^{o}C). Injections were done by a Spark Holland MIDAS system with an injection volume of 50 μL. The eluent was 1,1,1,3,3,3-hexafluoro-2-propanol (HFIP) at a flow rate of 0.8 mL/min. A short silica column was placed after the pump to catch free fluoride possibly to present in HFIP. Samples were filtered through a 0.2 μm PTFE filter placed between the columns and the UV detector to prevent small particles from entering the LS detector. Calibration was done using PMMA standard sets (Polymer Labs, EasyCal PM-1). Data acquisition and processing was performed using Viscotek, Omnisec 4.0 (all detectors) and Waters Empower 2.0 (UV and DRI detectors). A fifth order polynomial was used to fit the $\log_{10}$M vs. time calibration curve which appeared linear over the molecular weight range M = 3.71$\times$10^2-2.33$\times$10^6 g/mol.

3.4.3 MALDI ToF MS

MALDI ToF mass spectra were recorded on a Voyager–DE STR (Applied Biosystems, Framingham) equipped with a nitrogen (N$_2$) 337 nm laser in the reflector mode, at 25 kV accelerating voltage and with delayed extraction. The matrix was trans-2-[3-(4-tert-butylphenyl)-2-

methyl-2-propenylidene]malononitrile (Aldrich) and Potassium Trifluoro acetate (KTFA) (Aldrich) was used as the cationizing agent. In each analysis, the analyte sample was prepared by first making up the following concentrations of matrix, KTFA and sample, in THF, separately: 40 mg/mL matrix: 5 mg/mL KTFA: 1 mg/mL sample, before mixing them in the respective ration of 4:1:4 and hand spotting on the target plate. 1000 laser shots were obtained for each spectrum. All the MALDI ToF results reported in the rest of this work were obtained as described here.

3.5 Results and discussion

3.5.1 Control over the of molecular weight distribution

The alcohol functional Xanthate RAFT agent (HEECP) was prepared in high yields and excellent purity. The general reaction scheme for the polymerization is shown below:
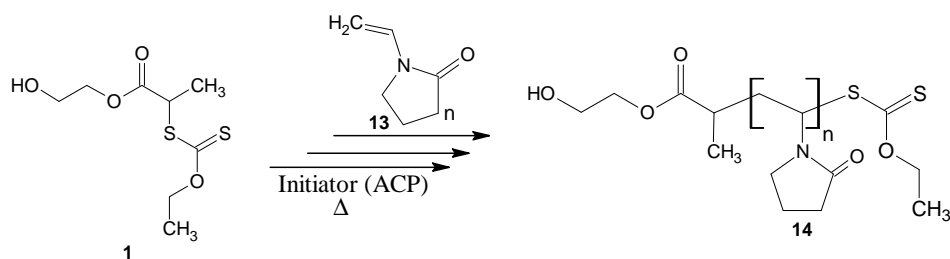
Scheme 3.2. General scheme for the RAFT mediated polymerization of NVP (13) with HEECP (1) as the RAFT agent to give PVP (14).

The RAFT-mediated polymerization of NVP proceeded with good control over molecular weight and molecular weight distribution. This will be shown below. ^{1}H NMR was used to determine conversion as a function of time by comparing monomer peak integrals to the polymer (PVP) and RAFT agent peak integrals. The residual monomer was quantified from the signal at 7.09 ppm (dd, N–CH=CH**H**). The overlapping resonances at 2.9–4.2 ppm (broad multiplet, PVP C**H$_2$**–NC**H**) and 3.52 (t, NVP C**H$_2$**N) were used to obtain the amount of residual monomer plus polymer.

Figure 3.3(a) shows the evolution of conversion with time. Conversion increased fairly linearly with time and about 45% conversion was attained in 7 h. The $\ln([M]_0/[M])$ vs. time plot is linear indicating that the kinetics were first order with respect to the monomer concentration and that there was a constant number of polymer radicals. Figure 3.3(b) shows the number-average molecular

weight (M_n) and polydispersity index (M_w/M_n) as a function of conversion. Molecular weights increased linearly with conversion. The maximum variation in M_w/M_n ratios is approximately 0.05, therefore they can be considered as constant within experimental error.
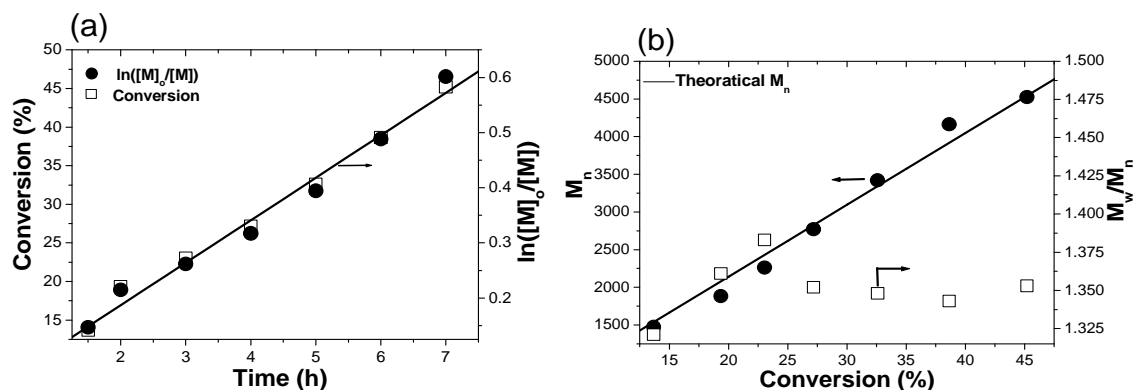
Figure 3.3 (a). Time-conversion and first-order kinetic plots and (b) M_n and M_w/M_n versus Conversion for the RAFT mediated bulk polymerization of NVP at 60 °C, with the initial molar ratios 436.0:10:1.0 for NVP, HEECP and ACP respectively.
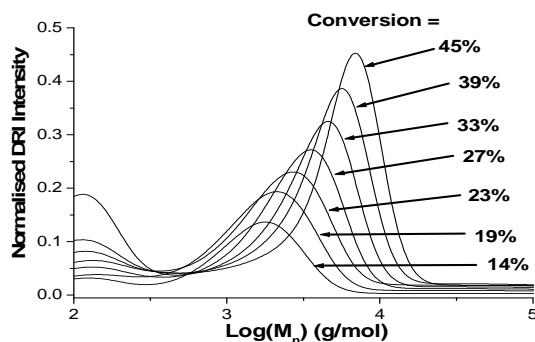
Figure 3.4: Evolution of SEC traces with conversion for the RAFT mediated bulk polymerization of NVP at 60 °C with the initial molar ratios 436.1:10:1.0 for NVP, HEECP and ACP respectively.

Figure 3.4 shows the normalized SEC traces, scaled to monomer conversion, which show that molecular weights progressively increase with conversion. No bimodality was observed. This is typical of well controlled living radical polymerization systems. Some tailing, however, is evident towards the low molecular weight region. This again could be attributed to chain breaking reactions like radical-radical coupling and disproportionation, resulting in dead chains. Degradation of the xanthate chain end moiety also produces dead chains. Good control, however, was maintained throughout the polymerization ($M_w/M_n < 1.4$).

3.5.2 Chain end structural analysis

3.5.2.1 ^{1}H-NMR analysis

^{1}H-NMR analysis was used to provide both qualitative and quantitative information on the polymer end groups. Only polymers with low degrees of polymerization were targeted in order to increase the concentration of end groups to avoid problems due to low resolution of the end group signals.
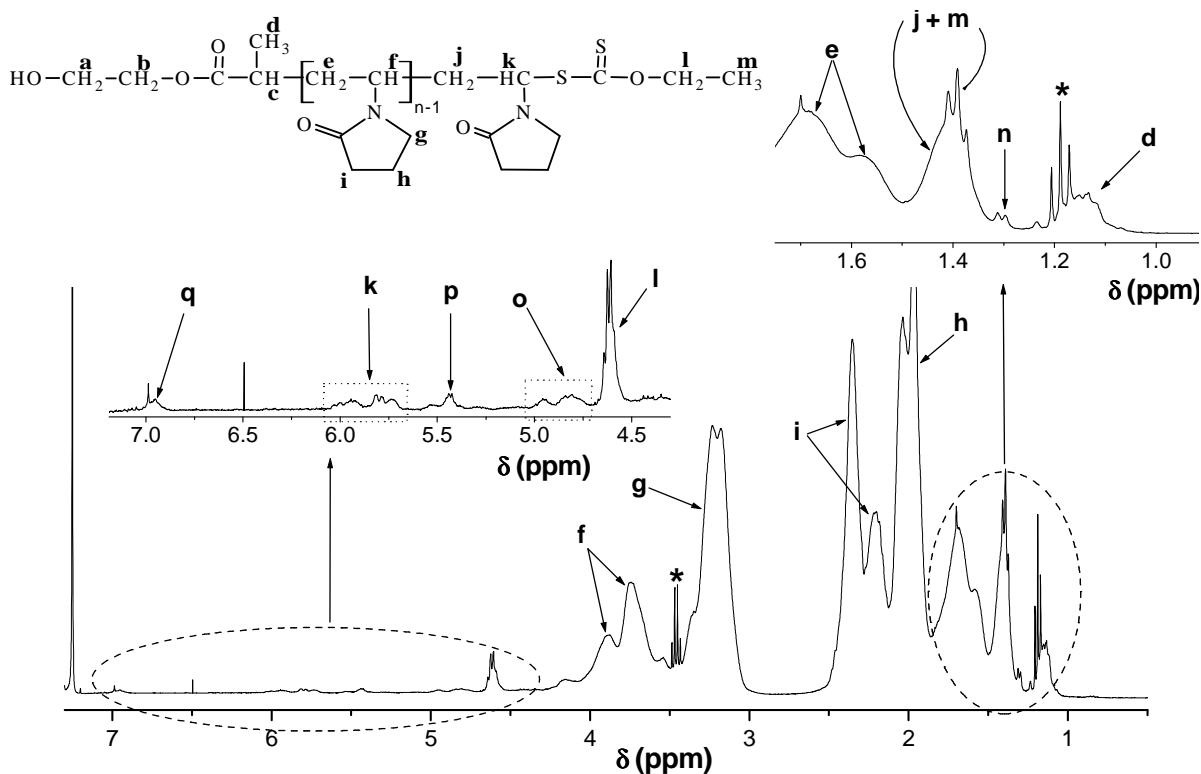
Figure 3.5. ^{1}H-NMR spectrum (CDCl₃) of PVP prepared by the RAFT mediated bulk polymerization of NVP at 60 °C with the initial molar ratios 224.5/5.3/1.0 for NVP, HEECP and ACP respectively.

A typical ^{1}H-NMR spectrum of the PVP prepared in this work is shown is Figure 3.5. Peak assignments were made based on the expected structure which is shown in the insert in Figure 3.5. The large signals at 1.3–2.6 ppm (*e, h, i* and *j*) and at 3.0–4.1 ppm (*f* and *g*) are due to the repeat units.[12] The peaks marked by an asterisk are due to diethyl ether. Insight into the end group composition of the polymer was provided by analyzing the several small signals in the baseline that are highlighted in the inserts. The signal at 1.15 ppm (*b*) was attributed to the methyl group of the R group of the RAFT agent, which is located at the α–chain end of the polymer. Signals *l* and *m* were assigned to the Z group –CH₂– and –CH₃ protons of the xanthate. Signal *m* overlaps with the signal

for the "head" $-CH_2-$ peak of the terminal repeat unit before the Z group of the xanthate). Several other RAFT agent signals, *a*, *b* and *c*, overlap with the broad signal of the polymer backbone in the region 3.0–4.2 ppm. The broad signal at 5.7–6.2 ppm was attributed to the $-CH-$ (*k*) of the terminal monomer unit attached to the S of the Z group. The signal at 4.60 ppm (*l*) from the ω-chain end was used to calculate the number-average molecular weight (M_n) from the ω-chain end. This was done by dividing the integration value of signal *f* of the polymer backbone by the xanthate chain end signal *l* as shown by equation 3.3.

$$M_n^{NMR} = f / (l/2) \times 111.14 \text{ g/mol} \qquad\qquad 3.3$$

M_n^{NMR} is the M_n value determined this way. 111.14 g/mol is the molar mass of NVP. The integration value for signal *l* is divided by two so as to equate it to that of *f*. The former signal is produced by two protons whilst the latter signal is produced by one proton. The M_n values determined in this way are shown in Table 3.1 as the M_n^{NMR} values. Agreement with the M_n values determined by SEC was good (see Table 3.1). Differences can be attributed to inaccuracies in determining the integral values due to overlap between polymer peaks and some end group peaks resulting in the overestimation of the integral values of the former. Also, not all of the polymer chains were eventually capped by the RAFT agent's thiocarbonyl thio moiety at the ω-chain end. This resulted in an overestimation of integral values of the polymer peaks. Bimolecular termination events like radical-radical coupling and disproportionation reduce the number of chains capped at the ω-chain end by the thiocarbonyl thio moiety. It also appears that this end group is very labile and it decomposes under mild conditions. This was verified by analyzing the small signals *o*, and *q* (Figure 3.5). Peaks *o* and *q* were assigned to protons on unsaturated end groups (Figure 3.6) due to their similarity to the signals of the monomer at 4.43 ppm (N–CH=CH**H**) and 7.09 ppm (N–CH=CH**H**) (downfield of TMS in CDCl$_3$). No evidence was found for a $-CH=CH_2$ end group. This end group is produced by backbiting (by the propagating radical) followed by β-scission.[13] This implies that this side reaction either did not take place or it occurred at undetectable levels.
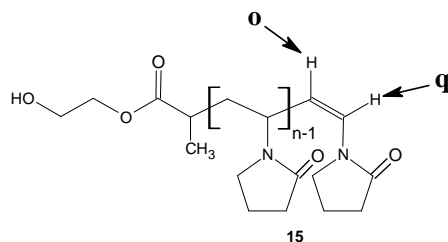
Figure 3.6. Illustration of unsaturated chain ends on PVP prepared by the RAFT mediated bulk polymerization of NVP at 60 $^{\circ}$C.

Analysis of the COSY spectra (Appendix 1) also showed that their cross peaks intersected on the diagonal line indicating that they were indeed coupled. This chain end unsaturation is attributed to disproportionation and/or thermal cleavage of the Z group at the ω-chain end. MALDI ToF MS analysis of the polymer, however, implied that this chain end unsaturation is largely caused by the thermal cleavage of the Z group. This is shown below. Legge *et al.*[14] assessed the thermal stability of a number of RAFT agents and found that for xanthates the breakdown temperature was at 75 $^{\circ}$C, it is possible therefore to conclude that the onset of this decomposition occurs at a much lower temperature as polymerizations in this case were ran at a much lower temperature (60 $^{\circ}$C). Liu *et al.*[15] also found that cumyl dithiobenzoate (CDB) decomposed to give α-methylstyrene and dithiobenzoic acid (DTBA) (Scheme 3.3). They determined the decomposition rate constant (k_{dec}) for this to be 4.64×10^{-5} s^{-1} at 60 $^{\circ}$C. High temperatures shift the equilibrium to the right.[15] In analogy with Liu's findings, the decomposition of the thiocarbonyl thio end group from the ω-chain end can also be rationalized as shown in Scheme 3.4.
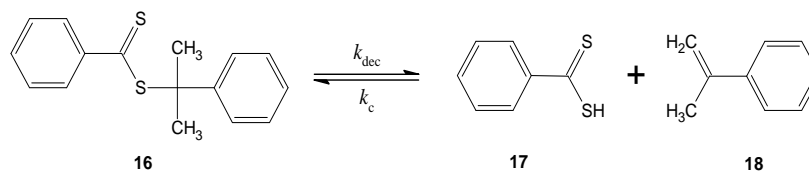
Scheme 3.3. Mechanism of decomposition of CDB.
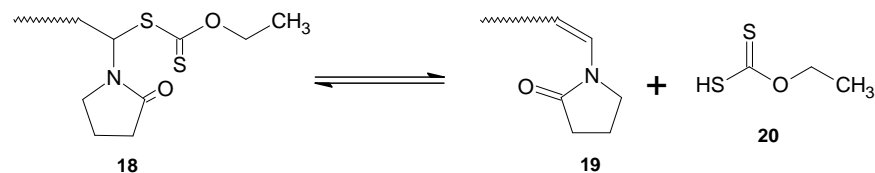
Scheme 3.4. Proposed thermal decomposition of thiocarbonyl thio end group from the ω-chain end of PVP prepared in this work.

In this work no attempt was made to isolate the *O*-ethyl xanthic acid, (**20**). However, in several polymerizations ran in this work, the unsaturation at the ω-chain end was estimated by ^{1}H-NMR, to between 3-5%. It was also observed, in a test sample from run 3, Table 3.1, that when the sample was kept on the bench, open to air, the chain end unsaturation increased from ~3.5% to 9% within 4 months.

The doublet at 1.3 ppm (*n*) and the quartet at 5.44 ppm (*p*) were assigned to **CH**₃ and **CH** signals respectively as this pattern is typical of a **CH**₃–**CH**–system. It was observed that their intensity could be increased by merely heating a freshly precipitated (once) polymer sample as a way of removing residual unreacted monomer and precipitating solvent (diethyl ether) in an open beaker at 50 °C for 24 h. Figure 3.7 shows the resulting ^{1}H-NMR spectrum of such an experiment. In comparison with Figure 3.5, the intensities of signals *n* and *p* in Figure 3.7 have clearly increased.
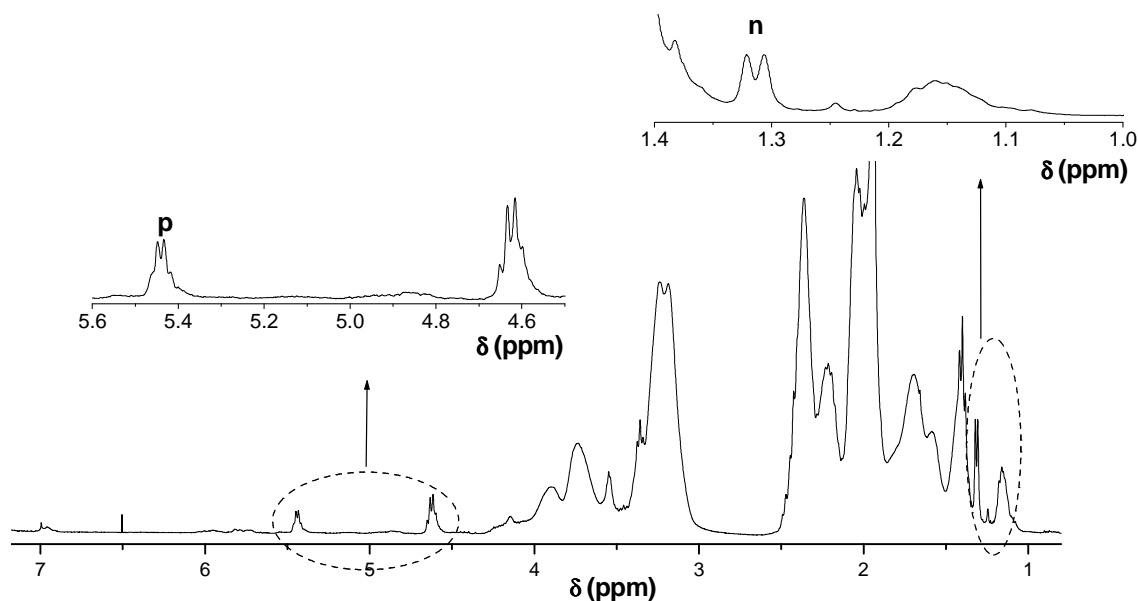
Figure 3.7. ^{1}H-NMR spectrum of PVP sample from Figure 3.5 after heating for 24 h at 50 °C.

2D NMR analysis (COSY) of this sample showed that the signals *n* and *p* were on adjacent carbon atoms as cross peaks were observed (Appendix 2). These peaks were assigned to end groups of dimeric derivatives. NVP is known to form a dimeric product (1,3-Bis[pyrrolidin-2-on-1-yl]but-1-ene) (**20**, Scheme 3.5) with itself under acid catalysis.[16] It also hydrolyses to 2-pyrrolidinone (**23**, Scheme 3.5) and acetaldehyde in aqueous solutions with acid catalysis.[17] The 2-pyrrolidinone (**23**) released by the hydrolysis can react with NVP (**13**) to form another dimeric product, an amidoethylpyrrolidinone derivative (**24**).[17,18]
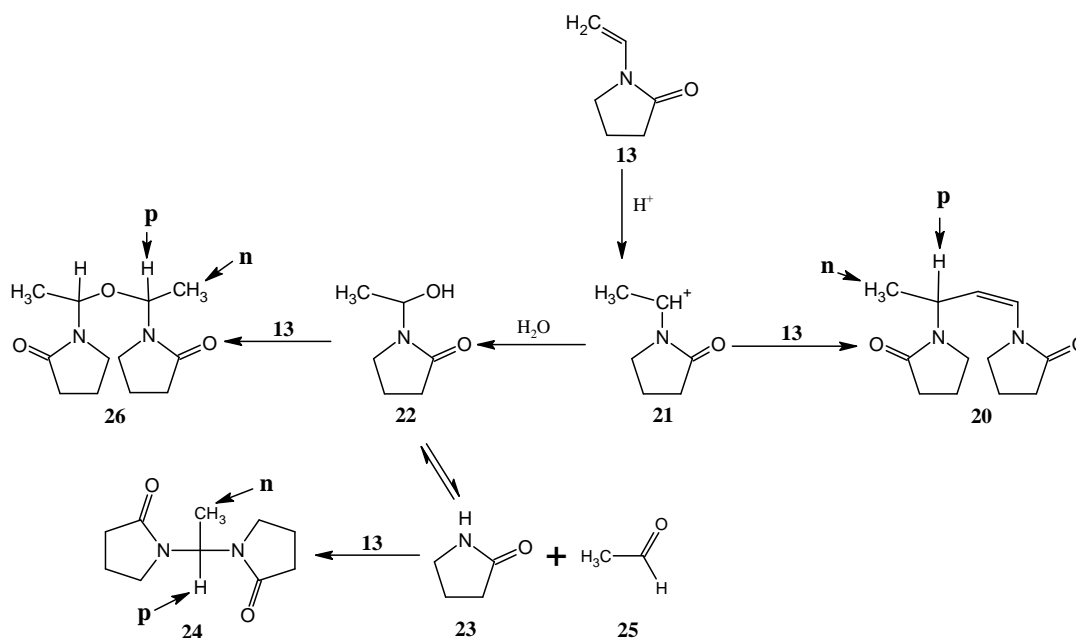
Scheme 3.5. Side reactions of NVP.

Reaction of the cation (**21**) with water to give **22** can also lead to the formation of the dimeric derivative (**26**). The protons expected to give the signals corresponding to *n* and *p* are indicated in Scheme 3.5. Whilst the monomer, NVP, used here was purified thoroughly, it is conceivable that there were traces of moisture. Considering also that the RAFT agent has an alcohol functionality this could lead to mildly acidic conditions which should catalyze the formation of any of the dimeric derivatives. It is unlikely that an end group structure analogous to **24** (**28**, Scheme 3.6) gives rise to the peaks *n* and *p*.
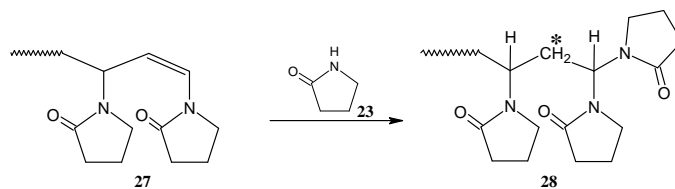
Scheme 3.6. Illustration of possible end group structure.

This is because the signal *n* is due to a CH_3 neighboring a CH. This only leaves end group structures analogous to **20** and **26**, Scheme 3.5, as an option.

3.5.2.2 MALDI ToF MS analysis

PVP end group structures were further analyzed by MALDI ToF MS. Figure 3.8 shows a typical MALDI ToF mass spectrum of a PVP oligomers prepared in this work.
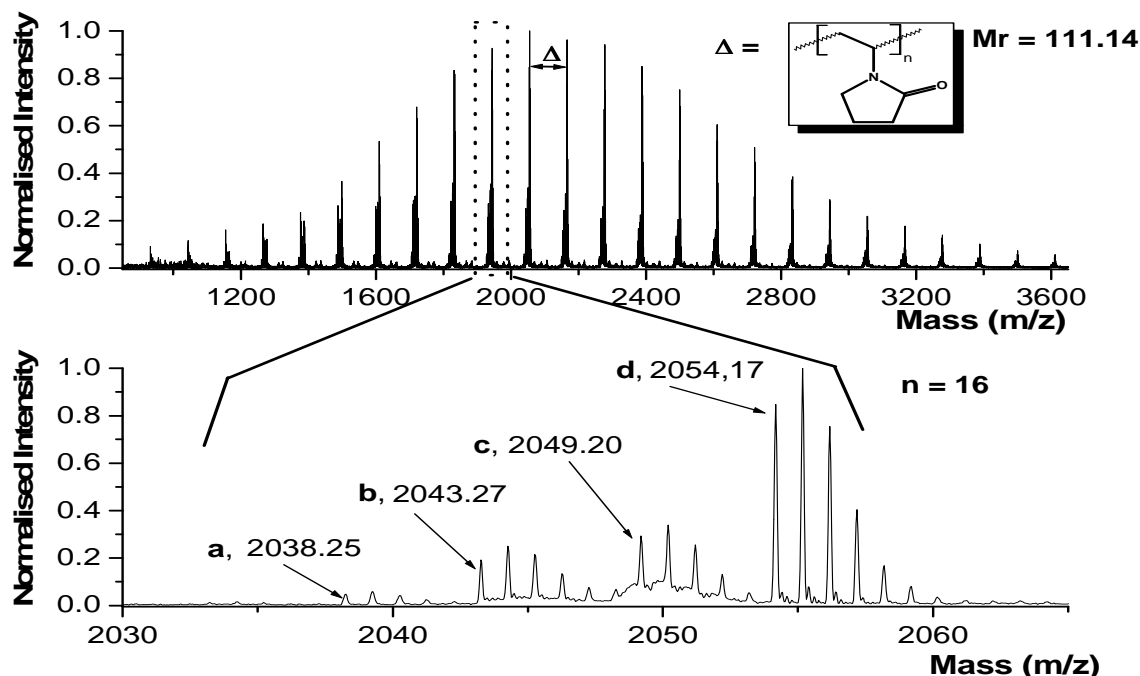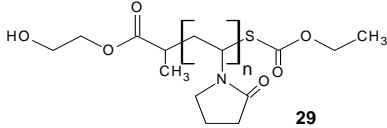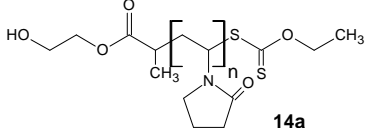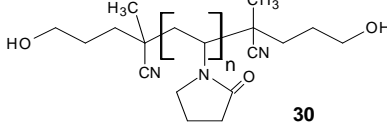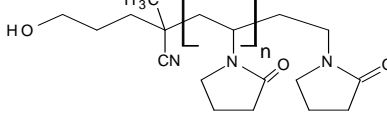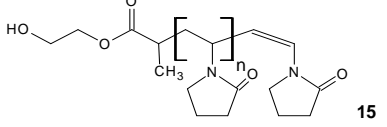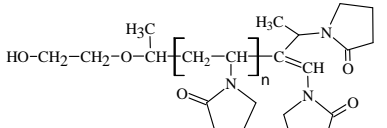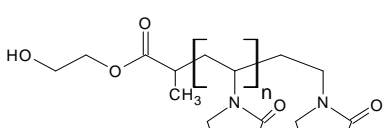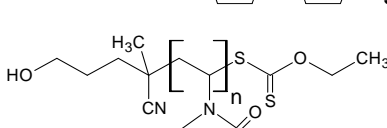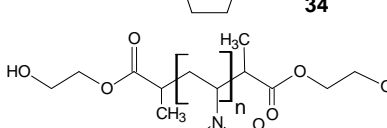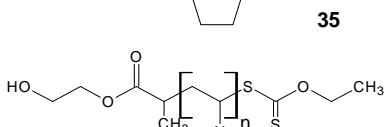
Figure 3.8. MALDI ToF mass spectrum of a PVP oligomer prepared by the RAFT mediated bulk polymerization of NVP at 60 °C, with the initial molar ratios 224.5/5.25/1.0 for NVP, HEECP and ACP respectively (run 1, Table 3).

The peaks in the main distribution, in Figure 3.8, are at intervals of 111.14 mass units from each other which corresponds to the molar mass of NVP, the repeat unit. Potassium trifluoro acetate was added as the cationizing agent hence all the chains, in the spectrum in Figure 3.8 (and in the rest of

this work), were cationized by potassium. This accounts for 39.10 Da of the experimental molar masses. The *m/z* region 2030–2065, expanded for illustrative purposes, shows that they were four signals, of varying intensity, for each peak, due to the natural abundance of the isotopes. Possible structures corresponding to these signals are shown in Table 3.2.

Table 3.2. Structural assignments for the MALDI ToF spectrum of PVP in Figure 3.10

Peak	Monoisotopic mass (+ K^+)		Structure	Cationization	[c]n
	[a]Expt.	[b]Theo.			
a	2038.25	2038.11	**29**	K^+	16
		2038.11	**14a**	Na^+	16
		2038.19	**30**	K^+	16
		2039.20	**31**	K^+	16
b	2043.27	2043.17	**15**	K^+	16
		2043.17	**32**	K^+	15
		2045.19	**33**	K^+	16
c	2049.20	2049.11	**34**	K^+	16
		2050.17	**35**	K^+	16
d	2054.17	2054.09	**14b**	K^+	16

[a.] experimentally determined number average molar mass, [b.] theoretical molar mass, [c.] degree of polymerization

In general MALDI ToF MS detects ions of the type $\{X–[M]_n–Y\}^{\cdots}C^+$. X and Y are the end groups, M is the repeat unit, n is the degree of polymerization and C^+ is the cationizing ion. End group analysis can be done by plotting Mass (*m/z*) against n to get a plot (as a straight line) of the type:

$$Mass\ (m/z) = (M_M)n + [(M_X + M_Y) + M_{C+}] \hspace{3cm} (3.4)$$

The slope of the line gives M_M, the molar mass of the repeat unit. The y–axis intercept, $[(M_X + M_Y) + M_{C+}]$, gives the combined masses of the end groups plus the cationizing ion respectively.[19,20] With knowledge of the synthetic procedure used, e.g. the RAFT mediated polymerization of NVP illustrated in Scheme 3.2, structural identification of the oligomer is made possible.

In Figure 3.8 the isotopic pattern with the greatest signal intensity, d, was assigned to structure **14b**, Table 3.2. This was as expected from Scheme 3.2 for the RAFT mediated polymerization of NVP with HEECP as the CTA. Figure 3.9 shows an excellent agreement between the theoretical and the experimentally determined isotopic distributions.

Figure 3.9. MALDI ToF mass spectrum of PVP, run 1 in Table 3.2, prepared as illustrated in Scheme 3.3, showing the experimental isotopic distribution (top) and the theoretical (bottom) corresponding to structure 14b in Table 3.4.

The isotopic distribution a (Figure 3.8) was attributed to four possible structures: **29**, **14a, 30 and 31**, Table 3.2. **29** corresponded to a dormant chain expected from Scheme 3.2 that has been oxidized. The oxidation of thiocarbonyl thio moiety in RAFT agents has also been observed by Favier *et al.*[21] They are oxidized to give the sulfine (**37**) initially, which subsequently gets oxidized to the (mono)thiolcarbonate[21,22] (**38,** Scheme 3.7).
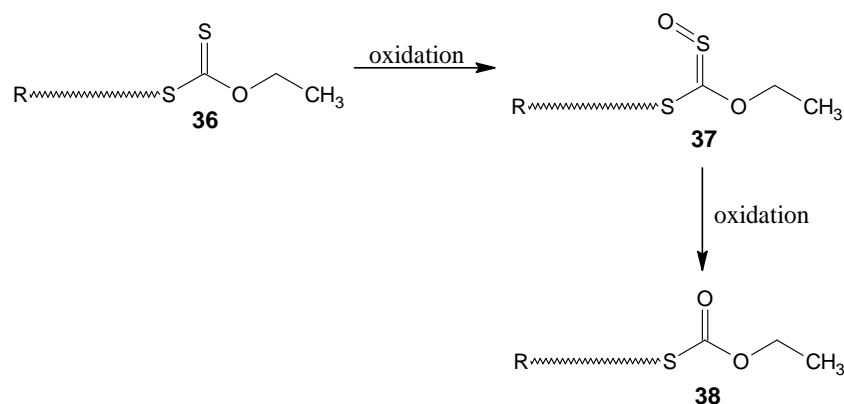
Scheme 3.7. Oxidation of the thiocarbonyl thio functionality.

Structure **14a** can be assigned to a "normal" RAFT mediated, dormant chain cationized by Na^+. This agrees well with a shift of 16 mass units down from peak d as the mass difference between Na^+ and K^+ is 16 g/mol. Even though KTFA was added to the sample, Na^+ ions can be anticipated to be present as impurities related to the sample history. **30** agrees with an initiator derived chain capped at the ω-chain end by another initiator fragment due to radical-radical coupling. Finally, from isotopic cluster a, it appears that **31** was either not present or was present in insignificant amounts. The isotopic cluster b, Figure 3.8, can be assigned to two possible structures (**15** and **32**). **15** is due to an R group derived chain that is capped at the ω–chain end by an unsaturated end group formed as described in Section 3.2.5.1. This chain end unsaturation can also be attributed to disproportionation. However, structure **33** which would also form as a result of disproportionation has a mass 1.92 Da higher than the observed value. This is outside the error range for this MALDI ToF MS analysis as the rest of the structures were within 0.14 Da. Although for this sample, run 1, Table 3.3, there was 3% chain end unsaturation it must also be noted that **15** can also arise due to fragmentation of the dithio moiety during the MALDI ToF MS analysis.[20,23] Structure **32** can be assigned to R group derived chains capped at the ω–chain end by a structure analogous to the NVP dimer (**20**, Scheme 3.6). It is interesting to note that structure **32** gives exactly the same isotopic pattern as **15**. This would imply that end group derivative **32** which is analogous to the NVP dimer (**20**) gives the peaks *n* and *p* in the NMR spectrum in Figure 3.7. The MALDI ToF MS spectrum of the sample used to acquire the NMR spectra in Figure 3.7 is shown in Section 3.5.2.3. below.

Finally the isotopic cluster c, Figure 3.8, is attributable to initiator derived chains capped at the ω-chain end by the normal thiocarbonyl thio moiety (**34**). Taking into account the $[HEECP]_0/[ACP]_0$ ratio of 5.25:1.0 used, run 1, Table 3.3, it is not surprising that they are observable. Destarac *et al.*[24]

and Schilli *et al.*[23] have also reported initiator derived chains using RAFT agent to initiator ratios of 5:3. Cluster c, could also be assigned to chains capped at both ends by the R group due to radical–radical coupling of R group derived chains (**35**). However, the mass for **35** is 0.97 Da higher than the experimentally observed value, which is higher than the errors for the other structures (± 0.14). A difference of 1 Da probably means that this is not the correct assignment. However, for the particular isotope peaks in this analysis (e.g. see Figure 3.10 below) the most abundant isotope peak was not located at the top of the isotope patterns. Therefore, this implies that structure **35** was probably present, but its isotopic pattern was overlapping with that for **34** and **14b**. This is shown in Figure 3.10 below.
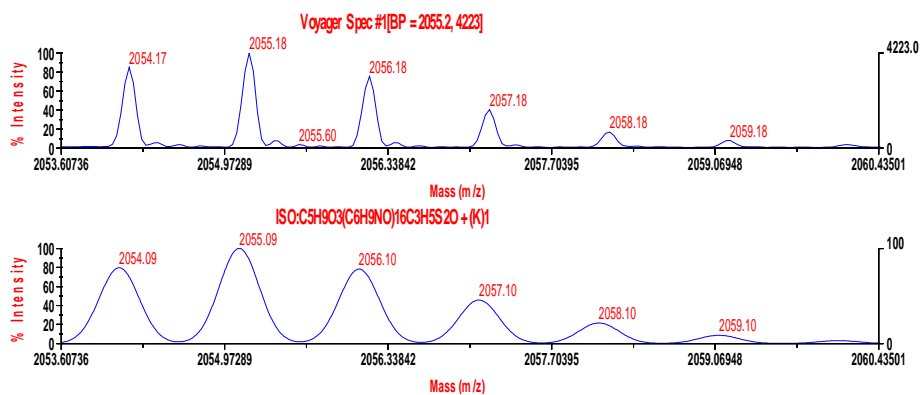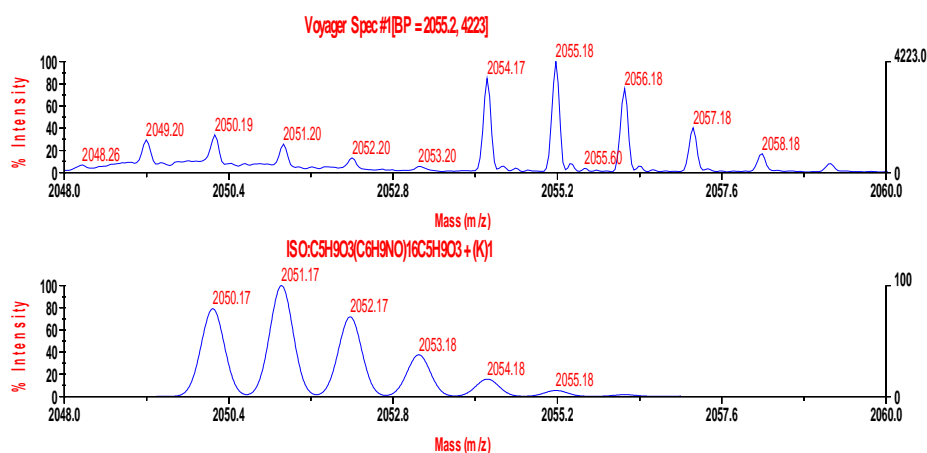

Figure 3.10. MALDI ToF spectrum of PVP, run 1 in Table 3.1, prepared as illustrated in Scheme 3.3, showing the experimental isotopic distribution (top) and the theoretical one (bottom) assigned to structure 35 in Table 3.4.

3.5.2.3 Analysis of peaks *n* and *p* by MALDI ToF analysis

The possibility of end group structure **28**, Scheme 3.6, was ruled out. This leaves two possible end group structures, **39** and **40**, in Figure 3.11, as the sources of peaks *n* and *p* in Figure 3.7. Both satisfy the criteria that the CH_3–CH– is isolated from the main chain.
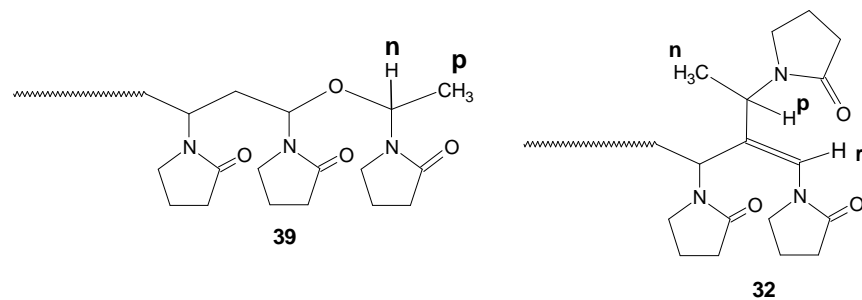
Figure 3.11. Proposed structures for end group giving signals *n* and *p*.

MALDI ToF analysis of the sample used to acquire the ^{1}H-NMR spectrum in Figure 3.8 is shown in Figure 3.12 below. The evolution of the peaks assigned to the end group in **32** (Figure 3.12) is marked by an asterisk.
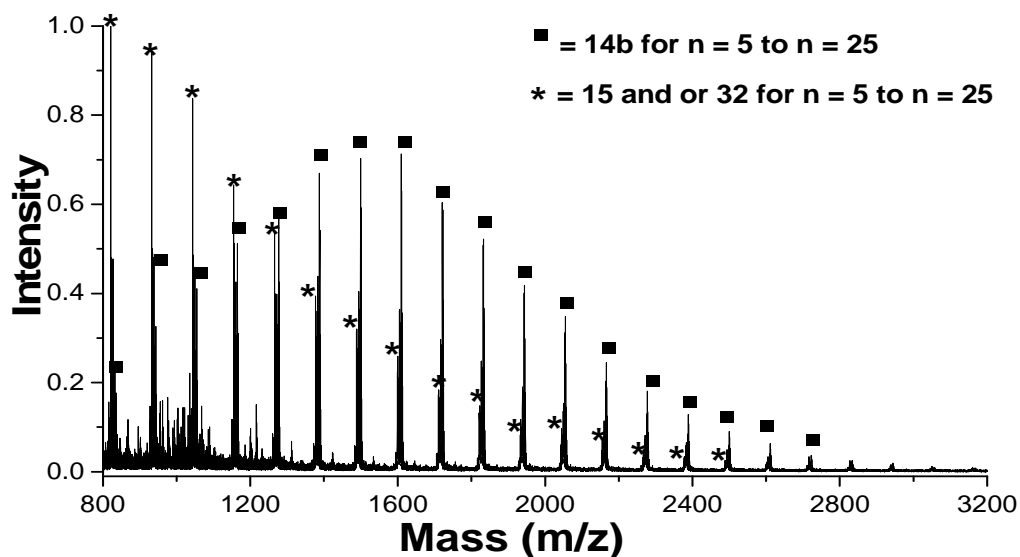
Figure 3.12. MALDI ToF mass spectrum of PVP sample used to acquire the NMR spectrum in Figure 3.7, with n as the degree of polymerization.

Although this series of peaks is attributed to both **15 and 32** (Table 3.2) it would seem on the basis of this evidence to imply that **32** is the origin of *n* and *p*. However, it is still plausible to presume that if signals *n* and *p* were given by **39**, this end group could be fragmenting during ionization step of the MALDI ToF. Beyou *et al.*[25] showed that for PS prepared by NMP the linkage between the terminal styrene unit and the O is weak and it cleaved during ionization. If **39** fragments, it would be indistinguishable from the isotopic cluster of **32**.
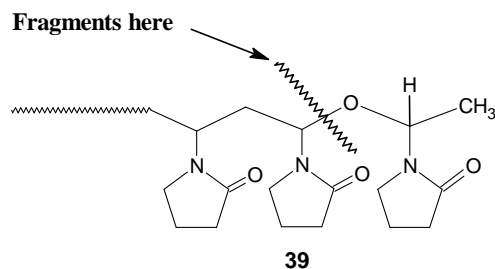
Figure 3.13. Illustrating the fragmentation of structure 39 in the MALDI ToF MS to give a structure with an isotopic pattern similar to that of structure 32.

3.6 Conclusions

α-Hydroxyl functional PVP was successfully synthesized with good control over molecular weight and PDI. To ensure that all the chains were α-hydroxyl functional, an alcohol functional initiator (ACP) was used. However, it was observed that a significant number of side reactions also take place. This is presumably due to the reactivity of the monomer used in this work. N-vinyl lactam monomers are highly reactive. This is due to conjugation of the vinyl group to the amide linkage which results in the carbon atom of the CH= in the vinyl group to be very susceptible to electrophilic addition reactions. In this work, it appears that this propensity for side reactions (mainly addition of protons to the vinyl group) seemed to be increased by the alcohol functionality. It probably causes mildly acidic conditions which favor these side reactions. This has also been observed in the RAFT-mediated polymerization of NVP with a carboxylic acid functional RAFT agent (**49**)[26] (Chapter 1). The extent of the side reactions was, however, small as the control attained in the final polymer was good.

The end groups were thoroughly characterized by ^{1}H-NMR spectroscopy as well as MALDI ToF MS. It was shown that the thiocarbonyl thio moiety is rather labile. The instability of thiocarbonyl thio end groups is known to increase with temperature. The evidence presented in this work implies that structure **32** is the source of the signals *n* and *p*. It was not established if the vinyl group of this end group is polymerizable and if so does it copolymerize with the monomer. Also it can be speculated that the proton *p* can be abstracted to give a very stable allylic radical. If so, its impact on the kinetics would need to be assessed as well.

References

(1)   M. L. Coote and L. Radom, *Macromolecules*, 2004. **37**: p.590-596.

(2)   S. Perrier and P. Takolpuckdee, *J. Polym. Sci., Part A: Polym. Chem.*, 2005. **43**: p.5347-5393.

(3)   G. Moad, E. Rizzardo and S. H. Thang, *Aust. J. Chem.*, 2005. **58**: p.379-410.

(4)   M. H. Stenzel, L. Cummins, G. E. Roberts, T. P. Davis, P. Vana and C. Barner-Kowollik, *Macromol. Chem. Phys.*, 2003. **204**: p.1160-1168.

(5)   L. Luo, M. Ranger, D. G. Lessard, D. L. Garrec, S. Gori, J.-C. Leroux, S. Rimmer and D. Smith, *Macromolecules*, 2004. **37**: p.4008-4013.

(6)   J. T. Lai and R. Shea, *J. Polym. Sci., Part A: Polym. Chem.*, 2006. **44**: p.4298-4316.

(7)   A. Theis, T. P. Davis, M. H. Stenzel and C. Barner-Kowollik, *Polymer*, 2006. **47**: p.999-1010.

(8)   V. Coessens, T. Pintauer and K. Matyjaszewski, *Prog. Polym. Sci.*, 2001. **26**: p.337-377.

(9)   S. Qin, D. Qin, W. T. Ford, D. E. Resasco and J. E. Herrera, *J. Am. Chem. Soc.*, 2004. **126**: p.170-176.

(10)   G. Clouet, M. Knipper and J. Brossas, *Polym. Bull.* , 1984. **11**: p.171-174.

(11)   A. Favier, M. T. Charreyre, P. Chaumont and C. Pichot, *Macromolecules*, 2002. **35**: p.8271-8280.

(12)   K. Dutta and A. S. Brar, *J. Polym. Sci., Part A: Polym. Chem.*, 1999. **37**: p.3922-3928.

(13)   A. Postma, T. P. Davis, G. Li, G. Moad and M. S. O'Shea, *Macromolecules*, 2006. **39**: p.5307-5318.

(14)   T. M. Legge, A. T. Slark and S. Perrier, *J. Polym. Sci., Part A: Polym. Chem.*, 2006. **44**: p.6980-6987.

(15)   Y. Liu, J. He, J. Xu, D. Fan, W. Tang and Y. Yang, *Macromolecules*, 2005. **38**: p.10332-10335.

(16)   J. C. Zhuo, *Molecules*, 1999. **4**.

(17)   E. Senogles and R. A. Thomas, *J. Chem. Soc. Perkin Trans.*, 1980. **2**: p. 825.

(18)   R. A. Hickner, C. I. Judd and W. W. Bakke, *J. Org. Chem.*, 1967. **32**: p.729.

(19)   G. Montaudo, F. Samperi and M. S. Montaudo, *Prog. Polym. Sci.*, 2006. **31**: p.277-357.

(20)   X. Jiang, P. J. Schoenmakers, J. L. J. v. Dongen, X. Lou, V. Lima and J. Brokken-Zijp, *Anal. Chem.*, 2003. **75**: p.5517-5524.

(21)   A. Favier, C. Ladavie, M. T. Charreyre and C. Pichot, *Macromolecules*, 2004. **37**: p.2026-2034.

(22)   F. Cerreta, A. M. L. Nocher, C. Leriverend, P. Metzner and T. N. Pham, *Bul.l Soc. Chim. Fr.*, 1995. **132**: p.67-74.

(23)   C. Schilli, M. G. Lanzendorfer and A. H. E. Muller, *Macromolecules*, 2002. **35**: p.6819-6827.

(24)   M. Destarac, D. Charmot, X. Franck and Z. Zard, *Macromol. Rapid Commun.*, 2000. **21**: p.1035-1039.

(25)   E. Beyou, P. Chaumont, F. Chauvin, C. Devaux and N. Zydowicz, *Macromolecules*, 1998. **31**: p.6828-6835.

(26)   G. Pound, J. B. McLeary, J. M. McKenzie, R. F. M. Lange and B. Klumperman, *Macromolecules*, 2006. **39**: p.7796-7797.

Chapter 4

Thiocarbonyl thio end group removal by an ATRA based radical exchange process for the preparation of α,ω-hydroxyl telechelic functional PVP

4.1 Introduction

The need for making end functional polymers has been pointed out in Chapter 2. They are essential building blocks for making block copolymers and polymer networks. For example telechelic hydroxyl functional polymers are precursors for making polyurethanes and polyesters. They can also be crosslinked using multi-functional isocyanates to form networks. Therefore, there is a great need for making telechelic polymers. Frequently, systems for making telechelic polymers are inherently designed in such a way that the initial polymer is α-end functional. The ω-end functionality is then introduced in extra post polymerization synthetic steps. Post polymerization end group modification for RAFT made polymers, at the ω-chain end, results in the removal of the thiocarbonyl thio end group. The advantages of this have been pointed out in Chapter 2 (Section 2.4.5.2).

In Chapter 3, details on how to prepare α-hydroxyl functional PVP by the RAFT process were presented. In this Chapter, a new approach to remove the thiocarbonyl thio ω-end group is presented. The process is based on radical induced reduction of the thiocarbonyl thio moiety. The radicals are generated as in ATRA.[1] ATRA and ATRP are based on the same mechanism. However, unlike with the latter, in ATRA only one molecule is added, there are no multiple monomer additions. Radicals are generated by the homolytic cleavage of the R-X bond of an appropriate alkyl halide (e.g. an α-bromo ester) catalyzed by a transition metal complex (e.g. a Cu complex). The transition metal catalyst simultaneously undergoes a one-electron oxidation step. In this work, Cu^{I} was generated in situ by reduction of Cu^{II} using ascorbic acid. The radicals then add to the thiocarbonyl thio moiety at the ω-chain end of the polymer as illustrated in Scheme 2.2 (Chapter 2). The sequence of reactions anticipated in this work is shown in Scheme 4.1. HEBP (**4**, Chapter 3) was used as the alcohol functional α-bromo ester. The use of radical reduction as a means of end

modifying RAFT made polymers has been described in Section 2.4.5.3 (Chapter 2). It takes advantage of the tendency of the thiocarbonyl thio moiety to react easily with radicals by addition-fragmentation.[2]
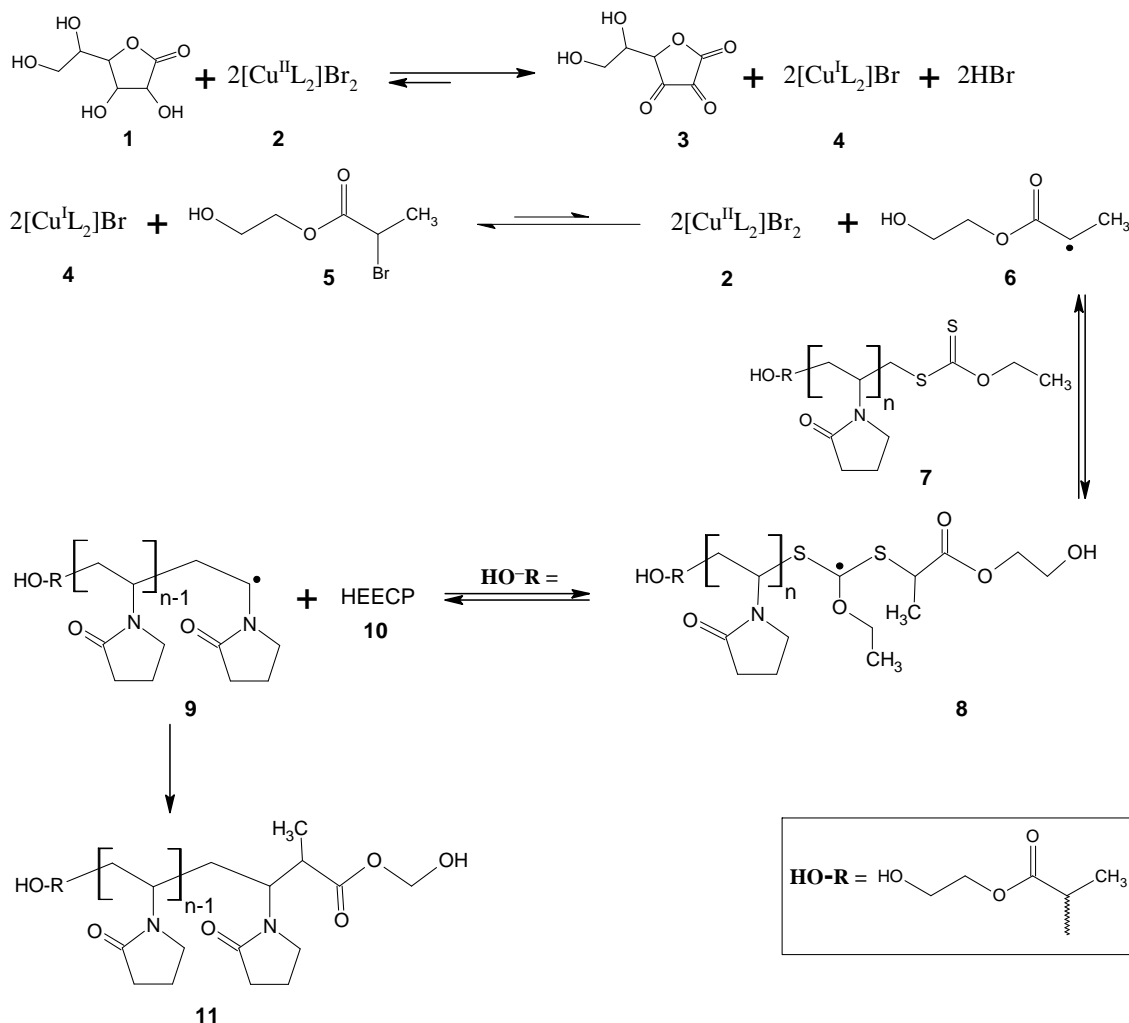
Scheme 4.1. Modification of RAFT made PVP's thiocarbonyl thio chain end moiety to produce ω-hydroxyl end functional PVP by ATRA.

The hydroxyl telechelic functional PVP was characterized by SEC, ^{1}H-NMR, UV-vis and MALDI ToF MS. Quantification of the hydroxyl functionality was done by derivatizing the hydroxyl end groups with TAI. This produced a well resolved ^{1}H-NMR signal for the α-methylene protons of the subsequent carbamate. By comparing the integration values for the α-methylene signal of the TAI derivatized PVP and those of the backbone of the polymer chain, quantitative information was obtained.

4.1.1 Materials

PVP oligomers from runs 1-3, Table 3.1 (Chapter 3) were used in this work. HEBP (**5**) was prepared as described before (Section 3.2.2, Chapter 3). $Cu^{II}Br_2$ (Aldrich), PMDETA (Across), ascorbic acid (Sigma) and TREN (Aldrich) were used as received. Dichloromethane was dried over anhydrous $MgSO_4$ overnight and distilled under normal pressure before use. TAI was from Fluka.

4.1.2 Synthesis of Me$_6$TREN

Me$_6$TREN was prepared exactly as described by Britovsek *et al.*[3] TREN, 3.00 mL (19.9 mmol), acetic acid, 135 mL, and acetonitrile (600 mL) were added to 1000 mL round bottom flask, followed by aqueous formaldehyde (49.0 mL, 660 mmol, 37 wt%). The mixture was stirred for an hour and subsequently cooled to 0 °C. Sodium borohydride 10.0 g (13.4 mmol) was then added slowly and the mixture was allowed to stir for 48 h. Afterwards all solvents were evaporated. The subsequent residue was made strongly basic with 3 M aqueous sodium hydroxide, and extracted 6 times with dichloromethane. The combined dichloromethane extracts were dried over anhydrous $MgSO_4$, overnight, and the solvent evaporated. The residue was dissolved in pentane, filtered, and the filtrate was dried under vacuum for 24 h to give 3.87 g (86 %) of Me$_6$TREN as pale yellow oil. ^{1}H-NMR (CDCl$_3$): δ (ppm) = 2.18 (s, 18 H, –NC**H**$_3$), 2.34 (m, 6 H, –NC**H**$_2$CH$_2$NCH$_3$), 2.57 (m, 6 H, –C**H**$_2$NCH$_3$).

4.2 Instrumentation

NMR, SEC, and MALDI ToF MS analysis was carried out as described in Section 3.3.2 (Chapter 3).

4.3 Results and discussion

Table 4.1. Initial results for the end group modification of PVP by Cu catalyzed radical reduction, in acetone at 65 °C for 15 h

[a]PVP	PVP:HEBP mol:mol	HEBP:Cat. mol:mol[c]	[b]Cat:[c]Asc. A mol:mol	[d]Modification	After modification M_n^{SEC}	PDI
1	1:10	10:1	4:1	>99%	2 483	1.30
1	1:20	10:1	4:1	>99%	2 599	1.26

[a]. These values are from the sample labeled as run 1, Table 3.1, Chapter 3, which was used for this particular experiment.

[b]. Cat. refers to the Cu catalyst ([CuL]Br$_2$), and L is the ligand.

[c]. Asc. A refers to ascorbic acid.

[d]. Modification refers to the relative extent of the removal of the thiocarbonyl thio moiety as estimated by ^{1}H NMR.

4.3.1 The catalyst system

The use of Cu catalysts is well documented in ATRA and in atom transfer radical cyclisation (ATRC) reactions.[1,4] The radical generation mechanism is very similar to that in ATRP.[5,6] A lot of progress has been made in increasing the catalytic efficiency of the Cu based catalyst systems by researches working in ATRP.[6] Aliphatic amines like PMDETA (**12**) and Me$_6$TREN (**13**) have been shown to be ligands that give very active Cu^I catalysts.[5,6]
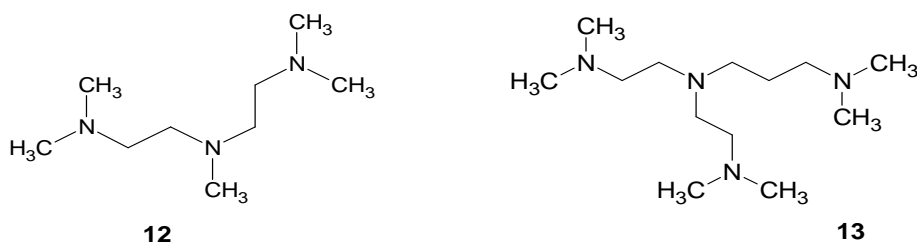
Figure 4.1. PMDETA (12) and Me6TREN (13).

In light of that, PMDETA was initially selected as the ligand as it is readily available commercially. The Cu^I complex was generated *in situ* by reduction of the Cu^{II} complex by ascorbic acid. This technique has been utilized in ATRP where it is termed AGET ATRP.[7-9] In the AGET ATRP system, one starts with an alkyl halide initiator and the Cu catalyst in the oxidatively stable Cu^{II} form. The activator (Cu^I catalyst) is generated by the addition of an appropriate reducing agent. In this work ascorbic acid (**1**) was used as the reducing agent. In the redox reaction, ascorbic acid (**1**) is oxidized to dehydroascorbic acid (**3**) whilst Cu^{II} is reduced to Cu^I, the activator.

In the AGET system the Cu^{II} complex, formed by termination reactions, is regularly reduced back to the active Cu^{I} form by ascorbic acid. Consequently lower amounts of Cu catalyst are therefore required as the active Cu^{I} form is constantly regenerated in the system. This has been termed activators regenerated (ARGET) ATRP by its inventors.[10] This system was therefore chosen as, due to the low catalyst loading, it would be fairly "green". Also the Cu^{II} precursor is air stable thereby improving the handling of the system.

4.3.2 ATRA end group modification

The anticipated mechanism for the end group modification is shown in Scheme 4.1. Ascorbic acid reduces the Cu^{II} complex to Cu^{I}. The Cu^{I} complex then homolytically cleaves the R–Br bond of the HEBP (**5**) to give the radical (**6**). The radical then adds to the reactive C=S bond of the thiocarbonyl thio moiety at the ω–chain end to give the intermediate radical **8**. The intermediate radical (**8**) can either fragment back to give **7** and **6** or fragment to give the macro radicals **9** and **10**. By applying a large excess of the alkyl radical **6**, the chances of the macroradical **9** (once formed) to react with the alkyl radical **6** are increased. The reaction between the radicals **6** and **9** to give the desired telechelic hydroxyl functional PVP (**11**) is irreversible so this reaction step is like a sink. Therefore these conditions should lead to an overall increase in the yield of the product (**11**).

4.3.3 Initial experiments

In the initial experiments PVP to HEBP ratios of 1:10 and 1:20 were used. Acetone was used as the solvent. In a typical experiment, the Cu complex was prepared separately by mixing equimolar amounts of CuBr$_2$ and the ligand (PMDETA) in a round bottom flask. The mixture was stirred, with some mild heating until all the CuBr$_2$ dissolved and the solution had a characteristic green color. The polymer and HEBP were weighed into a separate Schlenk flask followed by the addition of an appropriate amount of the Cu complex. Ascorbic acid was dissolved in acetone separately. Its dissolution was improved by adding small amounts of water. The polymer + HEBP + Cu complex (reaction mixture) as well as the ascorbic acid solutions were then degassed separately by 2 freeze pump thaw cycles. The reaction mixture was dipped into an oil bath preheated and thermostated at 65 ^{o}C. The experiment was started by adding the ascorbic acid solution to the reaction mixture. The reaction was stopped by removing the flask from the oil bath and diluting with an excess of THF. The polymer was then purified by running through a short column of neutral activated aluminum

oxide in order to remove the copper catalyst. It was eventually precipitated from diethyl ether. Recovery was typically low (40–60%). Sample was lost by running it through the column to remove the catalyst.

4.3.4 End group analysis

^{1}H-NMR analysis showed that, in both cases, there was complete removal of the xanthate chain end. However the polymers were largely terminated at the ω-end by unsaturated end groups and aldehyde functionality. The causes of each of this are now discussed individually.
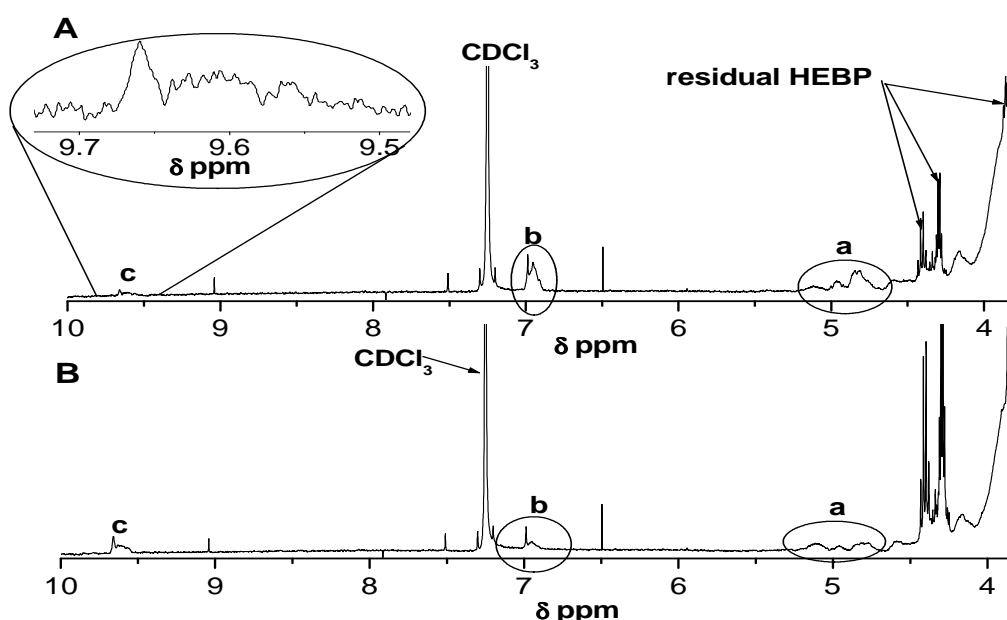
Figure 4.2. ^{1}H-NMR spectrum of PVP for PVP:HEBP = 1:10 (A) and PVP:HEBP = 1:20 (B). Peaks *a* and *b* were attributed to the unsaturated chain ends, N–CH=C*H* and N–C*H*=CH respectively. Peak *c* was attributed to aldehyde chain ends (–CH$_2$–CHO).

4.3.4.1 Unsaturated chain ends

Perrier *et al.*[11] attributed the occurrence of the unsaturated end groups to disproportionation reactions. It is possible that the chain end unsaturation here was also caused by disproportionation. Perrier *et al.*[11] also showed that this side reaction could be suppressed by using polymer to azo-initiator (radical source) of 1:20. Each azo compound (e.g. AIBN) decomposes to give 2 identical radicals (R•). In this work, however, each HEBP (**5**) molecule can only give one radical (**6**). Therefore, for run 2, Table 4.1, even with a 20 fold excess of HEBP the system will still be short of

radicals, by approximately half in order to totally suppress the disproportionation. From Figure 4.2, it is evident, though, that the extent of chain end unsaturation was much reduced with a 20 fold excess of HEBP.

In Chapter 3 (Section 3.5.2), it was shown that the xanthate end group is very labile and cleaves off under mild conditions to give unsaturated chain ends. As the reactions were carried out at 65 $^{\circ}$C, for 15 h, it can be assumed, therefore, that this side reaction was also contributing to give the chain end unsaturation. These side reactions are illustrated in Scheme 4.2 below.
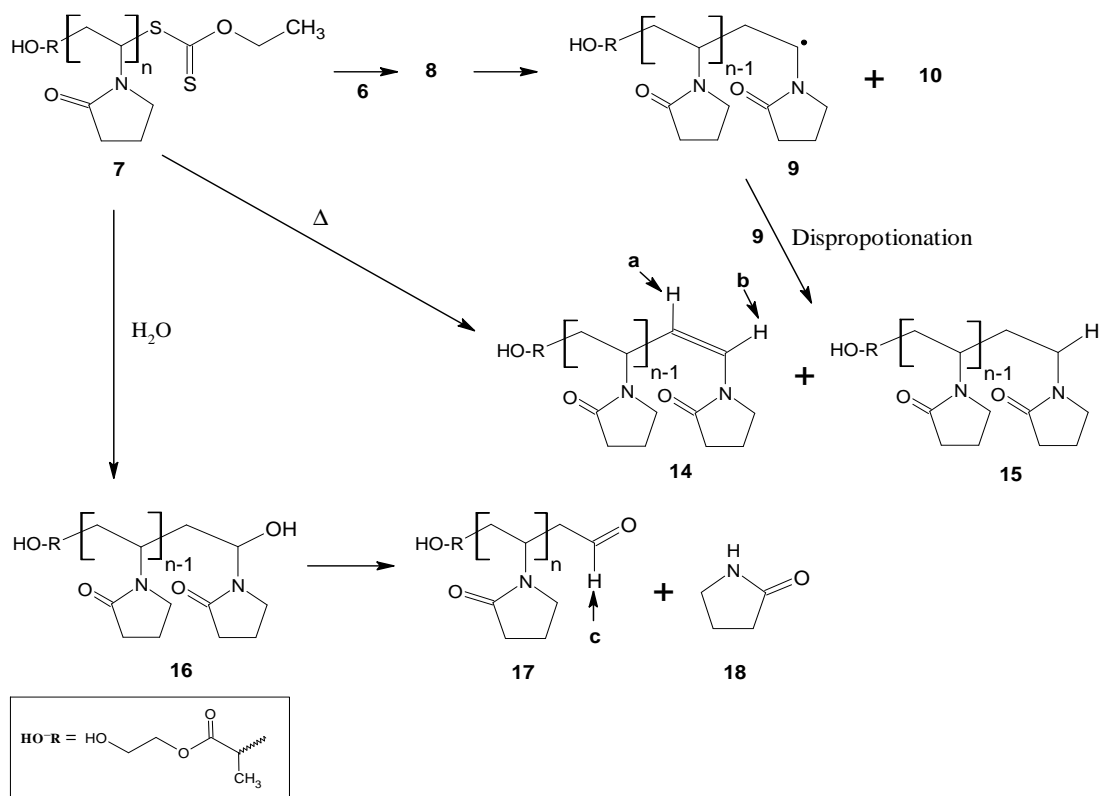
Scheme 4.2. Illustration of side reactions that give rise to the protons labeled *a*, *b* and *c* in Figure 4.2.

4.3.4.2 Aldehyde end groups

Aldehyde end groups are known to form in the polymerization of NVP in water with initiation by H_2O_2.[12] Polymers prepared in this way are terminated by hydroxyl groups. However, the hydroxyl end group at the ω-chain end (i.e. as with **16**, Scheme 4.2) splits off to give an aldehyde chain end functionality as well as pyrrolidone. Their appearance here was, however, surprising. The hydrolytic susceptibility of the thiocarbonyl thio moiety terminating RAFT made PVP has not been reported.

However, work in our group has shown that this end group can be hydrolyzed off under surprisingly mild conditions. It was observed that a significant amount of the xanthate end group was lost by merely dialyzing an aqueous solution of PVP as a way of removing residual monomer. The polymer had been isolated by precipitating three times from diethyl ether. It was found that by heating up the dialysis mixture to 40 ^{o}C for 16 h yielded PVP oligomers terminated with an OH end group as with **16**. Further heating at 120 ^{o}C for 20 h resulted in quantitative conversion of the hydroxyl end group to the aldehyde end functionality. The appearance of aldehyde chain ends in this case was therefore attributed to the hydrolysis of the xanthate chain ends initially to give **16**. This is then followed by the splitting off of the terminal pyrrolidone unit to give **17** and **18**. It is plausible to suggest that the electron withdrawing effect of the amide linkage, on the pyrrolidone, renders the C–S bond of **7** weak enough to be hydrolyzed under very mild conditions. In this work, the water had been added to aid the dissolution of ascorbic acid. However, it constituted only 2% of the solvent for the end group modification reactions. These end group assignments were confirmed by MALDI ToF MS analysis.

4.3.4.3 MALDI ToF analysis

Figure 4.3 shows the MALDI ToF MS spectrum of sample 2, Table 4.1. Two main series of peak were observed. The mass difference between clusters of peaks corresponds to the monomer unit in each series. An expansion of the *m/z* region 1700–1830 is shown for illustrative purposes. The structural assignments corresponding to each of these are given in Table 4.2.
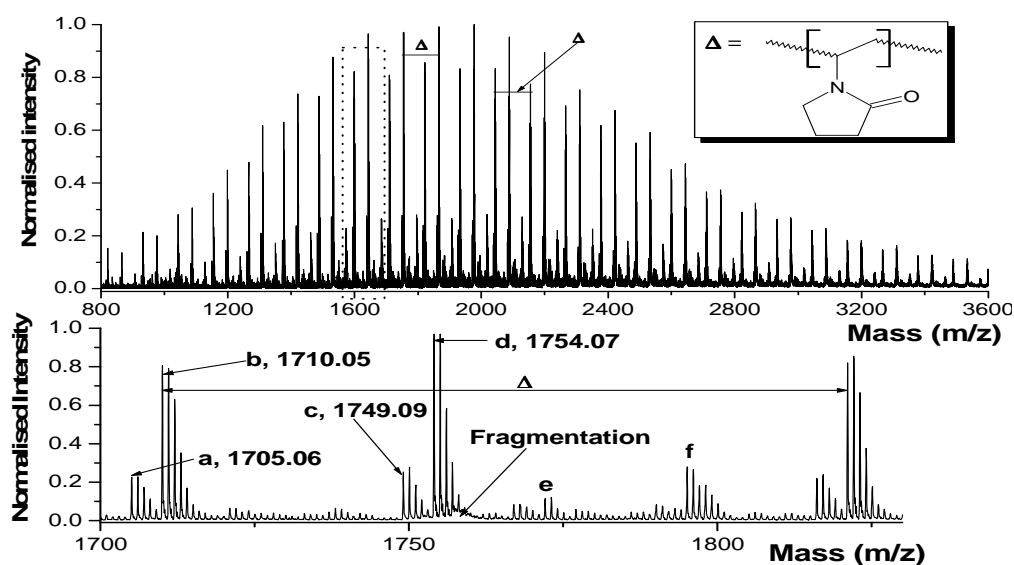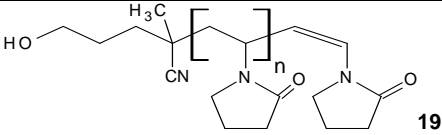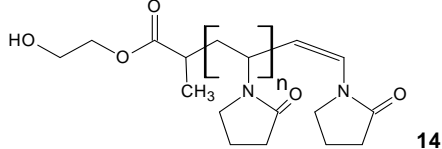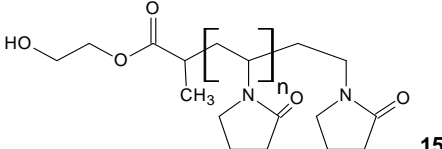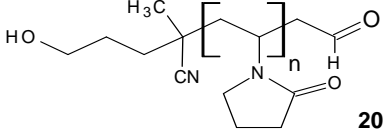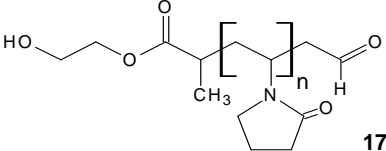

Figure 4.3. MALDI ToF MS spectrum for the end group modification reaction with PVP:HEBP = 1:20.

Table 4.2. Structural assignments for the MALDI TOF MS spectrum if Figure 4.3

Peak	Monoisotopic mass (+ K$^+$)		Structure	Cationization	n
	Expt.	Theo.			
a	1705.06	1704.97	**19**	K$^+$	13
b	1710.05	1709.97	**14**	K$^+$	13
		1711.98	**15**	K$^+$	13
c	1749.09	1749.02	**20**	K$^+$	14
d	1754.07	1753.99	**17**	K$^+$	14

The isotopic clusters represented by cluster d correspond to PVP oligomers capped at the α-end by the R group and at the ω-end by unsaturated end groups (**17**). Isotopic clusters a and b are attributable to chains terminated at the ω-chain end by unsaturated end groups. This is for both initiator and R group derived chains (**19** and **14**) respectively. Structure **15**, expected as a disproportionation product, if present, can not be clearly resolved from **14**, cluster b. However its calculated mass (1711.98) differs by almost 2 Da from the experimental value (1710.05). It is therefore highly probable that this end group was not formed, or was formed in very little amounts. This implies that the chain end unsaturation was largely caused by the decomposition of the thiocarbonyl thio end group as described in Chapter 3 (Section 3.5.2). The isotopic clusters c corresponds to initiator derived oligomers terminated at the ω-chain end by an aldehyde functionality (**20**). A lot of fragmentation was also evident under cluster d. The clusters of peaks labeled e and f were not assigned. It is possible that the macro radical **9** could have been deactivated by the Cu^{II} complex to give a PVP oligomer terminated by a bromine atom. The MALDI ToF analysis showed no evidence of such species. Terminal C–Br bonds have been shown to be labile at

the chain ends of PMMA prepared by ATRP.[13] Although the PMMA case is very system dependent, it is possible that if present in this case they are also labile and cleave off.

4.3.5 Optimized reactions

The results presented in the section 4.3.4 were generally reproducible. It was suggested that the lability of the xanthate end group required much milder reaction conditions to be used. This will minimize chances of it thermally cleaving off. It has been shown in ATRP that by using very efficient catalytic systems polymerizations can be ran at ambient temperature.[14] These can be prepared by complexing the copper with ligands like Me$_6$TREN (**13**).[14] Also from the last section it was evident that water had to be excluded from the reaction media to avoid formation of aldehyde chain ends. This could be achieved by using Cu^I (as in conventional ATRP) instead to using Cu^{II} and reducing it *in situ* to Cu^I. However, during the course of this work, Min *et al.*[15] showed that ascorbic acid could be used to regenerate the Cu^I complex under reaction conditions were its solubility in the reaction media was limited (heterogeneous conditions). This they showed by polymerizing a variety of acrylates in anisole using Cu^{II} and ascorbic acid to regenerate the Cu^I species. Ascorbic acid is sparingly soluble in anisole. The polymerization proceeded with good control over M$_n$ and PDI.[15]

In light of this it was decided that there was no need to add water in order to totally solubilize the ascorbic acid. Acetone is hygroscopic and takes up moisture from air very readily therefore it was decided to abandon it as a solvent for further reactions. The end group modifications reactions were therefore re-ran in acetonitrile at 35 ^{o}C. The PVP:HEBP was increased to ~1:35. In the end group modification method proposed by Perrier *et al.*[11], polymer to azo compound ratios of 1:20 were used. As illustrated in Scheme 2.2, Chapter 2, each azo compound produces two radicals. The initiator efficiency of dialkyldiazenes (azo initiators) typically ranges between 50 to 70% in low viscosity media.[16] Based on this it was estimated that the eventual radical to polymer ratio will be approximately 1:(20–30). Therefore it made sense to try the end modification at 1:35 for polymer to HEBP given that each molecule of the latter (**5**) can only give rise to one radical (**6**) Scheme 4.1.

Table 4.3. Results for the end group modification of PVP by Cu catalyzed radical reduction, in acetonitrile at 35°C for 40h

[a]PVP	PVP:HEBP mol: mol	HEBP:Cat. mol:mol	[b]Cat:Asc. A[c] mol:mol	[d]Modification.	After modification	
					M_n^{SEC}	PDI
2	1:35	5:1	2:1	>99%	2 473	1.23

[a,b,c, and d] are as described for Table 4.1.

The molar ratio of HEBP to the Cu catalyst was reduced to 5:1, whilst that of the catalyst to ascorbic acid was also reduced to 2:1. These changes were meant to increase the radical flux in the system. The end modified polymer was again analyzed by ^{1}H-NMR, MALDI ToF, SEC and UV-vis.

4.3.5.1 ^{1}H-NMR and UV-vis analysis

^{1}H-NMR analysis showed a complete removal of the thiocarbonyl thio moiety, Figure 4.4. Figure 4.4 shows a clear comparison of the unmodified and the end modified PVP samples. The characteristic xanthate chain end signal (a) in the unmodified PVP sample is marked. This signal is clearly removed by the end modification reaction as shown in the spectrum of the end modified sample. There was no evidence of aldehyde end groups. This was expected as the experiment was ran under (almost) total exclusion of moisture. Analysis by UV-vis also confirmed disappearance of the thiocarbonyl thio moiety. The xanthate end group of the polymer has a peak at λ_{max} = 280 nm, in water. This is illustrated in Figure 4.5.

unmodified
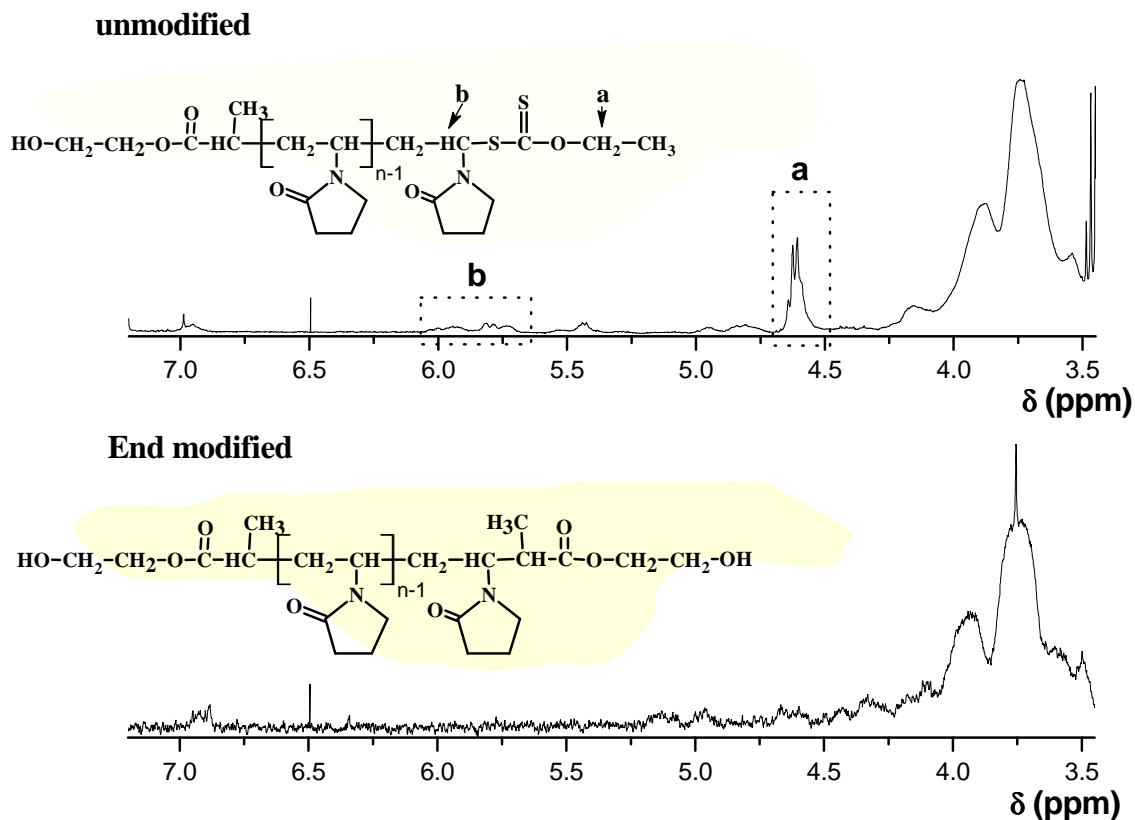
End modified

Figure 4.4. ^{1}H-NMR spectrum of unmodified (top) and end modified PVP (bottom) from Table 4.2.
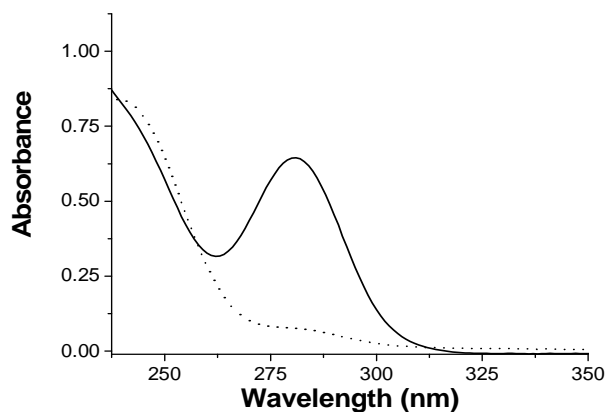
Figure 4.5. UV-vis spectra of the polymer capped with the Z group of the xanthate (bold line) and the end modified polymer (from Table 4.2), (dashed line) in water.

4.3.5.2 MALDI ToF MS analysis

MALDI ToF MS analysis also confirmed the end group modification. Figure 4.6 shows the MALDI spectrum and corresponding structures are shown in Table 4.4. The spectrum shows two series of peaks separated by a mass difference of ~16 which is the difference between Na and K. It can be

concluded therefore, that both series of peaks correspond to the same species cationized by the two different cations. The lower series is cationized by Na^+ and the higher one by K^+. KTFA was added to the sample as the cationizing agent, however, Na^+ must have been present as an impurity related to the sample history.
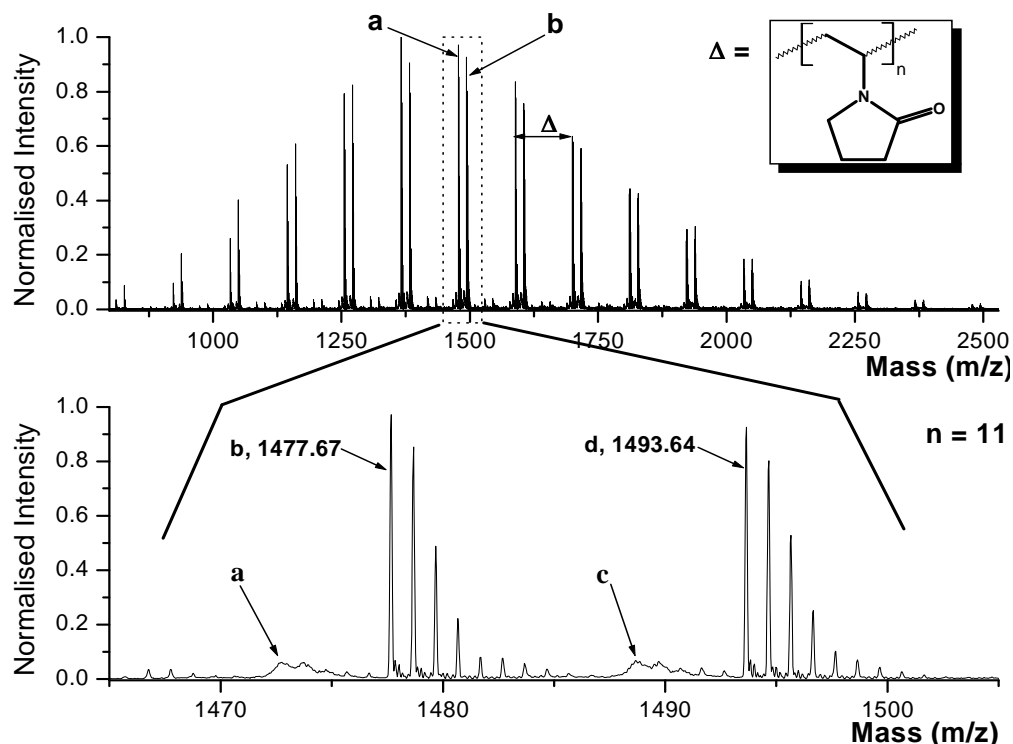
Figure 4.6. MALDI ToF MS spectrum of end modified PVP Table 4.2.

Fragmentation was observed under peaks labeled a and c. These positions are also where the signals for the disproportionation products (**14** and **15**) were expected. Oligomers capped at both ends by initiator fragments (**21**) were also expected to appear in this region. The fragmentation probably resulted from traces of oligomers capped by the xanthate end group. Peaks b and d were attributed to the desired alcohol telechelic functional oligomers (**11**) according to Scheme 4.1. However, the experimental mass was 1.04 Daltons lower than the calculated mass. This difference was consistent for both the Na^+ and K^+ cationized series of peaks. This difference is outside the error range for this technique. The peaks b and d do not correspond with any other structures conceivable considering the chemistry anticipated here even for the side products. This offset (1.04 Da) will probably be resolved with further research.

Table 4.4. Structural assignments for the MALDI ToF spectrum in Figure 4.6

Peak	Monoisotopic mass (+ K$^+$)		Structure	Cationization	n
	Expt.	Theo.			
a	?	1471.71	**14**	Na$^+$	10
	?	1473.73	**15**	Na$^+$	10
	?	1473.73	**21**	Na$^+$	11
b	1477.67	1478.85	**11**	Na$^+$	11
c	?	1487.69	**14**	K$^+$	10
	?	1489.70	**15**	K$^+$	10
	?	1489.70	**21**	K$^+$	11
d	1493.64	1494.68	**11**	K$^+$	11

Peaks b and d were assigned to **11** for the Na$^+$ and the K$^+$ cationized series. The molar mass distribution depicted in the MALDI ToF spectrum appears lower than of the original sample that was end modified (see Figure 3.1, Chapter 3). The PVP samples with the end groups modified by the ATRA based method were first purified by column chromatography using THF, in order to remove the Cu catalyst, and precipitated from diethyl ether. In this case the sample recovered was only 37.3% of the starting material. It is possible that some of the polymer sample (mainly the higher molecular weight fractions) could have been retained on the column and stayed behind. It is also plausible that some of the polymeric amide groups bind with the Cu catalyst, with the higher molar mass chains obviously binding more Cu. Therefore they get retained more on the column. The molar mass distribution shown, in Figure 4.6, can not, however, be considered to be truly reflective of that of the original sample. SEC analysis confirmed the lower M_n value, Table 4.3. The SEC plots are shown in Figure 4.7 below.
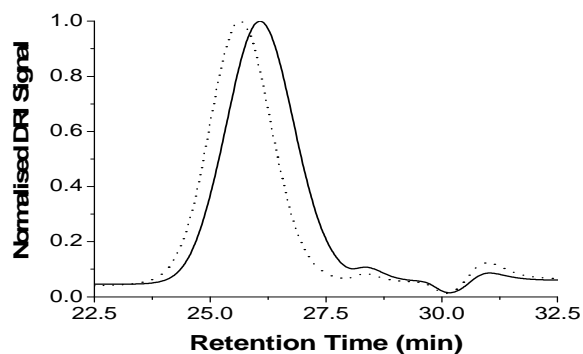
Figure 4.7. SEC plots before (bold line) and after end group modification (broken line) for the PVP samples described in Table 4.2.

This trend, of lower M_n and lower PDI values, described above, was typical. It is also observed in Table 4.1 where the M_n values after end modification were generally lower.

4.4 Quantification of the alcohol end functionality

Coessens and Matyjaszewski[17] as well as Moad *et al.*[18-20] have shown that protic end groups can be analyzed by ^{1}H-NMR, by derivatizing the polymers with TAI (**22**) and observing the signals produced. TAI reacts rapidly and quantitavely with protic end groups as illustrated in Scheme 4.3 below. The TAI is added into the NMR tube about 10–15 minutes before acquiring the ^{1}H-NMR spectrum. The derivatization reaction completes in the time it takes to set up the NMR experiment.
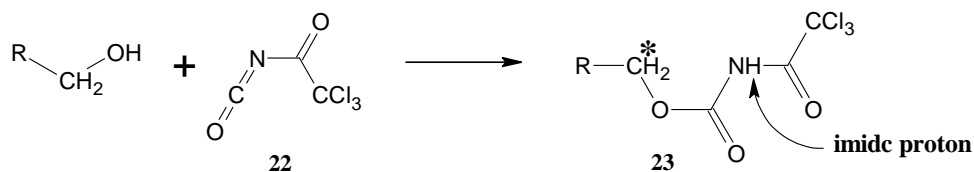
Scheme 4.3. Reaction of TAI (22) with hydroxyl groups to produce a carbamate, 23, with deshielded α-methylene protons (*) and an imidic proton.

Coessens and Matyjaszewski[17] used the technique in order to prove the incorporation of an allyl alcohol functionality that was introduced at the end of PMMA oligomers prepared by ATRP. They followed the signal of α-methylene protons (asterisked) (**23**, Scheme 4.3). It gave a clearly visible signal at 4.50 ppm in the ^{1}H-NMR spectrum (CDCl$_3$) which was not obscured by signals of the

polymer backbone. On the other hand, Moad *et al.*[18-20] were able to quantify the chain end protic groups using the signal produced by the imidic proton.

4.4.1 Derivatization procedure

The terminal hydroxyl functionality of the PVP prepared in this work was also quantified by the same technique. Unmodified PVP sample from run 2, Table 3.1, Chapter 3, and the end modified PVP from Table 4.4 above were selected. The analysis was carried out as described by Moad and coworkers.[20] A PVP sample, ~45 mg was dissolved in an appropriate amount of deuterated acetone (CD_3COCD_3) and was transferred to an NMR tube. An excess of TAI (~10 mg) was then added to the NMR tube and the reaction was assumed to be complete after about 15 minutes.
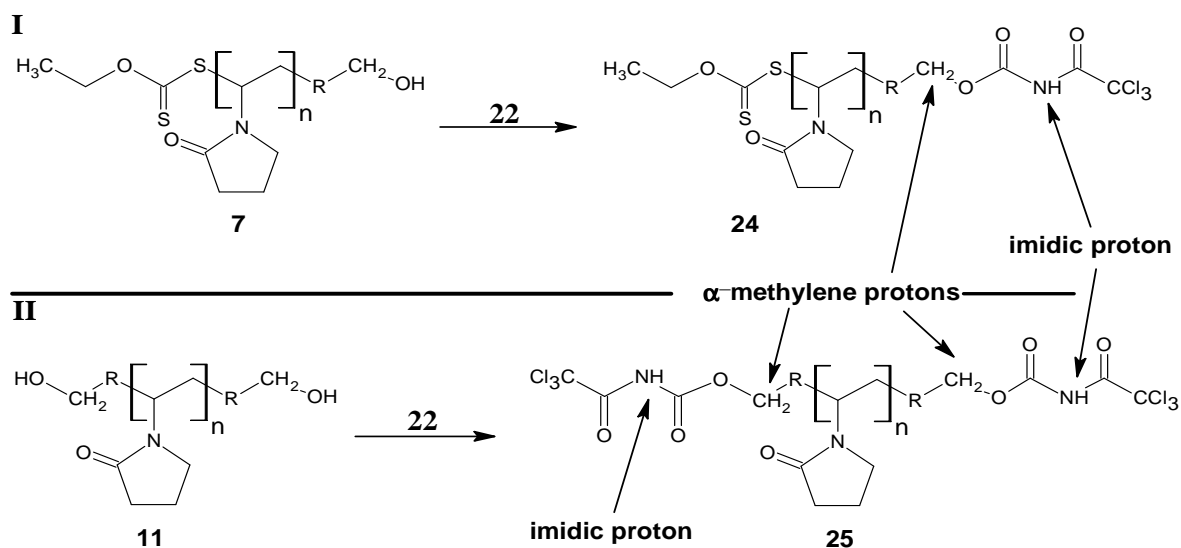
Scheme 4.4. Derivatization of hydroxyl end groups of PVP oligomers with TAI, 22 for unmodified (I) and end modified (II) samples. The PVP samples are described in Table 4.2.

Figure 4.8 shows the ^{1}H-NMR spectra of the derivatized end functional PVP, before and after the end group modification. From Figures 3.5 (Chapter 3) and 4.4 (Chapter 4), the α-methylene protons to the hydroxyl group can not be clearly observed by ^{1}H-NMR. They overlap with the polymer backbone signals at 3.0–4.2ppm. However, the derivatization with TAI to produce the carbamate deshields these protons. The deshielding has been estimated to produce a chemical shift difference of 0.5–0.9 downfield, for primary alcohols.[21] The connectivity of the deshielded α-methylene protons, at 4.35–4.55 ppm, in Figure 4.7, to the polymer backbone is demonstrated in the next chapter where the derivatized, end modified polymer was analyzed by two dimensional NMR. For

the end modified PVP prepared in this work (**11**) it was assumed that the α-methylene protons of the derivatized PVP (**25**) appear at the same chemical shift as the chain end functionality is similar.
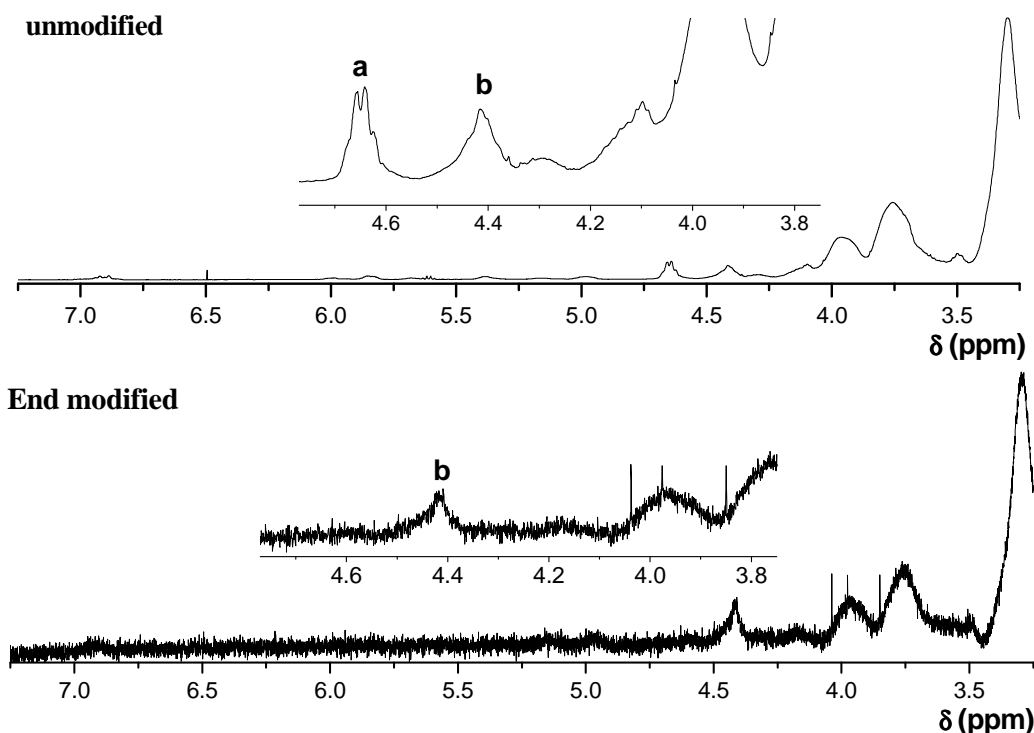
Figure 4.8 **^{1}H-NMR spectra of TAI derivatized α-hydroxyl-ω-xanthate functional PVP (top) and α,ω-hydroxyl functional PVP (bottom) oligomers (Table 4.2), in CD$_3$COCD$_3$. The signal *a* is due to the xanthate's –C*H*$_2$CH$_3$ protons, whilst that marked *b* is that of the α-methylene protons as indicated in Scheme 4.4.**

The relative proportion of hydroxyl end functionality was then estimated using equation 4.1 below.

$$\text{Relative OH end functionality } (f_n^{OH}) = \frac{M_n^{SEC}}{M_n^{NMR}} \tag{4.1}$$

The M_n^{SEC} value (2 473) was taken from Table 4.3. The M_n^{NMR} values were estimated by comparing the area of the signal due to the α-methylene protons of the carbamate (**25**) to those of the polymer backbone. For the polymer backbone, the broad signal at 3.0–4.2ppm (*f* + *g*, Figure 3.5, Chapter 3) was used.

The M_n^{NMR} values calculated using the signal for the α-methylene protons of the TAI derivatized PVP before and after end modifying, were 2513 and was 2630 respectively. This gave f_n^{OH} values of 1.08 and 1.88 respectively. A f_n^{OH} value of 1.08 (before end modifying) implies that about 8% of the chains already had hydroxyl functionality at both ends (were already telechelic). This would imply that there were a lot of termination reactions due to radical-radical coupling. The PDI of the polymer, however, was 1.29. This shows that the polymerization reaction still proceeded with good control; therefore this high value can only be attributed to inherent inaccuracies in this type of measurement. The fact that an alcohol functional initiator was used means that all chains formed had an alcohol functionality at the α-end. This serves to magnify the extent of termination by radical-radical coupling as any such event creates a hydroxyl telechelic functional oligomer. This, in turn, results in an increase in the relative "concentration" of hydroxyl functionality relative to the degree of polymerization. This technique therefore provides a way of estimating the relative extent of radical-radical coupling. The f_n^{OH} of 1.88 for the end functional sample in Table 4.5 means that 88% of the chains were telechelic since ~100% of the chains were α-hydroxyl functional. This shows that the technique developed here is a very useful method for preparing telechelic functional materials.

4.5 Conclusions

A method for preparing hydroxyl telechelic functional PVP was developed. The very reactive nature of the monomer, NVP, entails that the reaction conditions must by chosen carefully. This is more so when the precursor polymer, for the end group modification, is prepared by RAFT-mediated polymerization using a xanthate CTA. The labile nature of the C–S bond between the terminal NVP residue and the thiocarbonyl thio end group was shown in Chapter 3. It was shown that the use of very active Cu catalysts, resulting in the use of ambient temperature conditions, ensures that the xanthate chain end is removed only by the radical exchange with the alkyl radical. It would appear that this method of radical reduction is more effective, at preparing telechelic functional oligomers, than the one suggested by Perrier *et al*.[11] Radical reduction suffices for removing the thiocarbonyl thio moiety. However, the use of azo compounds to effect this requires elevated temperatures. For sensitive systems like PVP, side reactions will also become significant.

The main shortcoming of the system developed here is that the Cu catalyst has to be removed. The method of catalyst removal used here (column chromatography), although effective, lowers the yield of the recovered polymer significantly. This is a problem for scaling up. Also it has the effect of changing the sample composition as it appeared that the M_n^{SEC} for the end modified and purified values were lower than those for the original polymer sample. This was presumed to be due to the retention of the polymer sample in the column. This would mainly affect the higher molar mass oligomers. It is anticipated that improvements in ATRP, towards the reduction of the amount of catalyst used will be directly taken advantage of here.

References

(1)   J. Iqbal, B. Bhatia and N. K. Nayyar, *Chem. Rev.*, 1994. **94**: p.519-564.

(2)   S. Z. Zard, *Angew. Chem., Int. Ed. Engl.*, 1997. **36**: p.612-685.

(3)   G. J. P. Britovsek, J. England and A. J. P. White, *Inorg. Chem.*, 2005. **44**: p.8125-8134.

(4)   A. J. Clark, *Chem. Soc. Rev.*, 2002. **31**: p.1-11.

(5)   W. A. Braunecker and K. Matyjaszewski, *Prog. Polym. Sci.*, 2007. **32**: p.93-146.

(6)   N. V. Tsarevsky and K. Matyjaszewski, *Chem. Rev.*, 2007. **107**: p.2270-2299.

(7)   W. Jakubowski and K. Matyjaszewski, *Macromolecules*, 2005. **38**: p.4139-4146.

(8)   K. Min, H. Gao and K. Matyjaszewski, *J. Am. Chem. Soc.*, 2005. **127**: p.3825-3830.

(9)   J. K. Oh, K. Min and K. Matyjaszewski, *Macromolecules*, 2006. **39**: p.3161-3167.

(10)   W. Jakubowski, K. Min and K. Matyjaszewski, *Macromolecules*, 2006. **39**: p.39-45.

(11)   S. Perrier, P. Takolpuckdee and C. A. Mars, *Macromolecules*, 2005. **38**: p.2033-2036.

(12)   F. Haaf, A. Sanner and F. Straub, *Polym. J.* , 1985. **17**: p.143-152.

(13)   C. D. Borman, A. T. Jackson, A. Bunn, A. L. Cutter and D. J. Irvine, *Polymer*, 2000. **41**: p.6015-6020.

(14)   J. Xia, S. G. Gaynor and K. Matyjaszewski, *Macromolecules*, 1998. **31**: p.5958-5959.

(15)   K. Min, H. Gao and K. Matyjaszewski, *Macromolecules*, 2007. **40**: p.1789-1791.

(16)   G. Moad and D. H. Solomon, *The Chemistry of Radical Polymerization*. Second ed. 2006, Elsevier: Amsterdam.

(17)   V. Coessens and K. Matyjaszewski, *Macromol. Rapid Commun.*, 1999. **20**: p.127-134.

(18)   A. R. Donovan and G. Moad, *Polymer*, 2005. **46**: p.5005-5011.

(19)   A. Postma, T. P. Davis, A. R. Donovan, G. Li, G. Moad, R. Mulder and M. S. O'Shea, *Polymer*, 2006. **47**: p.1899-1911.

(20)   A. Postma, T. P. Davis, R. A. Evans, G. Li, G. Moad and M. S. O'Shea, *Macromolecules*, 2006. **39**: p.5293-5306.

(21)   J. C. Ronda, A. Serra, A. Mantecon and V. Cadiz, *Macromol. Chem. Phys.*, 1994. **195**: p.3445-3457.

Chapter 5

Facile end group modification, by radical exchange, with hydrogen peroxide and the subsequent synthesis of a PVP hydrogel

5.1 Introduction

This chapter represents a continuation of our pursuit for methods to remove the xanthate ω-end group from RAFT made PVP. In this work, radical exchange with H_2O_2 is introduced as an efficient and very clean method for removing the xanthate end group and also as a facile method of introducing alcohol end group functionality.

The use of H_2O_2 to remove the thiocarbonyl thio end group of polymers prepared by the RAFT process was first mentioned in the first publication on RAFT, by its inventors.[1] This was also cited by Moad *et al.*[2] in a later publication. However in the first reported work on RAFT, H_2O_2 was only made reference to in terms of its ability to oxidize thiocarbonyl thio compounds (**1**) to produce sulfines (**2**). This was in reference to work by Cerreta *et al.*[3] These workers found that oxidizing agents like peroxides can oxidize thiocarbonyl thio compounds firstly to sulfines (**2**). These subsequently converted to dithioperoxyesters (**3**) and thiolesters (**4**) if kept at room temperature for a few days.
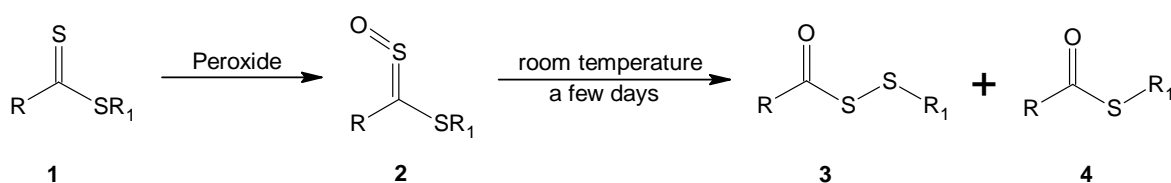
**Scheme 5.1. Oxidation of thiocarbonyl thio compounds by peroxides.**

The use of peroxides to oxidize the thiocarbonyl thio ω-end group of RAFT made polymers was also reported by Vana and coworkers.[4] They showed that this end group could be oxidized to the thiolester by simply stirring a mixture of the polymer with *tert*-butyl hydroperoxide at room

temperature for twelve hours. In Vana's work, however, the use of room temperature conditions ensures that the peroxide does not decompose to give radicals which can participate in radical exchange with the thiocarbonyl thio moiety. This end group modification method does not provide complete desulphurization.

The use of peroxide based systems to end modify RAFT end groups by radical reduction was reported, firstly, by Destarac *et al.*[5] and later by Chong *et al.*[6] The peroxide was used as an initiator in 2-propanol. Chong *et al.* used a toluene/2-propanol system. In all cases complete end group removal was claimed.

In this work we would like to propose a facile method of xanthate end group removal whereby the RAFT made polymer is simply heated with H_2O_2. H_2O_2 has traditionally been used as an initiator in the aqueous polymerization of NVP. In line with the radical exchange method introduced by Perrier *et al.*[7] and also used by us, in the previous chapter, this method works by applying a flood of radicals to a solution of the polymer. By using the α-hydroxyl functional PVP prepared as described in Chapter 3, this process affords a facile route to hydroxyl telechelic functional PVP. This is illustrated in Scheme 5.2.

Thermal decomposition of H_2O_2 (**5**) produces the highly reactive hydroxyl radicals (**6**). These then add to the C=S double bond of the xanthate end group of the native polymer (**7**) to produce the intermediate radical **8**. This process, again, takes advantage of the ability of thiocarbonyl thio compounds to react easily with radicals.[8] The intermediate radical (**8**) then fragments to give the macroradical (**9**). By using a very high ratio of H_2O_2 to polymer, the system will be flooded with hydroxyl radicals (**6**). This then ensures that the termination will be largely by combination between the macroradical and the hydroxyl radicals to produce dead chains. It was also assumed that the removed thiocarbonyl thio compound (**10**) does not participate in side reactions with the macroradical (**9**). The thermal stability of **10** was not assessed, since it was not isolated. The modified polymer was cleaned by precipitating from diethyl ether and washing the precipitate several times with diethyl ether. This provides a very clean method for not only removing the thiocarbonyl thio end group, but also for introducing hydroxyl end group functionality.
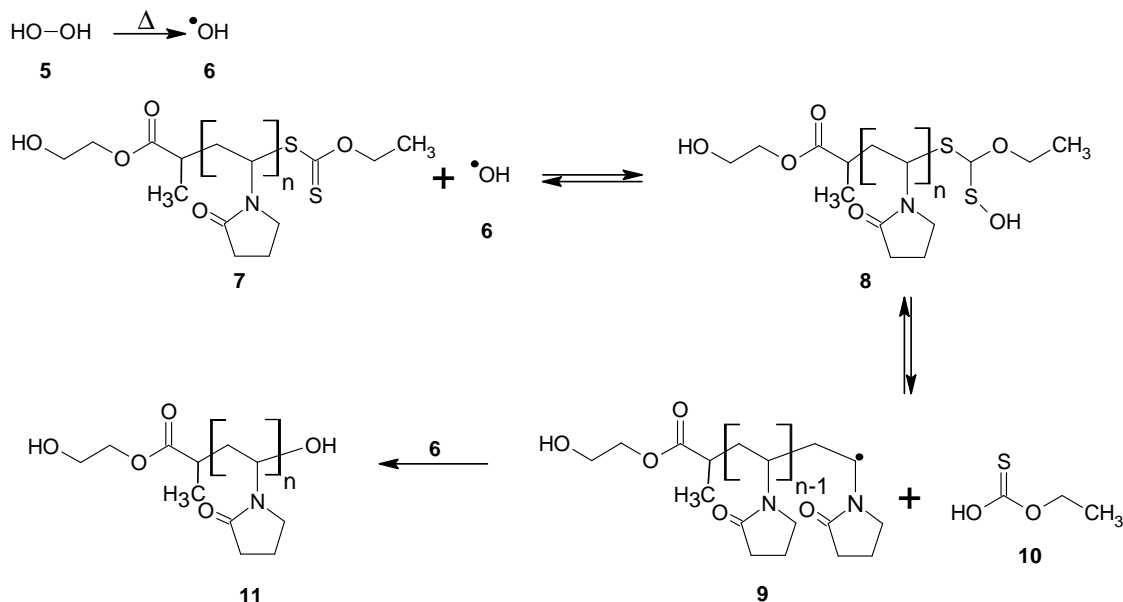
Scheme 5.2. Removal of the xanthate end group of RAFT made PVP, by H$_2$O$_2$, to produce hydroxyl telechelic functional PVP.

The end modified PVP produced here was characterized by SEC, ^{1}H-NMR and by MALDI ToF MS, as described in Chapters 3 and 4. As in Chapter 4, the extent of hydroxyl functionality was estimated by derivatizing with TAI and analyzing with ^{1}H-NMR. In order to demonstrate the usefulness of the end modification technique, the hydroxyl telechelic functional PVP produced here was crosslinked with a tri functional isocyanate to form a hydrogel. This is shown in Section 5.4.

5.1.1 Materials

The PVP sample 3, Table 3.1, (M$_n$^{SEC} = 2 483, PDI = 1.31) was used for the results presented in this chapter. H$_2$O$_2$ was obtained from R and S Enterprises as a 35% aqueous solution.

5.2 Experimental procedures and analysis

A typical experimental procedure is described here. PVP (0.5 g, 0.20 mmol) was dissolved in acetone (10 mL) in a 50 mL Schlenk flask. H$_2$O$_2$ (0.393 g, 4.03 mmol) was subsequently added to the reaction vessel and the mixture was stirred until it was homogenous. The reaction mixture was then degassed by two successive freeze pump thaw cycles and backfilled with argon before being dipped into an oil bath preheated to 60 ^{o}C in order to start the reaction. The reaction was stopped

after 16 h, by opening the flask and diluting the reaction mixture with THF. The polymer was isolated by precipitating it from diethyl ether. It was then washed several times with diethyl ether and dried under vacuum for 48 h. The end modified PVP prepared in this work was analyzed as described in Chapters 3 and 4.

5.3 Results and discussion

The anticipated process for the end group removal is shown in Scheme 5.2. In all cases, the end group removal was quantitative. This was confirmed by ^{1}H-NMR analysis, UV-vis and MALDI ToF MS. Figure 5.1 below shows a typical ^{1}H-NMR spectrum for end modified PVP.
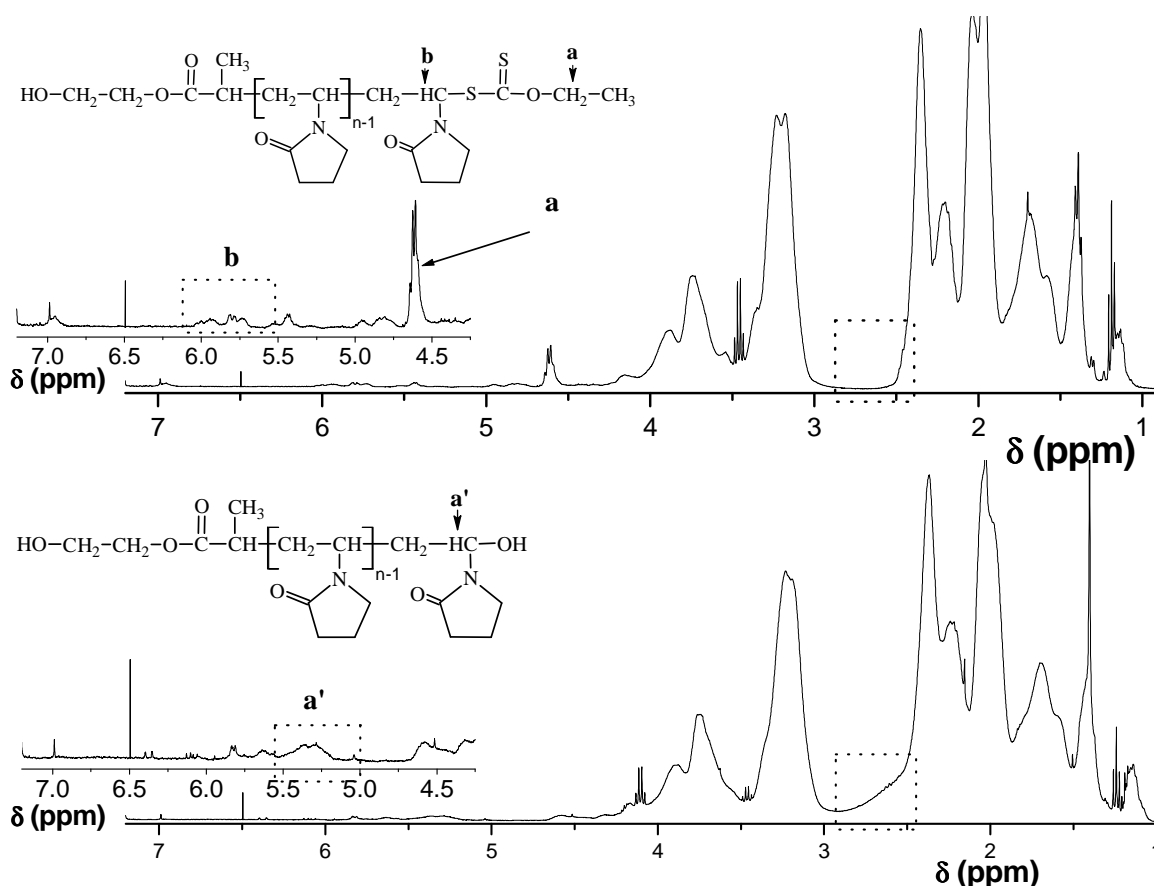

Figure 5.1. [1]**H-NMR spectra of** α**-hydroxyl-**ω**-xanthate end functional PVP (top) and** α,ω**-telechelic hydroxyl end functional PVP (bottom), prepared by heating** α**-hydroxyl-**ω**-xanthate functional PVP with H$_2$O$_2$ at 60 ^{o}C for 15 h. Both samples are described in Table 5.1.**

Figure 5.1 shows that the signal for the quartet at 4.6 ppm due to the –C**H$_2$**–CH$_3$ protons of the xanthate has disappeared from the spectrum of the end modified PVP sample. Another characteristic

signal, b, in the unmodified PVP sample is also missing after modification. This confirms the removal of the xanthate chain end. The broad signal, a', at 5.45–5.75 ppm, in the spectrum of the end modified sample, was attributed to the –N–**CH**– proton on the terminal repeat unit. The M_n^{NMR} calculated by comparing the integral value of the end group signal to the backbone signal was 2116 (M_n^{SEC} = 2508, see Table 5.1). This implies that about 82% of the chains were terminated by the hydroxyl end group as with structure (**11**), Scheme 5.2. It is also interesting to note that signals due to an unsaturated end group of the repeat unit, (–**CH** = **CH**), (see Figures 3.5 and 3.6, Chapter 3) were not observed in the spectrum of the end modified PVP sample. These signals are clearly observed in the spectrum of the unmodified PVP. Also in the spectrum of the PVP end modified by the ATRA based process (Chapter 4), these signals were always found. This implies that the hydroxyl radicals (**6**) are so reactive that they easily add to this end group and oxidize it. The aldehyde end group was also not observed. This was surprising given the findings in Chapter 4, were it was observed to form when the end modification reactions were carried out at 65 $^{\circ}$C for 15 h (see Section 4.3.4.2, and Scheme 4.2, Chapter 4). It appears improbable to speculate that the mere difference of 5 $^{\circ}$C, is enough to have caused this shift. This issue was not investigated further. The shoulder at, 2.50–2.80 ppm was attributed to –**CH$_2$**–CO$_2$H protons. These are poorly resolved from the polymer backbone signal. They arise possibly from hydrolysis of the lactam rings of the repeat unit by acid (impurity) catalysis.[9] The water is from the H$_2$O$_2$ which was a 35% aqueous solution. This is illustrated in Scheme 5.3 below.
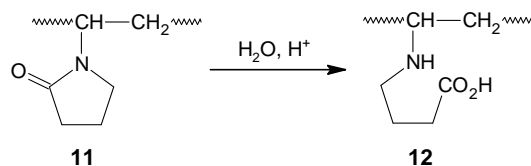
Scheme 5.3. Lactam ring opening side reaction of the NVP moiety to give a carboxylic acid derivative.

It will be shown below that the resolution of this carboxylic acid moiety can be improved by derivatizing with TAI.

5.3.1 UV-vis and SEC analysis

UV-vis analysis confirmed the removal of the xanthate end group. As in Chapter 4, the end group signal of the xanthate at λ = 280 nm was followed. This is shown in Figure 5.2.
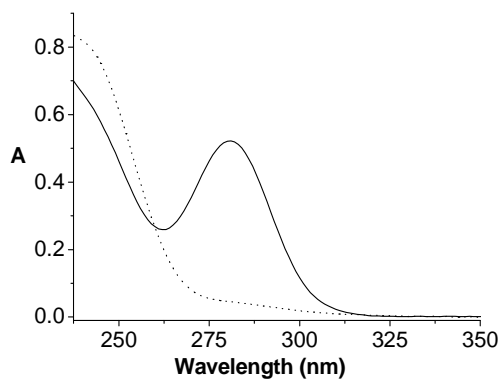
Figure 5.2. UV-vis spectra of RAFT made PVP (continuous line) and for PVP end modified by heating with H_2O_2 at 60 °C for 15 h (broken line), in water.

Table 5.1 below shows the M_n^{SEC} values before and after end modification.

Table 5.1 SEC analysis results

[a]PVP	[a]Before modification		[b]End group removal (%)	After modification	
	M_n	PDI		M_n	PDI
3	2483	1.31	>99%	2508	1.22

[a.] these values are for sample 3, Table 3.3, Chapter 3.

[b.] Removal of the xanthate end group was estimated by NMR.

The M_n values before and after end group modification were practically identical. The polydispersity index for the end modified PVP was, however, slightly lower. This could be due to baseline differences. Figure 5.3, below, shows the corresponding SEC plots.
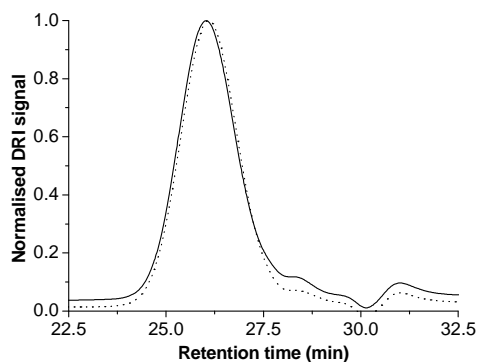

Figure 5.3. SEC plots for RAFT made PVP samples described in Table 5.1. PVP samples before and after end group modification are represented by a continuous line and by a broken line respectively.

5.3.2 MALDI ToF MS analysis

MALDI ToF analysis was carried out in order to obtain more structural information. Figure 5.4 shows the MALDI ToF MS spectrum of the end modified PVP sample in Table 5.1. Figure 5.4 shows that there was a main distribution, with the highest intensity, surrounded by several smaller distributions of less intensity. This pattern was largely typical for the PVP samples end modified by H_2O_2 treatment in this work. The corresponding structural assignments are shown in Table 5.2.
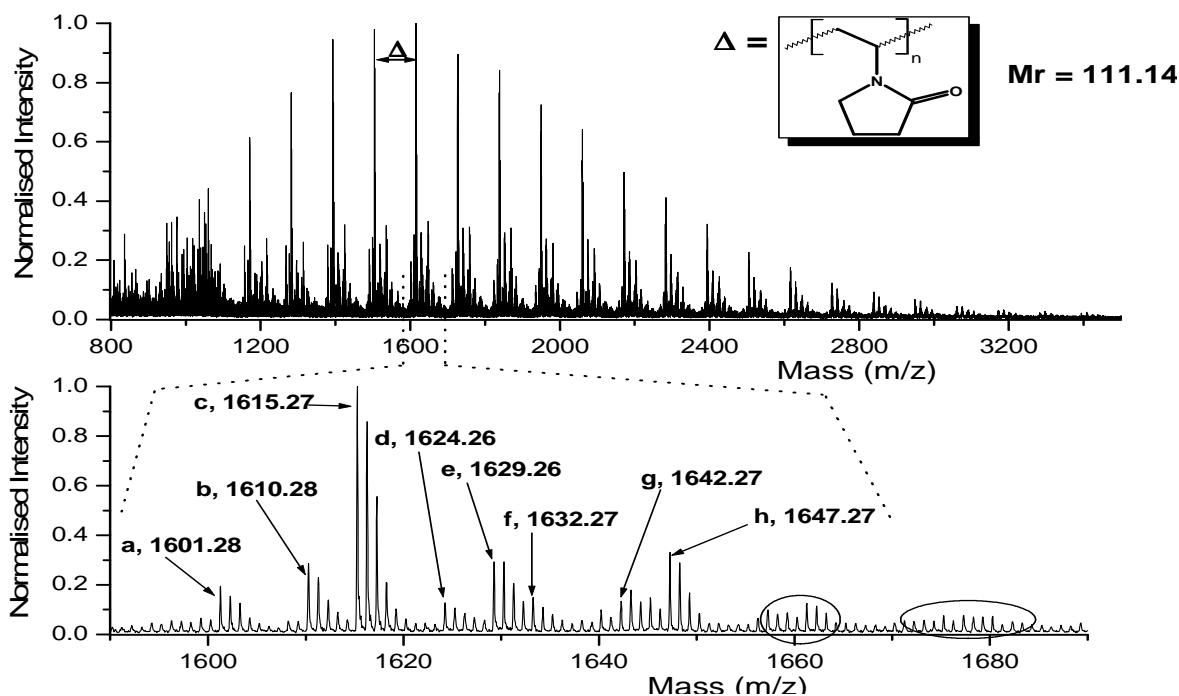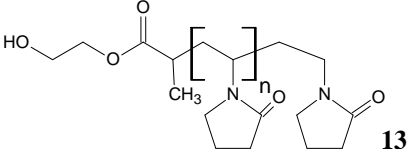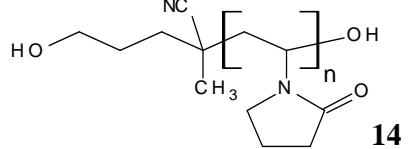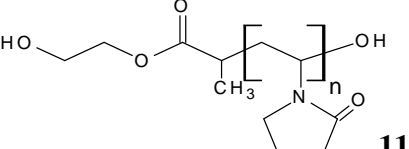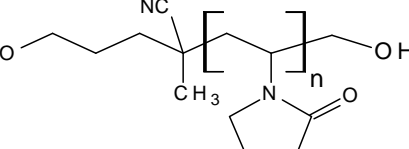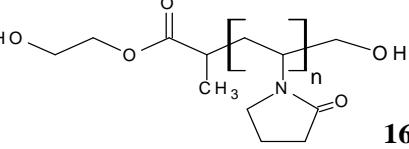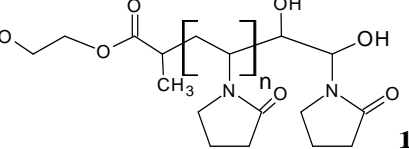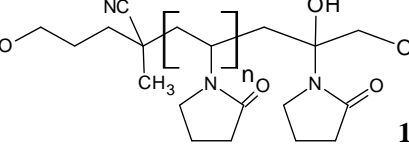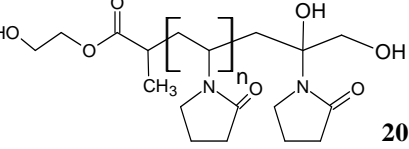

Figure 5.4. MALDI ToF mass spectrum of hydroxyl telechelic end functional PVP prepared by heating
α **-hydroxyl functional PVP with H_2O_2 at 60 ^{o}C for 15 h (same sample as in Figure 5.1).**

The peaks in the main distribution (top) are all separated by 111.14 Daltons which is the mass of the repeat unit. An enlargement of the *m/z* region 1590–1690 shows that there were seven main distinct masses. Two of very low intensity are encircled and were not assigned to any (tentative) structures. Cluster a was assigned to structure **13** which corresponded to oligomers terminated by a saturated repeat unit. Peak clusters b, c, d, and e could not be accurately assigned to their proposed structures (**14**, **11**, **15** and **16** respectively, Table 5.2). This is because the masses of the proposed structures differed from the experimentally determined masses by an average of 1.66, which again, is out of the acceptable error range for MALDI ToF MS. Their proposed structural assignments are the closest matches for the end groups which can be rationalized from the chemistry that can take place.

Nevertheless, their tentative structural assignments are now discussed. Cluster b and c were assigned to structures **14** and **11** for initiator and R group derived oligomers respectively, terminated by a hydroxyl group. This is as expected from Scheme 5.2. Clusters d and e were assigned to oligomers terminated by a –CH_2OH group. Anderson *et al.*[10] suggested that when crosslinking PVP with persulfate, SO_4^- and OH radicals are capable of abstracting hydrogen atoms from the backbone. This is illustrated in Scheme 5.3.

Table 5.2. Structural assignments for the MALDI ToF spectrum of PVP in Figure 5.4

Peak	Monoisotopic mass (+ K^{+})		Structure	Cationization	[c]n
	[a]Expt.	[b]Theo.			
a	1601.28	1600.92	**13**	K^{+}	13
b	1610.28	1611.93	**14**	K^{+}	13
c	1615.27	1616.91	**11**	K^{+}	13
d	1624.26	1625.95	**15**	K^{+}	13
e	1629.26	1630.93	**16**	K^{+}	13
f	1633.27	1632.91	**18**	K^{+}	12
g	1642.27	1641.94	**19**	K^{+}	12
h	1647.27	1641.94	**20**	K^{+}	13
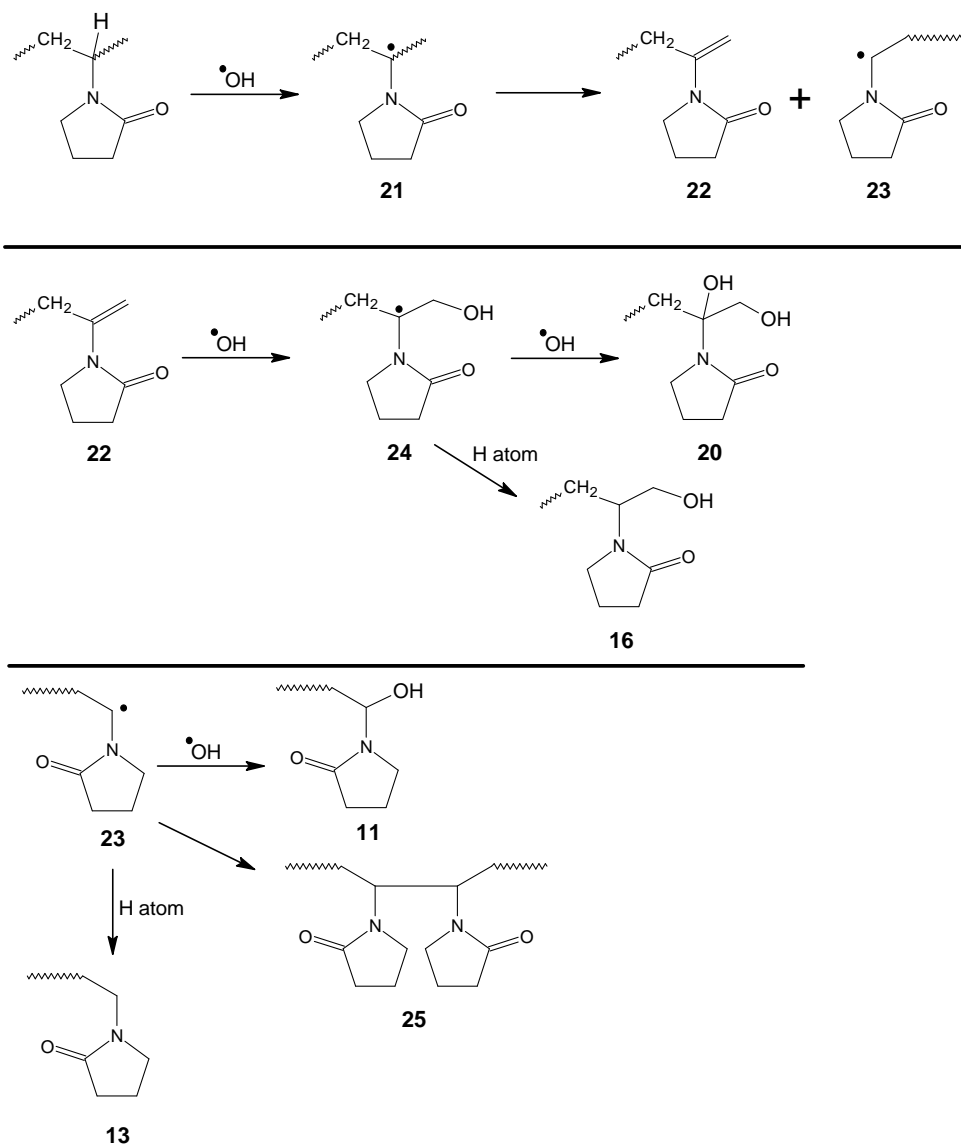
Scheme 5.3. Possible side reactions occurring during the end group modification of RAFT made PVP (7) with H₂O₂. All structures in this scheme are assumed to be R group α-hydroxyl functional.

Abstraction of a hydrogen atom from the backbone forms a macroradical which can rearrange to a more stable state by β-scission. This will lead to oligomers terminated by methylene groups (**22**) plus macroradicals (**23**). Further reactions of the oligomers terminated by the methylene group (**22**) with the hydroxyl radicals lead to structures **16** and **20** as shown. The macroradical **23** can terminate by radical-radical coupling with a hydroxyl radical or by abstracting a proton. This gives structures **11** and **13** respectively. The macroradical can also terminate by coupling with another macroradical like itself to give structure **25**. However, there was no evidence of structure **25** even within the wide

error range of 1.66 Daltons, as is the case for structures **14**, **11**, **15** and **16**. It is also possible that macroradical **21** can terminate by radical coupling with a hydroxyl radical.
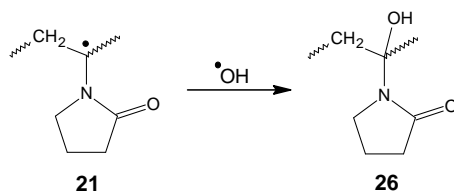
Scheme 5.4. Illustration of further reaction of macroradical (21).

If for a particular oligomer, just a single OH species is added along the chain as illustrated in Scheme 5.4, it would give a structure with a mass of 1632.91 Daltons. This serves to illustrate why there are so many small clusters in Figure 5.2. Structure **18** could form by reaction of oligomer terminated unsaturated repeat unit with hydroxyl radicals. In concluding this discussion, the MALDI ToF MS analysis did not provide conclusive evidence of the main structure (**11**) expected from Scheme 5.2. However it will be shown below that the end modified polymers had at least two hydroxyl functionalities per chain as they were successfully crosslinked. Also, the end modified PVP oligomers were reacted with TAI so as to estimate the extent of hydroxyl functionality.

5.3.3 Quantification of hydroxyl functionality by derivatizing with TAI

Derivatization with TAI (**27**) was shown to be a useful method to quantify the hydroxyl functionality in Chapter 4. The derivatization procedure was carried out for the H_2O_2 end modified PVP exactly as described in Chapter 4, see Section 4.4.1. This is illustrated below using structure **11** since 82% of the chains were terminated at the ω-chain end by the hydroxyl end group as shown.
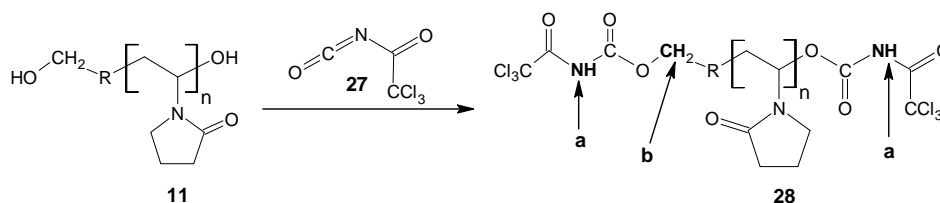
Scheme 5.5. TAI derivatization of hydroxyl end groups for end modified PVP showing the respective imidic, a, and the α-methylene protons, b, of the derivatized PVP.
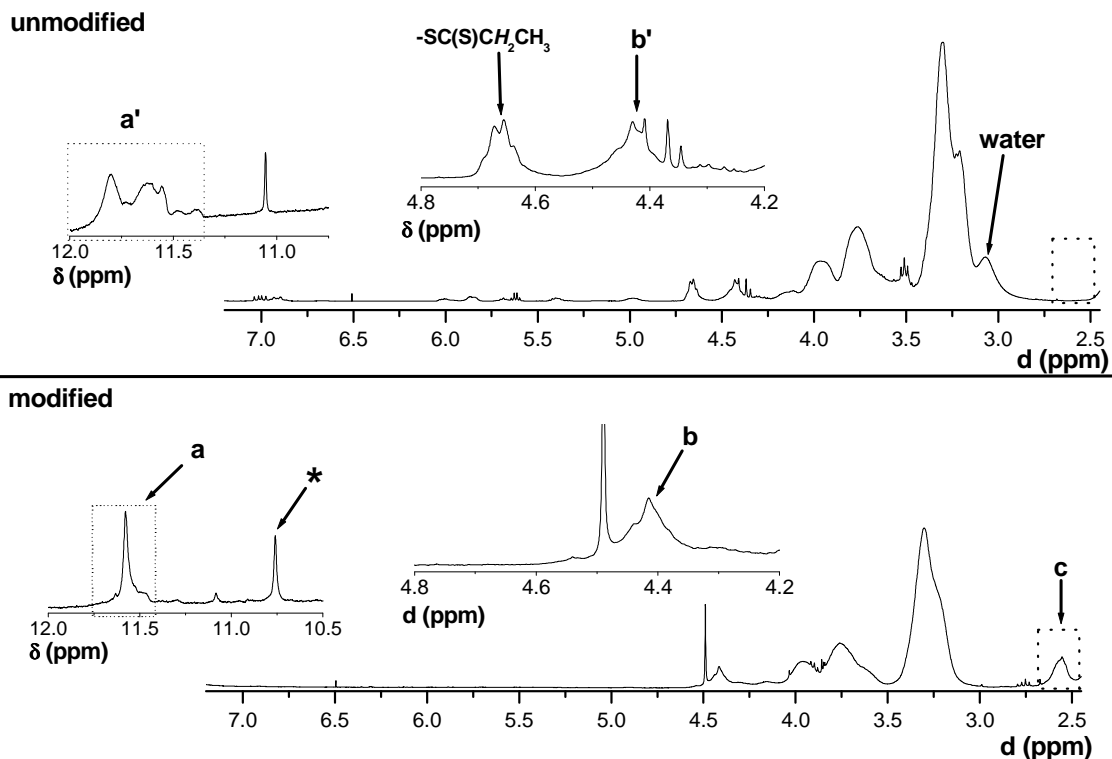
Figure 5.5. ^{1}H-NMR spectra of TAI derivatized α-hydroxyl-ω-xanthate functional PVP (top) and α,ω-hydroxyl functional PVP (bottom) oligomers, in CD$_3$COCD$_3$. The important signals a and a' and signals b and b' are assigned to the α-methylene protons and the imidic proton respectively.

The signal due to the α-methylene protons for the end modified telechelic hydroxyl functional PVP, b, had a shoulder which was probably due to an artifact or a solvent. Signal b was shown to be connected to a signal at 4.1–4.2 ppm (β–methylene protons signal) by a COSY experiment, (Appendix 3). The β–methylene protons are due to the –CH$_2$CH$_2$OC(O)– protons of the R group which are at the α-end of the derivatized PVP. The β-methylene protons, however, do not show connectivity to any other proton signal, apart from that of the α-methylene signal. This is because they are next to an ester linkage. Signal *a*, at 11.4–11.8 ppm, was assigned to the imidic proton. Imidic protons usually appear in the chemical shift region between 8–12 ppm.[11] The imidic protons did not show off-diagonal peaks in the COSY spectrum because they are not coupled to any other protons in the molecule (see a, **29**, Scheme 5.5). Signal c, at 2.6 ppm was attributed to α-methylene protons of a carboxylic acid TAI derivative. The carboxylic acid functionality is formed by ring opening of the lactam ring of the repeat unit as shown in Scheme 5.3. The α-methylene protons of, a chain end, carboxylic acid TAI derivative for RAFT made PMMA were reported to appear at 2.77 ppm by Postma *et al.*[11] Compared to Figure 5.1, in the chemical shift region marked a, it appears

that the TAI derivatization resolves the α-methylene protons of the carboxylic acid from the broad polymer backbone peak between 2.0–2.5ppm. In a COSY experiment (Appendix 4) these carboxyl α-methylene protons were shown to be connected to a signal buried under the –NH–CH$_2$CH$_2$– protons of the lactam ring (see signal h, Figure 3.5, Chapter 3). The protons giving rise to this signal are marked by an asterisk in structure **29** in Scheme 5.6 below.
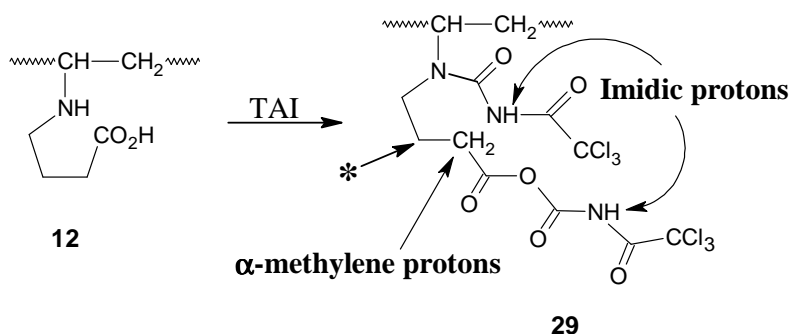
**Scheme 5.6. TAI derivatization of the carboxylic acid moiety.**

The ring opened lactam has two protic hydrogens, one on the carboxylic acid and the other on the amine group, (see **12**, Scheme 5.6). The amine proton also reacts with the TAI, as illustrated above, to give another imidic proton. The signal at 10.4–10.6 ppm was assigned to this particular imidic proton. This signal is marked with an asterisk (*****) in the spectrum of the derivatized end modified PVP above. The TAI derivatized carboxyl α-methylene protons were in a ratio of 1.11:1 with those of the TAI derivatized hydroxyl moiety, *b* (**29**, Scheme 5.5). This implies that there was approximately one ring opened lactam ring, of the NVP repeat unit, per oligomer. The imidic protons of **29** were assumed to appear in the same chemical shift region as those of **28**. Therefore TAI derivatized hydroxyl end groups make up about 47% on the integral value of the signal of the imidic protons. The 47% also includes other hydroxyl ω-end group derivatives (**15**, **16**, **18**, **19** and **20**) as illustrated in Table 5.2, Section 5.5 The M_n^{NMR} calculated, assuming that 47% of the signal for the imidic protons is for the hydroxyl end groups, was 2215. The subsequent f_n^{OH} value was 1.13, from the ω-chain end. The M_n^{NMR} calculated using the signal for the α-methylene protons (b, Figure 5.5) was 2328. This translated to a f_n^{OH} value of 1.08. This confirms that all the chains were hydroxyl functional at the α-chain end. Adding the two f_n^{OH} values up gave a total of 2.21. Therefore the H$_2$O$_2$ end modified RAFT made PVP was telechelic.

5.4 Synthesis of PVP hydrogel

To illustrate the usefulness of making hydroxyl telechelic functional polymers, the hydroxyl telechelic functional PVP made above was converted into a hydrogel. The uses of these materials were described in Section 2.6.4, Chapter 2. Hydrogels can either be (i) physically crosslinked or (ii) chemically crosslinked.[12,13] Physically crosslinked hydrogels are prepared by the crosslinking of (i) high molecular weight polymer chains due to entanglements or (ii) due to molecular interactions (e.g. van der Waals' forces, hydrogen bonds or ionic interactions) between polymer chain segments. Chemically crosslinked hydrogels are held together by covalent linkages between the polymer chains and can be prepared by a number of methods some of which are given below:[13]

- free radical induced crosslinking of high molecular weight polymer in solution initiated by free radical initiators (e.g. potassium persulfate[10]) or by high energy irradiation e.g. with gamma rays
- by copolymerizing the monomer with a crosslinking reagent or with a multifunctional macromer
- by reacting telechelic functional polymers with complementary multifunctional crosslinking agents

Physically crosslinked hydrogels are "cleaner" than chemically crosslinked hydrogels because the crosslinking agents used, for the latter hydrogels, may be toxic and carcinogenic and have to be extracted from the hydrogels before they can be used.[12] However, chemically crosslinked hydrogels have a better mechanical stability than the physically crosslinked ones.[13] Network formation by end linking telechelic functional polymers with multifunctional reagents with complementary functionalities gives the so called "model" networks. It is illustrated in Scheme 5.7.

End functional polymer

Multifunctional crosslinker

Hydrogel network
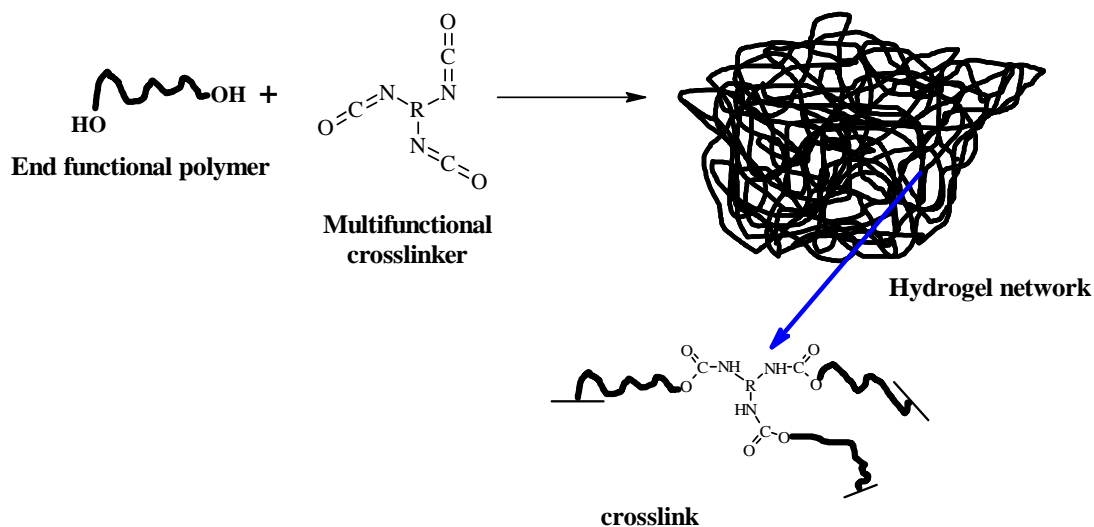
crosslink

Scheme 5.7. Schematic illustration of hydrogel network formation by reaction of end functional polymer with multifunctional crosslinking agent.

In order to ensure network formation, the chains used should have a minimum functionality of two. The end functional polymer is reacted stoichiometrically with multi functional molecules with complementary functionality.[13] As the precursor polymers will have known molecular weights and polydispersity indices, the average molecular weight between crosslinks (M_c) is known independently.[14] This is very important for establishing structure-property relationships.[14]

In this work, however, hydrogel formation was used as a way to illustrate that we had a telechelic functional material. Nevertheless, the swelling behavior of the hydrogel was also studied. Alcohols react with isocyanates to form urethanes.[13] Therefore, the hydroxyl telechelic functional PVP was crosslinked by reaction with a trifunctional isocyanate. This is shown in Scheme 5.8. This type of end linking reaction is well documented in literature as it provides ready access to "model" networks.[13] It has been used for polyisobutylene[15], polyethylene oxide[16] and polyacrylic acid[14] systems. In Scheme 5.8, structure **11** is used as it is predominant in the sample.
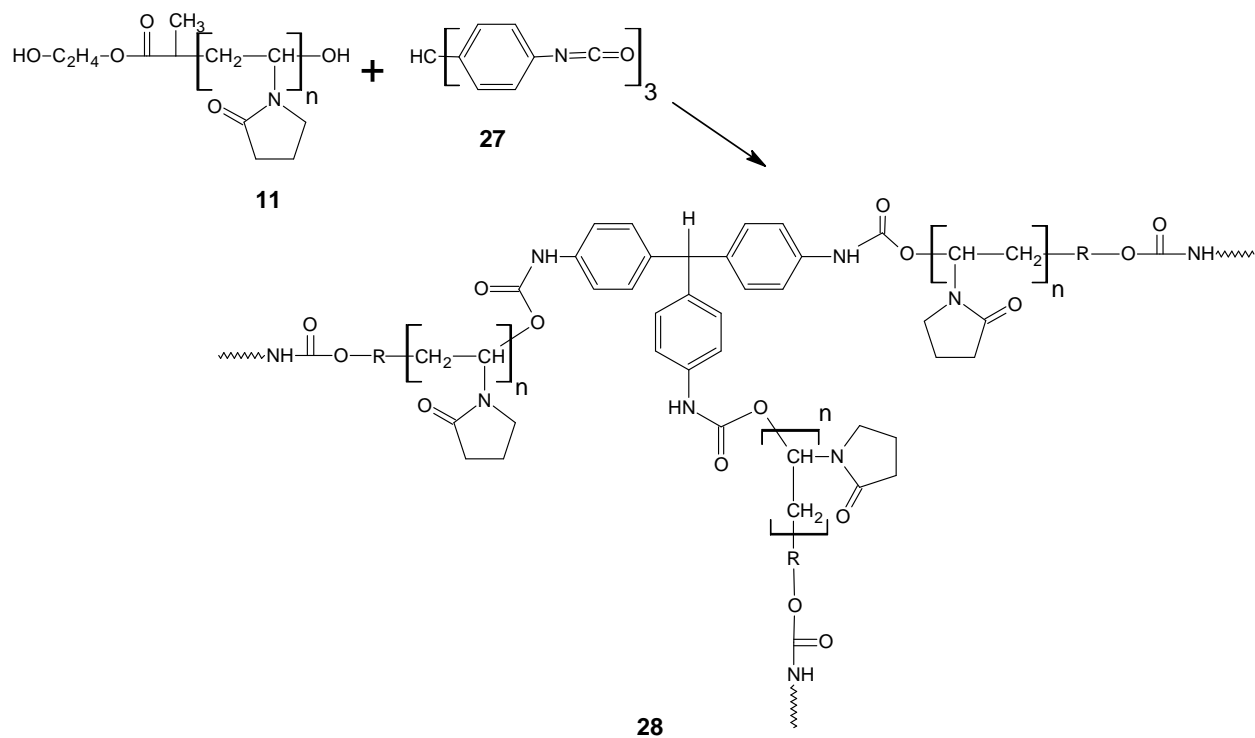
Scheme 5.8. Crosslinking reaction of hydroxyl telechelic functional PVP (11) with Desmodur R-E (27) to form PVP hydrogel network.

5.4.1 Materials

Hydroxyl telechelic functional PVP prepared as described in Section 5.2 was used. Desmodur R-E (Bayer) was a 35% solution of tris-(4-isocyanatophenyl)methane (**27**) in toluene. Dichloromethane (Saarchem) was dried over anhydrous $MgSO_4$ for 24 h and distilled over sodium metal, under a nitrogen atmosphere, and used immediately. The glassware used for the crosslinking reaction was dried in an oven at 150 ^{o}C for 24 h before use.

5.4.2 Crosslinking method

The PVP was freeze dried 24 h, immediately before use. PVP and tri-isocyanate (**27**) quantities were adjusted so that they were stoichiometrically balanced (–OH/–NCO = 1). The PVP was quickly weighed into a glass vial which was immediately sealed with a rubber septum. Freshly dried, distilled DCM was added via a degassed syringe. The mixture was gently swirled until all the PVP had dissolved. Afterwards the solution was degassed by gently bubbling nitrogen through the solution for 5 minutes and it was kept under a nitrogen atmosphere afterwards. Caution was required

so as not to evaporate the solvent during the degassing procedure. The appropriate amount of crosslinker was then added by a degassed syringe followed immediately by the addition of a catalytic amount of pyridine.[14] The mixture was then swirled gently so as to evenly mix the reagents thoroughly. Gel formation was observed in about 10 min. The reaction was allowed to proceed for 24 h so as to maximize the extent of crosslinking. Afterwards the gel was carefully cut out of the glass vial. The gel was then cleaned by soxhlet extraction with DCM. This step also served to give an estimation of the extent of crosslinking as the soluble fractions from the extraction were weighed and their combined mass was less than 35%, by weight, of the starting material. The cleaned gel was cut into cylinders of roughly 2.5 mm thick and 10 mm diameter. These were dried in a vacuum oven at 50 ^{o}C for 48 h and weighed to give W_d, (the weight of the dry gel). The gel had a typical red color. The chromophore is probably formed by the conjugation between the urethane linkage and the aromatic moiety, (see **28**, Scheme 5.8). Complete consumption of the tri-isocyanate was confirmed by infrared (IR) spectroscopy. The IR spectra were recorded on a Perkin Elmer FTIR spectrometer, Paragon 1000PC, fitted with a photoacoustic adapter model 300.

5.4.3 Swelling studies

The hydrogel prepared as described above was placed in DDI water at 37 ^{o}C ($\pm$ 2 ^{o}C). The gels were taken out at timed intervals, dried superficially, by blotting lightly with a tissue, and weighed to get W_s (the weight of the swollen gel). The equilibrium water content (EWC) of the gel was determined using equation 5.1.

$$EWC = \frac{W_s - W_d}{W_s} \times 100$$

5.1

5.4.4 Results and Discussion

The synthesis of PVP gels was carried out satisfactorily. The complete consumption of the isocyanate was confirmed by IR spectroscopy. Isocyanates have a broad and intense absorption near 2300 cm^{-1}. Figure 5.5 shows an FTIR spectrum of the PVP gel.

The swelling studies were done in duplicate and the results reported here are the averages. Figure 5.6 shows the EWC as a function of time. Water uptake increases with time and levels off after about 2.5 h. Figure 5.6 shows that a hydrogel with a water uptake of about 60 % was synthesized.
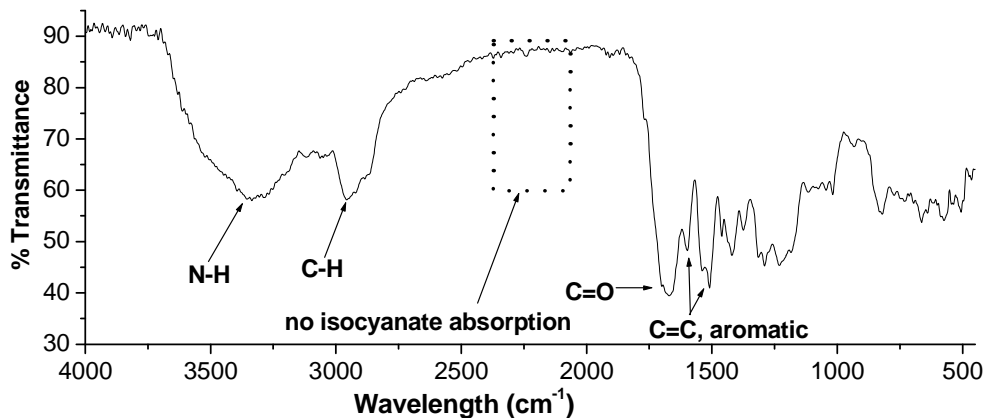

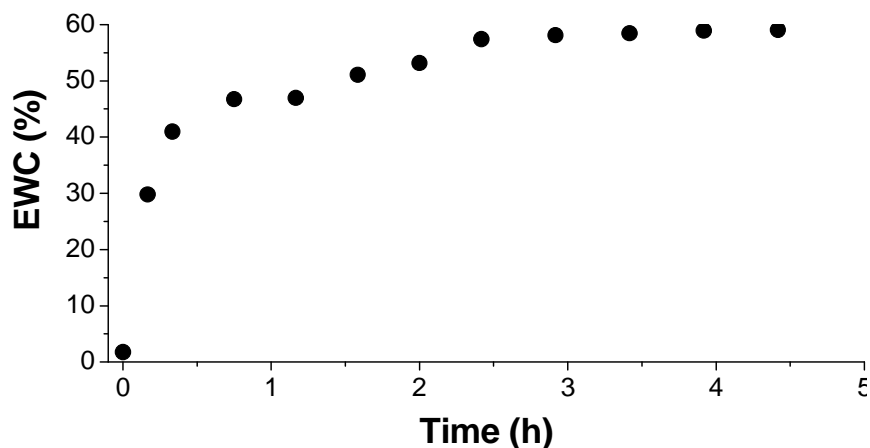**Figure 5.6. ATR-FTIR spectrum of PVP hydrogel.**

Figure 5.7. Swelling behavior of PVP hydrogel in DDI water at 37 °C.

Figure 5.8 below shows the EWC response in the long term. The EWC starts to drop after about 4 days. This is probably because some uncrosslinked PVP was diffusing out of the gel.[17]
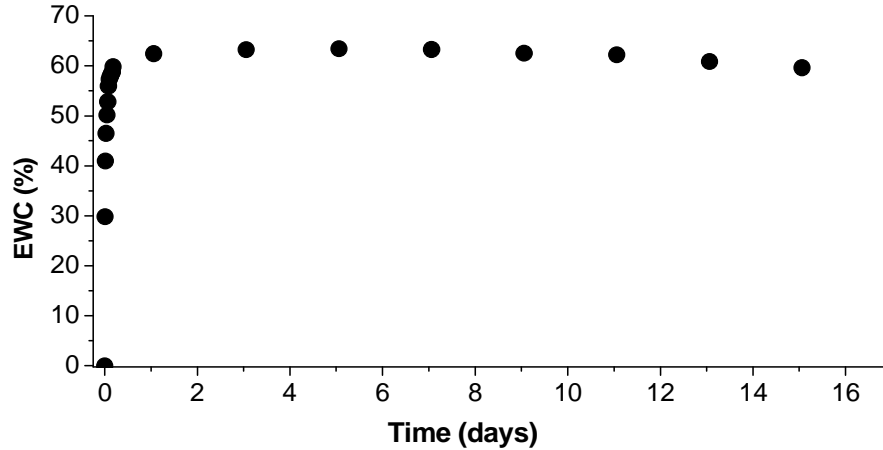
Figure 5.8. Long term swelling behavior of PVP hydrogel in DDI water at 37 $^{\circ}$C.

The diffusion behavior of the PVP hydrogel was also investigated. This was done by fitting the swelling data of each sample into equation 5.2.[18,19]

$$f = \frac{W_t}{W_\infty} = Kt^n \qquad\qquad 5.2$$

f is the fractional water content at time t. W_t and W_∞ are the weights of water in the hydrogel at time t, and at equilibrium swelling, respectively. K is a constant related to the structure of the hydrogel whilst n is a constant related to the type of diffusion. The constant n can be used to relate the rate of water uptake to time. When $n < 0.5$ swelling is diffusion controlled, whilst Fickian behavior is observed when $n = 0.5$. Between 0.5 and 1, the diffusion behavior is anomalous, i.e. it is affected by both the rate of relaxation and diffusion.[17,18] Linearizing equation 5.2 gives equation 5.3:

$$\ln f = \ln K + n\ln t \qquad\qquad 5.3$$

In the plot: $\ln f = \ln K = n\ln t$, $n = 0.38$, $r = 0.972$; axes labeled $\ln f$ (vertical) and $\ln t$ (horizontal).
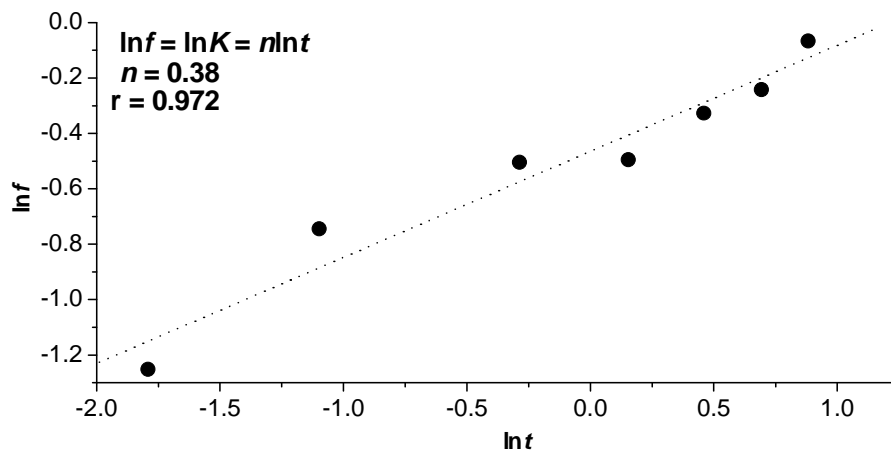
Figure 5.9. A plot of the time dependence of the rate of water uptake for PVP hydrogel.

Equation 5.3 was used to model water diffusion into the hydrogel and it gave a fairly linear plot, with a correlation coefficient of 0.97, as shown in Figure 5.9. The value of n determined here, 0.38, shows that swelling was diffusion limited. This means that the rate of diffusion of water into the hydrogel was slower than the rate of relaxation of the polymer.[17]

5.5 Conclusions

A new and facile method for removing the thiocarbonyl thio end groups of RAFT PVP was introduced. The method involves simply heating the polymer solution with H_2O_2. The method was also shown to be a simple way of introducing hydroxyl functionality at the ω-chain end.

The end modified polymers were characterized by NMR, SEC, UV-vis and MALDI ToF MS. To further prove that the material prepared here was indeed telechelic, the end modified polymer was crosslinked with a trifunctional isocyanate to form a hydrogel. The swelling behavior of the hydrogel network was characterized, in DDI water at 37 $^{\circ}$C.

The versatility of this simple end group modification procedure is now being extended to other RAFT made polymer systems.

References

(1)   J. Chiefari, Y. K. B. Chong, F. Ercole, J. Krstina, J. Jeffery, T. P. T. Le, R. T. A. Mayadunne, G. F. Meijs, C. L. Moad, G. Moad, E. Rizzardo and S. H. Thang, *Macromolecules*, 1998. **31**: p.5559-5562.

(2)   A. Postma, T. P. Davis, G. Moad and M. S. O'Shea, *Macromolecules*, 2005. **38**: p.5371-5374.

(3)   F. Cerreta, A. M. L. Nocher, C. Leriverend, P. Metzner and T. N. Pham, *Bull. Soc. Chim. Fr.*, 1995. **132**: p.67-74.

(4)   P. Vana, L. Albertin, L. Barner, T. P. Davis and C. Barner-Kowollik, *J. Polym. Sci., Part A: Polym. Chem.*, 2002. **40**: p.4032-4037.

(5)   M. Destarac, C. Kalai, L. Petit, A. Z. Wilczewska, G. Mignani and S. Z. Zard, *Polym. Prepr. (Am. Chem. Soc., Div. Polym. Chem.)*, 2005. **46**: p.372-373.

(6)   Y. K. Chong, G. Moad, E. Rizzardo and S. Thang, *Macromolecules*, 2007. **40**: p.9262-9271.

(7)   S. Perrier, P. Takolpuckdee and C. A. Mars, *Macromolecules*, 2005. **38**: p.2033-2036.

(8)   S. Z. Zard, *Angew. Chem., Int. Ed. Engl.*, 1997. **36**: p.612-685.

(9)   Y. E. Kirsh, *Water Soluble Poly-N-Vinylamides. Synthesis and Physicochemical Properties*. 1998, John Wiley and Sons: New York.

(10)   C. C. Anderson, F. Rodriguez and D. A. Thurston, *J. Appl. Polym. Sci.*, 1979. **23**: p.2453-2462.

(11)   A. Postma, T. P. Davis, A. R. Donovan, G. Li, G. Moad, R. Mulder and M. S. O'Shea, *Polymer*, 2006. **47**: p.1899-1911.

(12)   W. E. Hennink and C. F. v. Nostrum, *Adv. Drug Delivery Rev.*, 2002. **54**: p.13-36.

(13)   A. S. Hoffman, *Adv. Drug Delivery Rev.*, 2002. **43**: p.3-12.

(14)   A. Shefer, A. J. Grodzinsky, K. L. Prime and J. P. Busnels, *Macromolecules*, 1993. **26**: p.5009-5014.

(15)   T. Miyabayashi and J. P. Kennedy, *J. Appl. Polym. Sci.*, 1986. **31**: p.2523-2532.

(16)   B. Laik, L. Legrand, A. Chausse and R. Messina, *Electrochim. Acta*, 1998. **44**: p.773-780.

(17)   K. B. Keys, F. M. Andreopoulos and N. A. Peppas, *Macromolecules*, 1998. **31**: p.8149-8156.

(18)   A. Patel and K. Mequanint, *Macromol. Biosci.*, 2007. **7**: p.727-737.

(19)   J. V. Cauich-Rodriguez, S. Deb and R. Smith, *J. Appl. Polym. Sci.*, 2001. **82**: p.3578-3590.

Chapter 6

Conclusions and Outlook

In Chapter three, a facile method for making α-hydroxyl end functional PVP by RAFT mediated polymerization was introduced. A hydroxyl functional xanthate chain transfer agent was prepared and used as the RAFT agent. The subsequently made polymers had all the characteristics of a polymer prepared by a living radical polymerization process which include controlled molecular weight and low polydispersity index.[1] The presence of the thiocarbonyl thio moiety at the ω-chain end was confirmed by NMR and MALDI ToF MS. It was observed this end group is very labile and decomposes under very mild conditions leading to chains terminated by an unsaturated repeat unit. The N-vinylpyrrolidone repeat unit also introduces a very reactive moiety in the polymer. This is probably due to the amide linkage of the monomer. A tendency to participate in side reactions with extraneous water was observed and the subsequently produced end groups were characterized. It is imperative to keep the polymerization system as dry as possible in order to increase the retention of the xanthate end group at the ω-chain end. This is important when this site is the locus for the application of end group chemistry that is needed to make the polymer telechelic end functional.

In Chapter four, a simple method for removing the xanthate end group was introduced. This was via addition-fragmentation, and subsequent termination by combination with an α-haloester. Radicals are generated by an atom transfer radical addition based process using a Cu complex catalyst. Optimum conditions for this technique were determined. NMR analysis showed that the xanthate end group was removed quantitatively. On its own this is very important as the thiocarbonyl thio end moiety imparts some undesirable characteristics like color and smell to the polymer. It is also thermally unstable and unstable in the presence of nucleophilic reagents. By using a hydroxyl functional α-haloester and α-hydroxyl functional PVP, telechelic hydroxyl functional PVP was obtained. Quantitative information on the extent of hydroxyl functionality was obtained via derivatizing the end functionality with trichloro acetyl isocyanate and comparing integrated NMR signals. MALDI ToF analysis of the end modified PVP oligomers was, however, not conclusive.

The experimentally determined masses of the PVP oligomers differed from the theoretical ones by more than the acceptable error range for this technique. This was not investigated further.

In Chapter five, a facile route for removing the xanthate end group by merely heating the polymer solution with hydrogen peroxide was introduced. Again, by using α-hydroxyl functional PVP this method yielded telechelic hydroxyl functional PVP. The xanthate end group is directly replaced by a hydroxyl end group. Characterization was as in Chapters three and four, by NMR and MALDI ToF MS. As in Chapter four, MALDI ToF MS analysis was not conclusive. This method of end group modification is very green as all that was required was a sample of the RAFT made polymer, dissolved in an appropriate solvent and hydrogen peroxide and simply heating the reaction mixture. The telechelic hydroxyl functional PVP was subsequently crosslinked by reacting with a trifunctional isocyanate to give a PVP hydrogel. This approach was used as an alternative way to show that the polymer was indeed telechelic hydroxyl functional. The swelling kinetics of the gel were assessed in double deionized water.

The facile end group modification procedure, by heating with H_2O_2 will now be extended to other RAFT made polymer systems. These are polystyrene and polymethyl methacrylate prepared by the RAFT process using cyanoisopropyl dithiobenzoate and 4-cyano-4-((thiobenzoyl)sulfonyl) pentanoic acid as the chain transfer agents. Polyvinyl acetate prepared by RAFT using a xanthate chain transfer agent will also be used. Of main interest will be to confirm the presence of the hydroxyl group at the ω-chain end. This will be verified by analyzing the subsequently end modified polymers by NMR and MALDI ToF mass spectrometry.

The end modified polymers should also be analyzed by advanced liquid chromatographic techniques like Liquid Chromatography under Critical Conditions. In LCCC the polymers are separated on the basis of end group functionality.[2] This technique can be used to provide quantitative information, which can be used to complement the structural information provided by NMR and MALDI ToF MS It will also be very important to verify if the end group modification does not disturb the integrity of the polymer sample. For example, some acrylate systems are known to undergo backbiting reactions followed by β-scission.[3] This technique will afford a facile and cheap method of accessing hydroxyl functional polymers. Since the only ingredients are the polymer sample and hydrogen peroxide, it will be a relatively cheap and clean process.

References

(1)   J. Chiefari, Y. K. B. Chong, F. Ercole, J. Krstina, J. Jeffery, T. P. T. Le, R. T. A. Mayadunne, G. F. Meijs, C. L. Moad, G. Moad, E. Rizzardo and S. H. Thang, *Macromolecules*, 1998. **31**: p.5559-5562.

(2)   H. J. A. Philipsen, *J. Chromatogr., A*, 2004. **1037**: p.329-350.

(3)   A. Postma, T. P. Davis, G. Li, G. Moad and M. S. O'Shea, *Macromolecules*, 2006. **39**: p.5307-5318.

<u>Appendices</u>

Appendix 1

COSY spectrum of RAFT made PVP showing the connectivity of proton signals on an unsaturated terminal repeat unit
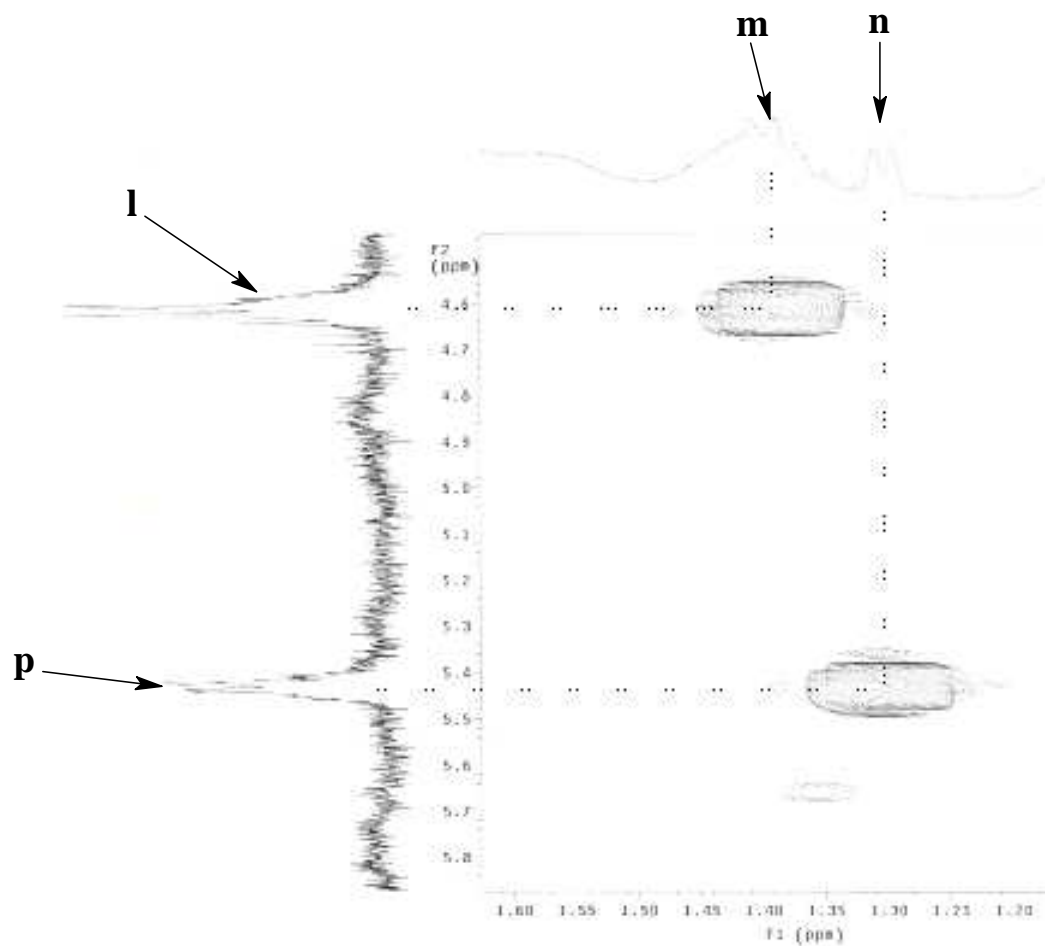
The COSY spectrum shows the connectivity of the –NC**H**=C**H**– protons on an unsaturated terminal repeat unit as illustrated in Figure 3.6, Chapter 3, for structure **15**. The small signal at 4.75–5.0 ppm (*o*, Figure 3.5) was assigned to –NCH=C**H**– whilst that at 6.8–7.0 ppm (*q*, Figure 3.5) was assigned to –NC**H**=CH–.the connectivity of these signals is illustrated using the dashed lines.
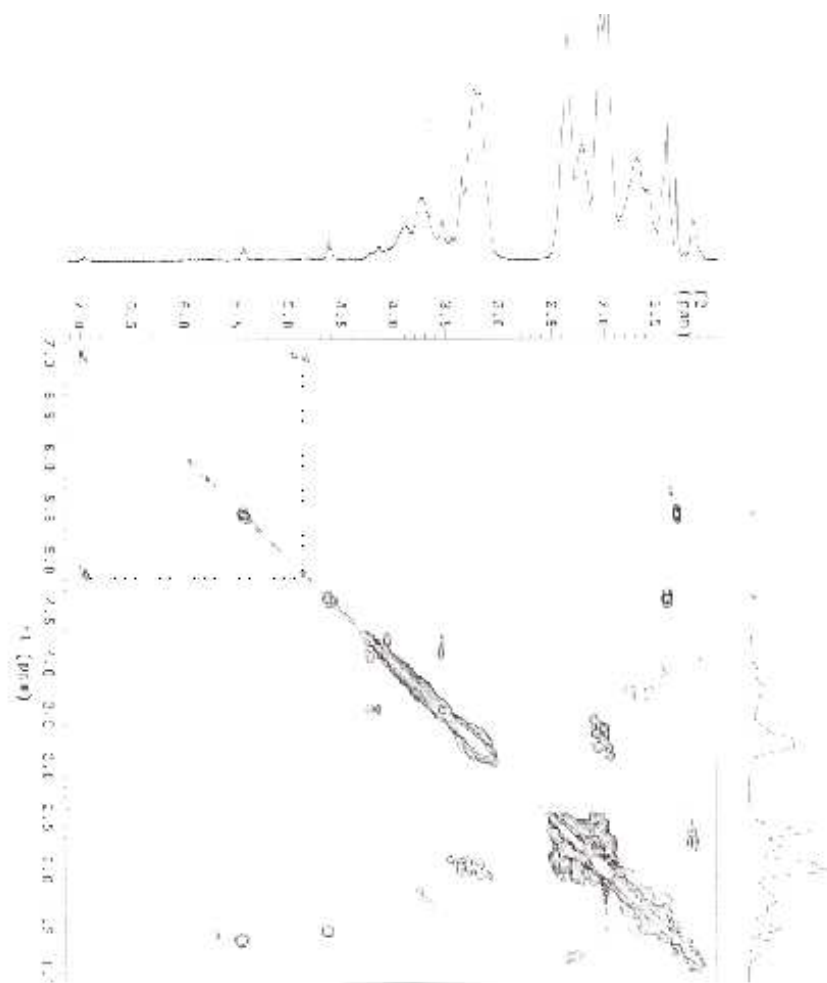
Appendix 2

## COSY spectrum of RAFT made PVP showing the connectivity of proton signals attributed to PVP dimer end group

The COSY spectrum shows the connectivity of the signals *n* and p, Figure 3.7, Chapter 3. This spectrum also shows the connectivity the xanthate chain end group, *m* and *l*. The signal *m* also overlaps with a broad polymer backbone signal.

Appendix 3

COSY spectrum of TAI derivatized peroxide modified PVP, showing the connectivity of the α-methyelene protons to the polymer backbone

The COSY spectrum of TAI derivatized α,ω-hydroxyl end functional PVP showing the connectivity of the signal for the α-methyelene protons to a signal 4.1–4.2 ppm which was assigned to the β-methylene protons of the R group's $–CH_2CH_2–O–C(O)–$ moiety in Chapter 5.
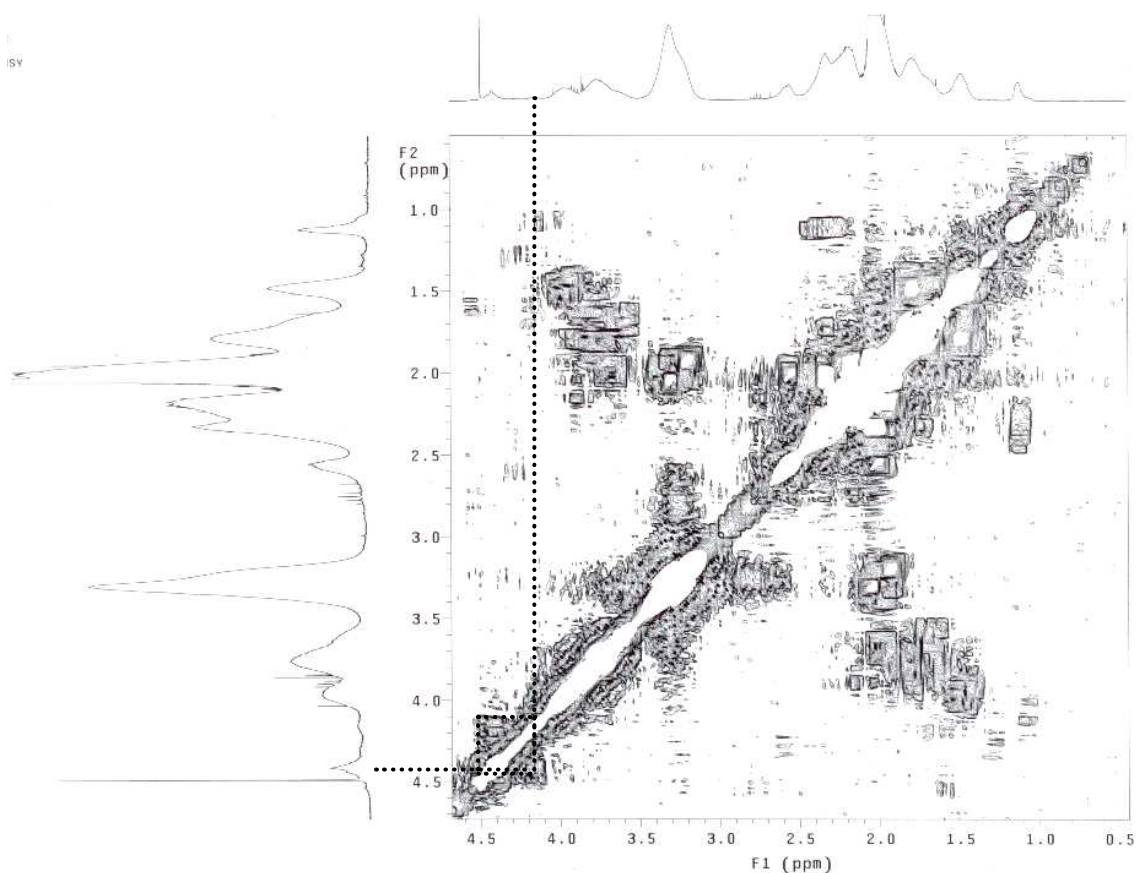
Appendix 4

COSY spectrum showing the connectivity of TAI derivatized carboxylic acid side chain's α-methylene protons to the polymer backbone